Validation of the bifurcation diagram in the 2D Ohta-Kawasaki problem

Jan Bouwe van den Berg* J.F. Williams†

April 13, 2016

Abstract

We develop a rigorous numerical method to compare local minimizers of the Ohta-Kawasaki functional in two dimensions. In particular, we validate the phase diagram identifying regions of parameter space where rolls are favorable, where hexagonally packed spots have lowest energy and finally where the constant mixed state does. More generally, we present a method to rigorously determine such features in problems where optimal domain sizes are not known a priori.

Contents

*VU University Amsterdam, Department of Mathematics, De Boelelaan 1081, 1081 HV Amsterdam, The Netherlands, `janbouwe@few.vu.nl`; partially supported by NWO-VICI grant 639033109.

†Simon Fraser University, Department of Mathematics, 8888 University Drive Burnaby, BC, V5A 1S6, Canada, `jfwillia@sfu.ca`.

1 Introduction

1.1 Overview of the problem

In recent decades, the mathematical study of pattern formation has often been motivated by computer simulations of specific partial differential equations (PDEs) modelling physical, chemical and biological phenomena. These computations have provided much inspiration and intuition. However, little attention is usually paid to the validity of the numerical computations. Do the images on the computer screen reflect the true behaviour of solutions of the PDEs or are we observing artefacts of the algorithmic implementation? These issues become more important the more interesting the results are and, typically, the more mathematically difficult the problem.

In this paper we address this concern of spurious numerical solutions in the context of the Ohta-Kawasaki [25] energy. This is a variational problem for an order parameter u with fixed proportion $m \in (-1, 1)$. Specifically, we want to minimize:

$$E(u) = \frac{1}{|\Omega|} \int_\Omega \frac{1}{2\gamma^2} |\nabla u|^2 + \frac{1}{4}(1 - u^2)^2 + \frac{1}{2}|\nabla \phi|^2 \, dx, \tag{1.1}$$

where u is a periodic function on the domain Ω, $m = \frac{1}{|\Omega|} \int_\Omega u(x)dx$ is its average, $-\Delta\phi = (u - m)$ and γ is a model parameter related to physical properties of the system. This non-local non-convex energy has three competing elements. The first two are familiar from the Ginzburg-Landau energy and are minimized by smooth connections between the two preferred states $u(x, t) = \pm 1$. The third however is nonlocal and penalizes deviations from the mean m. This additional term prefers mixed-phase regions of space wherein u is essentially constant.

The competition between the three terms leads to oscillations about the mean with an intrinsic length-scale *not set by the domain size or boundary conditions.* The relative strengths of the three terms are determined by the parameters (m and γ) and, on a sufficiently large domain, these alone determine the energy minimizing patterns.

The Ohta-Kawasaki energy was originally derived in the context of diblock copolymers [25]. These are linear-chain molecules consisting of two sub-chains joined by a covalent bond. The two sub-chains are made of monomers which weakly repel each other causing the sub-chains to segregate. This tension between attraction and repulsion induces large scale separation into regions containing only one type of monomer [25]. The geometric form of the energetically favourable states depends on system parameters. Because of this self-organization these materials are widely studied in material science, see [4, 21] for overviews.

It was shown by Choksi and Ren [12] that the energy 1.1 can be formally derived from an appropriate mean field theory connecting this simple mathematical model directly to the physical

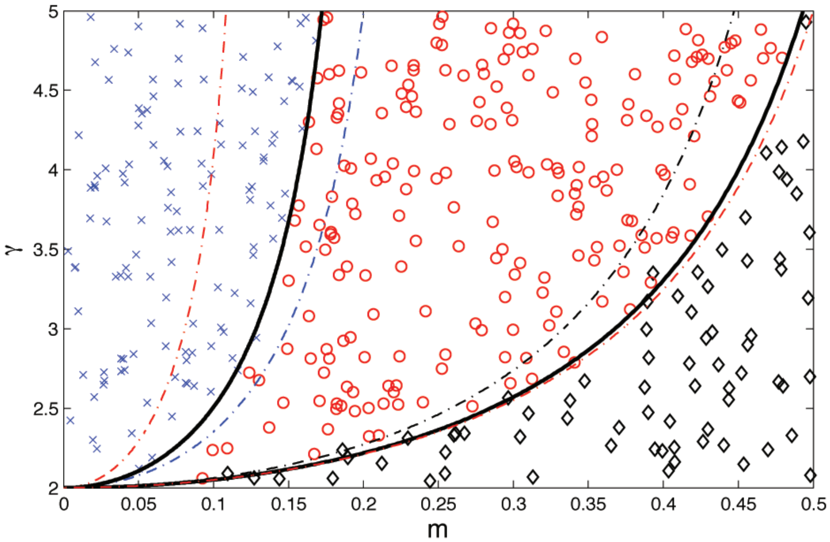

Figure 1.1: A previous approach to constructing the bifurcation diagram was done by simply evolving (1.2) from random initial conditions and randomly chosen parameter values and then identifying the final state. In this figure the crosses represent stripes, the circles represent spots and the diamonds represent the mixed state. The solid lines are asymptotic approximations to the bifurcation curves and the dashed lines indicate changes in linear stability (these are not relevant to the current discussion). Figure reproduced from [8].

problem in a quantitative way. Thus we may consider this as a mathematical paradigm for pattern formation when there are competing short-range attractive interactions and long-range repulsive Coulomb interactions or as a simplified description of an important physical system valid in a certain realistic limit.

Whether one is trying to predict the states formed by a specific diblock copolymer at a specific temperature or trying to understand the abstract mathematical problem the fundamental question is the same:

For a given set of parameters what pattern minimizes the energy overall possible patterns?

While some work has been done numerically [28, 11, 8, 19, 24, 30, 31], formally [8, 25] and analytically in certain limits [9, 10, 7, 12] this is in general an open and seemingly impossible problem. Of these [19] is the only prior work to attempt to determine an optimal domain size as part of the solution procedure.

The energy 1.1 is highly non-convex and known to be extraordinarily flat in some regions of parameter space. One previous approach to studying minimizers has been to start with random initial data and evolve the time-dependent PDE. Performing the gradient descent in H^{-1} makes the PDE local and mass preserving:

$$u_t = -\Delta \left(\frac{1}{\gamma^2} \Delta u + u - u^3 \right) - (u - m). \tag{1.2}$$

However, the long-time PDE evolution is very difficult as one is plagued by stiffness [20] and metastability issues [29, 8]. Moreover, a sensible domain size is not known a-priori. Direct minimization of the energy from arbitrary initial conditions has similar problems [28].

In this paper we consider only the two dimensional problem. In some regions of parameter space the optimal solutions in three dimensions are lower dimensional but the full physical problem is truly three dimensional. The 3D problem is even more computationally challenging and has fewer exploitable symmetries. It will be addressed in future work.

Figure 1.2: Solutions computed with $m = 0.11, \gamma = 2.5$. Energy increasing from left to right. The leftmost two solutions are solved with optimal domain size (for that pattern). The right three are not. For these parameter values the hexagonally packed spots have lower energy than the stripes but it is easy to find a spot pattern with *higher* energy than the stripes. Each spot solution is presented by copying the unit cell twice in each direction. The solutions have very different values of κ (defined in Section 3) and thus correspond to different physical domains.

By considering $|m| \ll 1$ Choksi et al [8] constructed asymptotic solutions in the limit $m \to 0, \gamma \to 2$. The following picture emerged (cf. Figure 1.1). There are curves $\Gamma_1(m), \Gamma_2(m)$ such that if $\gamma > \Gamma_1(m)$ then the stripe solutions are energetically favourable, if $\Gamma_1(m) < \gamma < \Gamma_2(m)$ then hexagonally packed spots have lowest energy and if $\gamma < \Gamma_2(m)$ the mixed state ($u \equiv m$) is lowest. The authors explored these curves numerically for parameter values away from the bifurcation point by evolving the PDE from random initial data, see Figure 1.1; over this region of parameter space the problem was solved on a fixed grid with no attempt to optimize the domain. Rigorous bounds on Γ_2 were computed in [9] and [28]. The first rigorously in the limit $\gamma \to \infty$ and the latter using a novel numerical algorithm.

The domain size has been seen experimentally to scale with various physical parameters and also proven to scale with $\gamma^{-2/3}$ as $\gamma \to \infty$. However, its significance has been largely ignored in previous numerical studies. Indeed, little to no optimization of the domain size was considered for m significantly away from the bifurcation point ($m = O(1)$). As mentioned before, the choice of domain size is nontrivial. Ideally one would like to work on arbitrarily large domains; at the very least one would like to work on domains that are much larger than the intrinsic length scale of the patterns, so that boundary effect are negligible.

Figure 1.2 illustrates that ignoring the domain size is indeed an oversight. Here we present three solutions with fixed parameters and two on optimal domain sizes. The right three spot-like solutions were all solved on fixed domain sizes and found to have higher energy than the stripes. However, when we optimize over spot solutions with respect to domain size we find that the best pattern are the hexagonally packed spots and that it has considerably lower energy than any of the solutions with fixed arbitrary domain size.

To overcome these obstacles we take the following approach:

1. Start from the known bifurcation point where all patterns can be found analytically and ordered energetically and the optimal length scale determined exactly.

2. Include the length scale as an unknown in the problem.

3. Continue in parameter space on curves where the energies of different patterns are equal. This means solving for the coefficients of the solution expansions, the parameters m and γ and the domain sizes simultaneously.

4. Rigorously prove that the computed curve of finite numerical approximations is "close" to that of the true continuous curve of solutions. Close here means that we have a computed bound on the size of the cylinder containing the true curve centred on our numerical curve.

The latter point is an important step as we show that our solutions are true solutions independent of discretization method, size of finite approximation or any other numerical detail that can plague such delicate calculations. For instance, suppose we have what appears to be a static solution to the evolutionary PDE (and hence a local minimizer of the energy). When considering only the numerical approximation it can be difficult to distinguish between the effects of numerical error and those of an exponentially small eigenvalue of the linearized problem *of either sign*. By considering the linearization about our numerical solution in the full infinite-dimensional setting we categorically rule out fictive purely numerical solutions (cf. the spurious solution of the Emden equation on a rectangle [27]).

1.2 Overview of relevant rigorous numerics

We develop a rigorous numerical method to efficiently explore the parameter space by identifying those curves along which different patterns have the same energy. Rigorous numerics are hybrid numerical/analytical schemes where each computation is truly an existence proof as we compute a solution to a truncated problem, but also show that the numerical solution is at the centre of a ball in which there is, by fixed point arguments, a unique solution to the infinite dimensional problem and that this holds along the path connecting all computed solutions. Computations involving floating point numbers are performed rigorously through the use of interval arithmetic.

We use a functional analytic approach, as opposed to a more geometric one (see e.g. [1, 38]), to rigorous computing. In particular, given an abstract nonlinear problem

$$\text{find } x \in X \text{ such that } F(x) = 0$$

posed on some Banach space X, we proceed as follows:

- Obtain a numerical approximation $\overline{x}_N$ such that $F_N(\overline{x}_N) \approx 0$, where F_N is a finite approximation (truncation) of F.
- Form a Newton-like fixed point operator $T(x) = x - AF(x)$ such that $x = T(x) \Rightarrow F(x) = 0$. Here A is a conveniently chosen approximation of $(DF)^{-1}(\overline{x}_N)$.
- Determine analytical estimates on T to test if it is a local contraction map.
- Use interval arithmetic to rigorously verify that these conditions hold in an infinite dimensional ball around the numerical approximation $\overline{x}_N$.

The result of this procedure is then an existence proof as we determine a rigorous bound on the radius of the ball centered on $\overline{x}_N$ which contains the solution $\tilde{x}$ of $F(x) = 0$. Note that this approach uses interval arithmetic only once an approximate solution has been generated and is thus not plagued by the artificial growth of intervals caused by some iterative schemes. In the entire analysis we treat the radius r of the ball $B_r(\overline{x}_N)$ as a parameter (not fixed a priori) that is chosen in the final step of the algorithm only. Choosing r small leads to the best bounds on the location (in X) of the solution, whereas large r give the best region of uniqueness.

Although the particular application leads to several novel aspect (which we outline in more detail in Section 2), we stress that such an functional analytic, rigorous numerical approach in itself is not new, and we refer to [2, 3, 37, 23, 13], and the references therein, for a host of applications of these techniques (see also Section 6 for additional references). Furthermore, in [36] the one dimensional Ohta-Kawasaki equation was studied using similar, although more Sobolev space based, methods.

The following theorem formulates precisely which bounds we need in order to prove that T is a contraction mapping on $B_r(\overline{x}_N)$, see Section 6 for more details.

Newton-Kantorovich type Theorem. Let F be a map from X to X', where X is a Banach space with norn $\|\cdot\|_X$. Let A and $A^\dagger$ be linear operators mapping $X' \to X$ and $X \to X'$, respectively. Assume $T : X \to X$, defined by $T(x) = x - AF(x)$, is Fréchet differentiable. Assume that A is injective. Fix $r^* > 0$ and let Y_0, Z_0, Z_1 and Z_2 be constants such that

$$\begin{aligned}
\|AF(\overline{x})\|_X &\leq Y_0 \\
\|I - AA^\dagger\|_{B(X)} &\leq Z_0 \\
\|A(A^\dagger - DF(\overline{x})\|_{B(X)} &\leq Z_1 \\
\|A(DF(b) - DF(c))\|_{B(X)} &\leq Z_2 \|b - c\|_X \quad \text{for all } b, c \in \overline{B_{r^*}(\overline{x}_N)}.
\end{aligned}$$

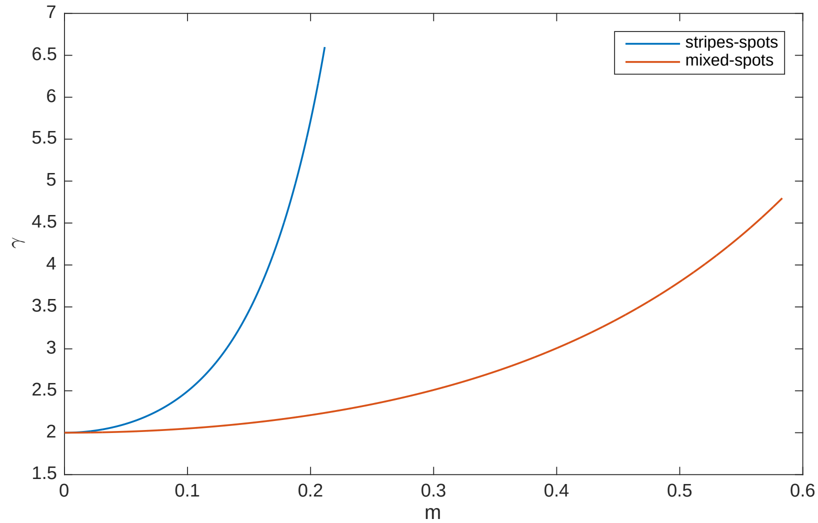

Figure 2.1: Curves of equal energy in the (m, γ)-plane. Along the left curve spots and stripes have equal energy, whereas along the right the spots and mixed state are energetically equal. These curves are rigorous and the rigorous error bounds are much smaller than the line width, in the sense explained in the main text.

If there exists and $r \in (0, r^*)$ such that

$$p(r) \stackrel{\text{def}}{=} Y_0 - (1 - Z_0 - Z_1)r + Z_2 r^2 < 0, \tag{1.3}$$

then there exists a unique $\tilde{x}$ such that

$$\tilde{x} \in B_r(\overline{x}_N) \quad \text{and} \quad F(\tilde{x}) = 0.$$

The proof of existence of a solution is thus "reduced" to carefully choosing the operators A and $A^\dagger$, obtaining explicit bounds Y_0, Z_0, Z_1 and Z_2 defined above, and verifying the polynomial $p(r)$ in 1.3 is negative for some $r \in (0, r^*)$. The choices of A and $A^\dagger$ are discussed in detail in Section 6, while the estimates are carefully outlined in Section 7, calculated in detail in the Appendices and then verified in the accompanying matlab code.

2 Main contributions of this work

In this paper we use rigorous numerics to construct the curves Γ_1 and Γ_2 defined thus: a pair (m, γ) lies on the curve Γ_1 if there are stripe and hexagonal spot solutions at this point with equal energy, these patterns are both optimal with respect to their respective domain sizes, and the point lies on the unique continuous curve of such points that emanates from the bifurcation point $(m, \gamma) = (0, 2)$. The curve Γ_2 is defined similarly except now the hexagonal spot pattern and mixed state must have the same energy. These curves are presented in Figure 2.1. We obtain smooth parametrized curves in the parameter plane with rigorous error bounds of size $2 \cdot 10^{-7}$ for the stripes-spots curve Γ_1 and of size 10^{-6} for the mixed-spots curve Γ_2. These errors are dwarfed by the line width.

In terms of the practical realities of applying the rigorous numerics ideas, this work represents a significant step forward past clean-cut test problems to more elaborate variational problems in pattern formation.

On the applied side, this is the first paper to carefully and fully consider the impact of domain size optimization in the Ohta-Kawasaki problem. If we believe that any physical system is "large

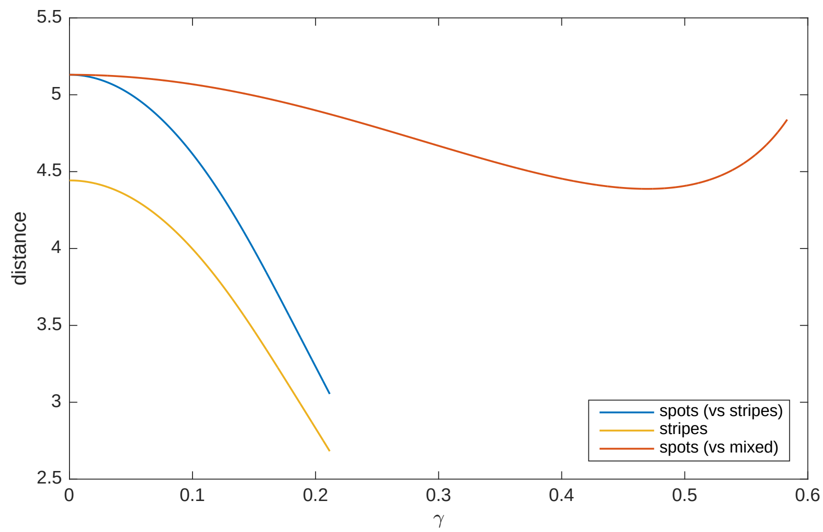

Figure 2.2: Optimal distances between subsequent maxima of stripes and spots along the stripes-spots curve Γ_1 (yellow and blue) and the mixed-spots curve Γ_2 (red).

enough" to avoid finite size effects, we must compute on very large domains to replicate this. However, this quickly becomes impractical. To overcome this obstacle we focus on the two patterns that appear exclusively in simulations on large domains: stripes and spots. We consider the distance between stripes as well as the distance between the spots as unknown variables that we have to optimize for as part of the variational problem.

One of our findings is that the domain size is critically important. Indeed, we note that the curves in Figure 2.1 deviate substantially from the ones in Figure 1.1 which were reported previously [8] (and which were supported by asymptotics in the limit $m \to 0$). The rigorously computed curves lie much lower in the parameter plane, meaning that the transitions to spots and stripes occur for lower values of γ or higher values of μ (depending on which parameter is varied) than could be predicted from those earlier simulations. Besides, Figure 2.2 shows both the distance between the stripes and the distance spots as a function of m, see also Remark 3.2. The optimal distances decrease by 40% from their asymptotic ($m = 0$) values for the stripes-spots curve, while this is around 10% for the mixed-spots curve. We note the similar shapes of the curves for the optimal distances in the stripes-spots energy balance. The distance between spots has a multiplicative factor (dictated by the geometry) of $\sqrt{4/3}$ compared to the distance between stripes. When taking this geometric factor into account the ratio between these distances varies only by 3% along the depicted stripes-spots curves.

On the algorithmic side, we work in a weighted space where the weights are chosen algorithmically in order to make the computations as efficient as possible. Indeed, while simpler implementations of these rigorous numerics techniques for continuation problems have been developed previously [34, 5, 14, 17], due to the complexity of the system of equations under consideration, we had to develop a novel weight-choosing algorithm.

To trace the curve in parameter space rigorously, we need weights that vary over *four* orders of magnitude (see Figure 9.3). We explain this procedure in Section 9 and also show that we have close to the optimal weights at all times, see Remark 9.2.

Finally, to trace the curves Γ_1 and Γ_2 all the way into the bifurcation point $(m, \gamma) = (0, 2)$ we need to perform an asymptotic "blowup" analysis near the bifurcation point. Since essentially all patterns originate from this point, the rescaling is subtle and a notable advance beyond a somewhat analogous treatment of the Hopf bifurcation point in Wright's delay equation [22]. In Section 8 we derive this desingularized problem and then in Section 9 show how to connect a solution branch coming out of the bifurcation point to a "global" branch of solutions.

The paper is organized as follows. We focus on the detailed analysis of the stripes-spots curve throughout the paper and indicate briefly the changes needed to adapt this analysis to the mixed-spots curve. First, in Section 3 we write the differential equations under consideration in Fourier space and then detail the necessary Banach spaces in Section 4. The contination problem is outlined in Section 5 and the functional analytic setup is presented in Section 6. The structure of the estimates is explained in Section 7. We identify the crucial terms needed for the bounds, but defer their individual determination to Appendix A. Indeed, once the problem has been carefully formulated, each term (and there are many in our problem) requires careful consideration, but the individual estimates are less illuminating and would break the flow of the main text. Next, in Section 8 we give the analogous analytical and computational details of the hybrid construction for the asymptotic limit problem (at and near the bifurcation point $\mu = 0$, $\gamma = 2$). The construction of the rescaled problem at and near the bifurcation point is delicate, although the detailed estimates are in fact somewhat less gruelling than in the general case, see Appendix B. Finally, in Section 9 we discuss extensively the main computational and algorithmic issues. The reader wishing to recreate the proof of the full problem is referred to the appendices and the matlab codes available at [35].

3 Formulation of the Ohta-Kawasaki problem

We consider the functional

$$E(u) = \frac{1}{|\Omega|}\int_\Omega \frac{1}{2\gamma^2}|\nabla u|^2 + \frac{1}{4}(1-u^2)^2 + \frac{1}{2}|\nabla\phi|^2\,dx,$$

where u is a periodic function on the rectangular domain $\Omega = [0, L_1]\times[0, L_2]$ and $m = \frac{1}{|\Omega|}\int_\Omega u(x)dx$ is its average. The function ϕ is the unique solution of the elliptic problem

$$-\Delta\phi = u - m \tag{3.1}$$

with periodic boundary conditions and $\int \phi = 0$. Taking the H^{-1} gradient of E gives us the Euler-Lagrange equation

$$-\Delta(\gamma^{-2}\Delta u + u - u^3) - \sigma(u - m) = 0$$

for the critical points of E. We aim to find the minimum of E for fixed m, but varying L_1 and L_2. As explained in the introduction, we only consider stripes and hexagonal spot patterns. In particular, we would like to find the curve in parameter space for which stripes and spots have equal energy and the energies are optimized over the domain sizes.

To fix the domain and to simplify the algebra in the formulas somewhat, let us change variables $\beta \stackrel{\text{def}}{=} \gamma^{-2}$, $\mu \stackrel{\text{def}}{=} m^2$ and $\ell_i \stackrel{\text{def}}{=} \frac{L_i}{2\pi}\gamma$. We introduce the rescalings $u \to mu$, $\phi \to m\gamma^{-1}\phi$, $x_i \to \frac{L_i}{2\pi}x_i$ and $m^{-2}(E - \frac{1}{4}) \to E$:

$$E(u) = \frac{1}{4\pi^2}\int_0^{2\pi}\int_0^{2\pi} \frac{1}{2}|\nabla_\ell u(x)|^2 - \frac{1}{2}u(x)^2 + \frac{\mu}{4}u(x)^4 + \frac{\beta}{2}|\nabla_\ell\phi(x)|^2\,dx,$$

with $\nabla_\ell = \left(\ell_1^{-1}\frac{\partial}{\partial x_1}, \ell_2^{-1}\frac{\partial}{\partial x_2}\right)^T$. We require that $\frac{1}{4\pi^2}\int_0^{2\pi}\int_0^{2\pi} u(x)dx = 1$ and the rescaled $\phi(x)$, solves

$$-\Delta_\ell\phi(x) = u(x) - 1 \quad \text{on } x \in [0, 2\pi]\times[0, 2\pi], \qquad \text{and} \qquad \int \phi = 0,$$

where

$$\Delta_\ell = \nabla_\ell\cdot\nabla_\ell = \ell_1^{-2}\frac{\partial^2}{\partial x_1^2} + \ell_2^{-2}\frac{\partial^2}{\partial x_2^2}.$$

The differential equation becomes $\Delta_\ell^2 u + \Delta_\ell[u - \mu u^3] + \beta(u - 1) = 0$. To compare stripes and hexagonal spots we need to solve for both simultaneously. The stripes solve the 1D problem

$$u_1'''' + \kappa_1[u_1 - \mu u_1^3]'' + \kappa_1^2\beta(u_1 - 1) = 0$$

where $\ell_1 = \kappa_1^{1/2}$ and $\ell_2 = 1$ and there is no dependence on x_2. The energy in these variables is

$$E_1(u_1) = \frac{1}{2\pi}\int_0^{2\pi} \frac{1}{2\kappa_1}|u_1'|^2 - \frac{1}{2}u_1^2 + \frac{\mu}{4}u_1^4 + \frac{\kappa_1\beta}{2}|\phi_1'|^2\,dx_1$$

where ϕ_1 (once again rescaled, namely $\phi \to \kappa_1\phi_1$) solves $-\phi_1'' = u_1 - 1$. To optimize over κ_1 we require $\frac{\partial E_1}{\partial \kappa_1} = 0$, i.e.,

$$\int_0^{2\pi} \frac{1}{2\kappa_1^2}|u_1'|^2 - \frac{\beta}{2}|\phi_1'|^2\,dx_1 = 0.$$

We look for a symmetric solution and pose

$$u_1 = 1 + 2\sum_{k=1}^{\infty} a_k \cos kx_1 = \sum_{k=-\infty}^{\infty} a_k e^{ikx_1}, \tag{3.2}$$

with the convention $a_{-k} = a_k$, and $a_0 = 1$. This transforms the equation into Fourier space:

$$k^4 a_k - \kappa_1 k^2[a_k - \mu\langle a^3\rangle_k] + \kappa_1^2\beta a_k = 0, \qquad k \geq 1, \tag{3.3}$$

where $\langle\cdot\rangle$ denotes the convolution in both one and two dimensions:

$$\langle a\tilde{a}\rangle_k \stackrel{\text{def}}{=} \sum_{j\in\mathbb{Z}} a_{k-j}\tilde{a}_j \qquad \text{and} \qquad \langle b\tilde{b}\rangle_{m_1,m_2} \stackrel{\text{def}}{=} \sum_{j_1,j_2\in\mathbb{Z}} b_{m_1-j_1,m_2-j_2}\tilde{b}_{j_1,j_2}.$$

These represent the Fourier coefficients of the product $u(x)\tilde{u}(x)$. We also denote $\langle a^2\rangle = \langle aa\rangle$ and $\langle a^3\rangle = \langle\langle a^2\rangle a\rangle$, etc. For algebraic simplicity later on, we rewrite the optimal domain size condition as

$$\sum_{k\in\mathbb{Z}\setminus 0} (k^2 - \kappa_1^2\beta k^{-2})a_k^2 = 0. \tag{3.4}$$

Clearly this can also be written as $2\sum_{k=1}^{\infty}(k^2 - \kappa_1^2\beta k^{-2})a_k^2 = 0$, but the notation (3.4) will be more convenient since it mirrors the two-dimensional setup below. For the 2D hexagonal spot problem, we set $\ell_1 = \kappa_2^{1/2}$ and $\ell_2 = 3^{-1/2}\kappa_2^{1/2}$, and solve

$$\Delta_2^2 u_2 + \kappa_2\Delta_2[u_2 - \mu u_2^3] + \kappa_2^2\beta(u_2 - 1) = 0, \quad \text{with} \quad \Delta_2 = \frac{\partial^2}{\partial x_1^2} + 3\frac{\partial^2}{\partial x_2^2}. \tag{3.5}$$

The energy is now

$$E_2(u_2) = \frac{1}{4\pi^2}\int_0^{2\pi}\int_0^{2\pi} \frac{1}{2\kappa_2}|\nabla_2 u_2(x)|^2 - \frac{1}{2}u_2(x)^2 + \frac{\mu}{4}u_2(x)^4 + \frac{\kappa_2\beta}{2}|\nabla_2\phi_2(x)|^2\,dx,$$

with $\nabla_2 = (\frac{\partial}{\partial x_1}, \sqrt{3}\frac{\partial}{\partial x_2})^T$ and $-\Delta_2\phi_2 = u_2 - 1$. Hence $\frac{\partial E_2}{\partial \kappa_2} = 0$ corresponds to

$$\int_0^{2\pi}\int_0^{2\pi} \frac{1}{2\kappa_2^2}|\nabla_2 u_2(x)|^2 - \frac{\beta}{2}|\nabla_2\phi_2(x)|^2\,dx_1 dx_2 = 0.$$

Writing

$$u_2 = \sum_{m_1=-\infty}^{\infty}\sum_{m_2=-\infty}^{\infty} b_{m_1,m_2}e^{im_1x_1}e^{im_2x_2} \tag{3.6}$$

with $b_{-m_1,m_2} = b_{m_1,-m_2} = b_{-m_1,-m_2} = b_{m_1,m_2}$, we obtain the equations

$$(m_1^2 + 3m_2^2)^2 b_{m_1,m_2} - \kappa_2(m_1^2 + 3m_2^2)[b_{m_1,m_2} - \mu\langle b^3\rangle_{m_1,m_2}] + \kappa_2^2\beta b_{m_1,m_2} = 0 \tag{3.7}$$

for the Fourier coefficients with $(m_1, m_2) \in \mathbb{N}^2 \setminus (0,0)$, and $b_{0,0} = 1$, as well as the optimal domain size condition

$$\sum_{(m_1,m_2)\in\mathbb{Z}^2\setminus(0,0)} \Big[(m_1^2 + 3m_2^2) - \kappa_2^2\beta(m_1^2 + 3m_2^2)^{-1}\Big]b_{m_1,m_2}^2 = 0. \tag{3.8}$$

Finally, to determine for which value of the parameter μ stripes and hexagonal spots have the same energy we require that

$$E_a[a,\beta,\mu,\kappa_1] - E_b[b,\beta,\mu,\kappa_2] = 0, \tag{3.9}$$

which in Fourier coefficients can be expressed via

$$E_a = \sum_{k\in\mathbb{Z}\setminus 0} \left[\frac{1}{\kappa_1}k^2 - 1 + \kappa_1\beta k^{-2}\right] a_k^2 + \frac{\mu}{2}\left[\langle a^4\rangle_0 - 1\right],$$

$$E_b = \sum_{(m_1,m_2)\in\mathbb{Z}^2\setminus(0,0)} \left[\frac{1}{\kappa_2}(m_1^2+3m_2^2) - 1 + \kappa_2\beta(m_1^2+3m_2^2)^{-1}\right] b_{m_1,m_2}^2 + \frac{\mu}{2}\left[\langle b^4\rangle_{0,0} - 1\right].$$

Here we have introduced a multiplicative factor 2 for algebraic convenience. Moreover, we have subtracted the energy of the uniform state. Hence, energies are calibrated to the reference energy of the uniform state, see also Remark 5.1.

Our problem is to solve the system (3.3)–(3.9) with variables $(\beta,\mu,\kappa_1,\kappa_2,a_k,b_{m_1,m_2})$, with $k\geq 1$ and $(m_1,m_2)\in\mathbb{N}^2\setminus(0,0)$, recalling that $a_0=1$ and $b_{0,0}=1$. This problem has a one parameter family of solutions. To find a numerical approximation of the solution curve, we need to choose a finite dimensional truncation of the problem and perform a pseudo-arclength continuation. Additionally, we need to choose a functional analytic framework to validate these numerical computations.

Remark 3.1. *The hexagonal spot pattern has additional symmetries beyond the ones expressed by the cosine series* (3.6)*. Namely, let*

$$H = \begin{pmatrix} \frac{1}{2} & -\frac{3}{2} \\ \frac{1}{2} & \frac{1}{2} \end{pmatrix},$$

and let $\mathbb{Z}^2_H = \{m\in\mathbb{Z}^2 : m_1+m_2 = \text{even}\}$*. Then H is a linear operator on the sublattice $\mathbb{Z}^2_H$. When we introduce* $B_H = \{(b_m)_{m\in Z^2} : b_m = 0 \text{ for } m\notin\mathbb{Z}^2_H\}$*, then we may define the linear operator $\tilde{H}$ on B_H by $(\tilde{H}b)_m = b_{Hm}$. The action of $\tilde{H}$ on B_H in Fourier space corresponds to a rotation over $\pi/3$ around the origin in physical space. The hexagonal spot patterns are described by $b\in B_H$ with the symmetry $\tilde{H}b = b$ (as well as the periodicity and up-down and left-right symmetry inherited from the cosine series).*

We do not use this additional rotational symmetries in the present paper. We do not attempt to prove that the solutions that we find have this additional symmetries either, but rather leave such an analysis for future research.

Remark 3.2. *Taking into account the rescalings of the spatial variables in this section as well as the geometry of the hexagonal packing, it is not hard to derive that the distance between the stripes is $2\pi\kappa_1^{1/2}\beta^{1/2}$, while the distance between two nearest neighbor spots is $(4/3)^{1/2}\pi\kappa_2^{1/2}\beta^{1/2}$. Both distances are depicted as a function of m in Figure 2.2. We note that at the bifurcation point $(m,\beta) = (0,\frac{1}{4})$ we have $\kappa_1 = 2$ and $\kappa_2 = 8$.*

4 Functional analytic setting: an analytic Fourier space

Rigorous numerics requires a careful balance between computational and analytical simplicity. In this regard we work in an exponentially weighted Fourier space as this will give us the computational advantage of using Fourier methods, control of the tail remainders of our truncated approximations and a good way to bound convolution terms.

The expression

$$\mathbf{m} \stackrel{\text{def}}{=} \left(m_1^2 + 3m_2^2\right)^{1/2}$$

appears throughout in the analysis as the multiplier in Fourier space corresponding to the differential operator Δ_2, see (3.5).

We restrict to Fourier spaces of analytic functions by using exponential weights in the norms:

$$\|a\|_1 \stackrel{\text{def}}{=} \sum_{k\in\mathbb{Z}} |a_k|\, \xi_1^{|k|} \qquad \text{and} \qquad \|b\|_2 \stackrel{\text{def}}{=} \sum_{m\in\mathbb{Z}^2} |b_{m_1,m_2}|\, \xi_2^{|m|}, \tag{4.1}$$

with decay rates $\xi_1 > 1$ and $\xi_2 > 1$ to be chosen later (see Section 9). The norm $|m|$ on $\mathbb{Z}^2$ (appearing in $\|\cdot\|_2$ above) is chosen to have the symmetry $|(m_1,m_2)| = |(-m_1,m_2)|$, that fits well the cosine series (3.6). Specifically, we have used both the 1-norm $|m| \equiv |m_1| + |m_2|$ and the ∞-norm $|m| \equiv \max\{|m_1|,|m_2|\}$, ultimately settling (somewhat arbitrarily) on the 1-norm in the final proof.

The Banach spaces corresponding to the norms in (4.1) are denoted $X_1^{\exp}$ and $X_2^{\exp}$. Since the weights are exponentially growing, any point in $X_1^{\exp}$ or $X_2^{\exp}$ correspond to a smooth symmetric function via (3.2) or (3.6), respectively.

The norms on $X_{1,2}^{\exp}$ behave nicely under the convolution namely as a Banach algebras:

$$\|\langle a\tilde{a}\rangle\|_1 \le \|a\|_1 \cdot \|\tilde{a}\|_1 \qquad \text{and} \qquad \|\langle b\tilde{b}\rangle\|_2 \le \|b\|_2 \cdot \|\tilde{b}\|_2. \tag{4.2}$$

Here we have used that $|m|$, being a norm, satisfies the triangle inequality.

We work in affine subspaces and define the symmetric spaces

$$X_1^{\text{sym}} \stackrel{\text{def}}{=} \{a \in X_1^{\exp} : a_{-k} = a_k \text{ for all } k \in \mathbb{Z}\},$$
$$X_2^{\text{sym}} \stackrel{\text{def}}{=} \{b \in X_2^{\exp} : b_{m_1,m_2} = b_{|m_1|,|m_2|} \text{ for all } m \in \mathbb{Z}^2\}$$

and

$$X_1^1 \stackrel{\text{def}}{=} \{a \in X_1^{\text{sym}} : a_0 = 1\} \qquad\qquad X_1^0 \stackrel{\text{def}}{=} \{v^a \in X_1^{\text{sym}} : v_0^a = 0\}$$
$$X_2^1 \stackrel{\text{def}}{=} \{b \in X_2^{\text{sym}} : b_0 = 1\} \qquad\qquad X_2^0 \stackrel{\text{def}}{=} \{v^b \in X_2^{\text{sym}} : v_0^b = 0\}.$$

The spaces X_i^1 are the (affine) spaces where our variables live, whereas the variations live in the linear spaces X_i^0. The spaces X_1^1, X_1^0 and X_2^1, X_2^0 are hyperplanes in X_1^{sym} and X_2^{sym} respectively. These hyperplanes have a_0 and $b_{0,0}$ fixed due to the mass constraint in our problem. We define the sets

$$\mathbb{N}_0 \stackrel{\text{def}}{=} \mathbb{N} \setminus 0, \qquad \mathbb{Z}_0 \stackrel{\text{def}}{=} \mathbb{Z} \setminus 0, \qquad \mathbb{N}_0^2 \stackrel{\text{def}}{=} \mathbb{N}^2 \setminus (0,0), \qquad \mathbb{Z}_0^2 \stackrel{\text{def}}{=} \mathbb{Z}^2 \setminus (0,0).$$

It will also be useful to interpret $a \in X_1^{\exp}$ and $b \in X_2^{\exp}$ as linear operators, i.e., as elements of the dual space. Since $X_{1,2}^{\exp}$ are weighted l^1 spaces, their dual spaces are weighted l^∞ spaces. We will need the following variants:

$$\|a\|_1^* \stackrel{\text{def}}{=} \sup_{k\in\mathbb{Z}} |a_k|\xi_1^{-|k|} \qquad \text{so that } \Big|\textstyle\sum_{k\in\mathbb{Z}} a_k\phi_k\Big| \le \|a\|_1^* \cdot \|\phi\|_1 \quad \text{for all } \phi \in X_1^{\exp},$$
$$\|a\|_1^{*\text{s}} \stackrel{\text{def}}{=} \sup_{k\in\mathbb{Z}} \tfrac{1}{2}\big(|a_k| + |a_{-k}|\big)\xi_1^{-|k|} \qquad \text{so that } \Big|\textstyle\sum_{k\in\mathbb{Z}} a_k\phi_k\Big| \le \|a\|_1^{*\text{s}} \cdot \|\phi\|_1 \quad \text{for all } \phi \in X_1^{\text{sym}},$$
$$\|a\|_1^{*\text{s}0} \stackrel{\text{def}}{=} \sup_{k\in\mathbb{Z}_0} \tfrac{1}{2}\big(|a_k| + |a_{-k}|\big)\xi_1^{-|k|} \qquad \text{so that } \Big|\textstyle\sum_{k\in\mathbb{Z}} a_k\phi_k\Big| \le \|a\|_1^{*\text{s}0} \cdot \|\phi\|_1 \quad \text{for all } \phi \in X_1^0.$$

We note that $\|a\|_1^{*\text{s}0} \le \|a\|_1^{*\text{s}} \le \|a\|_1^* \le \|a\|_1$.

For $a \in X_1^{\text{sym}}$ the factor $\frac{1}{2}\big(|a_k| + |a_{-k}|\big)$ reduces to $|a_k|$. Hence $\|a\|_1^{*\text{s}} = \|a\|_1^*$ for $a \in X_1^{\text{sym}}$ and $\|a\|_1^{*\text{s}0} = \|a\|_1^{*0}$ for $a \in X_1^{\text{sym}}$, where for convenience we introduce the notation

$$\|a\|_1^{*0} \stackrel{\text{def}}{=} \sup_{k\in\mathbb{N}_0} |a_k|\xi_1^{-k}.$$

The definitions of $\|b\|_2^*$, $\|b\|_2^{*\text{s}}$, $\|b\|_2^{*0}$ and $\|b\|_2^{*\text{s}0}$ are entirely analogous, with $\frac{1}{2}\big(|a_k| + |a_{-k}|\big)\xi_1^{-|k|}$ replaced by

$$\tfrac{1}{4}\big(|b_{m_1,m_2}| + |b_{-m_1,m_2}| + |b_{m_1,-m_2}| + |b_{-m_1,-m_2}|\big)\xi_2^{-|m|},$$

which reduces to $|b_m|$ for $b \in X_2^{\mathrm{sym}}$.

The variables that we will use are $x = (\beta, \mu, \kappa_1, \kappa_2, a, b)$, where $a = (a_k)$, $k \in \mathbb{N}_0$ and $b = (b_m) = (b_{m_1,m_2})$ with $m = (m_1, m_2) \in \mathbb{N}_0^2$. The space of such collections of variables is denoted by $X = \mathbb{R}^4 \times X_1^1 \times X_2^1$. Throughout the paper we will use the notational conventions $a_k = a_{|k|}$ for all $k \in \mathbb{Z}_0$ and $a_0 = 1$, as well as $b_{m_1,m_2} = b_{|m_1|,|m_2|}$ for all $m \in \mathbb{Z}_0^2$ and $b_{0,0} = b_0 = 1$. We use projections $\pi^c x = (\pi_1^c x, \pi_2^c x, \pi_3^c x, \pi_4^c x) = (\beta, \mu, \kappa_1, \kappa_2)$, $a = \pi^a x$, $a_k = \pi_k^a x$, $\pi^b x = b$, $\pi_m^b x = b_m$. On X we use the L^∞ product norm:

$$\|x\| \stackrel{\text{def}}{=} \max\{\|\pi^c x\|_c, \omega_a^{-1}\|\pi^a x\|_1, \omega_b^{-1}\,\|\pi^b x\|_2\},$$
$$\|\pi^c x\|_c \stackrel{\text{def}}{=} \max\{\,\omega_{c,n}^{-1}\,|\pi_n^c x| \,:\, n = 1,2,3,4\},$$

where ω_a, ω_b and $\omega_{c,n}$, $n = 1,2,3,4$ are weights. When clarity is more important than compactness we will use the alternative notation

$$\big(\omega_{c,1}, \omega_{c,2}, \omega_{c,3}, \omega_{c,4}\big) \equiv \big(\omega_\beta, \omega_\mu, \omega_{\kappa_1}, \omega_{\kappa_2}\big).$$

Since we are working in an affine Banach space, it pays of to introduce notation for variations in X, and in particular for the ball of radius 1 in the tangent space $TX \cong \mathbb{R}^4 \times X_1^0 \times X_2^0$, i.e. $\mathcal{B} = \{v \in TX \,:\, \|v\| \le 1\}$, which is characterized by

$$v = (v^c, v^a, v^b) \in \mathcal{B} \Leftrightarrow \begin{cases} |v_n^c| \le \omega_{c,n},\ n = 1,2,3,4 \\ v_0^a = 0,\ v_{-k}^a = v_k^a,\ \|v^a\|_1 \le \omega_a \\ v_0^b = 0,\ v_{m_1,m_2}^b = v_{|m_1|,|m_2|}^b,\ \|v^b\|_2 \le \omega_b. \end{cases} \tag{4.3}$$

Throughout we use the notation

$$\pi^a v = v^a, \qquad \pi^b v = v^b, \qquad \pi^c v = (v_\beta, v_\mu, v_{\kappa_1}, v_{\kappa_2}),$$

and assume the symmetries $v_{-k}^a = v_k^a$ and $v_{m_1,m_2}^b = v_{|m_1|,|m_2|}^b$. Furthermore, we use the convention $v_0^a = 0$ and $v_0^b = 0$.

Remark 4.1. *The characterisation of the dual spaces is helpful when estimating convolution terms of the form $\langle ay^a\rangle_k$ and $\langle by^b\rangle_m$ uniformly for and $\|y^a\|_1 \le 1$, $\|y^b\|_2 \le 1$.*

(i) Let $a, y^a \in X_1^{\exp}$ with $\|y^a\|_1 \le 1$. Then $|\langle ay^a\rangle_0| \le \|a\|_1^*$, which improves to $|\langle ay^a\rangle_0| \le \|a\|_1^{*\mathrm{s}}$ and $|\langle a\tilde{y}^a\rangle_0| \le \|a\|_1^{*\mathrm{s}0}$ for $y^a \in X_1^{\mathrm{sym}}$ and $\tilde{y}^a \in X_1^0$, respectively. If $a \in X_1^{\mathrm{sym}}$ then the expression for $\|a\|_1^{*\mathrm{s}}$ reduces further, as mentioned above.

(ii) To estimate $\langle ay^a\rangle_k$ for $k \neq 0$ we first note that $\langle ay^a\rangle_k = \langle(\sigma_{-k}a)y^a\rangle_0$, where the shift operator is defined via

$$(\sigma_k a)_{k'} \stackrel{\text{def}}{=} a_{k'-k} \qquad \text{and} \qquad (\sigma_m b)_{m'} \stackrel{\text{def}}{=} b_{m'-m}\,.$$

We then use the estimates from part (i) of this remark to obtain $|\langle ay^a\rangle_k| \le \|\sigma_{-k}a\|_1^*$ for all $y^a \in X_1^{\exp}$ with $\|y^a\|_1 \le 1$. This improves to $|\langle ay^a\rangle_0| \le \|\sigma_{-k}a\|_1^{*\mathrm{s}}$ and $|\langle a\tilde{y}^a\rangle_0| \le \|\sigma_{-k}a\|_1^{*\mathrm{s}0}$. for $y^a \in X_1^{\mathrm{sym}}$ and $\tilde{y}^a \in X_1^0$, respectively. We note that $\|\sigma_{-k}a\|_1^{*\circ} = \|\sigma_k a\|_1^{*\circ}$ for $a \in X_1^{\mathrm{sym}}$ and any of the three dual norms ($*\circ = *, *\mathrm{s}, *\mathrm{s}0$). However, clearly $\sigma_{-k}a \notin X_1^{\mathrm{sym}}$ for $k \neq 0$. The estimates for $|\langle by^b\rangle_0|$ are analogous.

(iii) Finally, we note that

$$\|\sigma_k a\|_1^{*\mathrm{s}0} \le \|\sigma_k a\|_1^{*\mathrm{s}} \le \|\sigma_k a\|_1^* \le \|a\|_1 \xi_1^{-|k|}, \tag{4.4}$$

and similarly for $\sigma_m b$ (using the triangle inequality for $|m|$). This gives rougher, but computationally simpler, estimates. In Remark A.1 we return to the issue of balancing computation time and sharpness of the estimates.

(iv) For notational simplicity *we will use the estimates $|a_k| \le \|a\|_1 \xi_1^{-k}$ for all $k \ge 0$ and $|b_m| \le \|b\|_2 \xi_2^{-|m|}$ for all $m \in \mathbb{N}^2$ throughout. Clearly, for $a \in X_1^{\mathrm{sym}}$ this could be improved to $|a_k| \le \frac{1}{2}\|a\|_1 \xi_1^{-k}$ for $k \ge 1$, but not for $k = 0$. A similar improvement can be made for $b \in X_2^{\mathrm{sym}}$. However, in the present paper, which is heavy on notation already, we choose to give up some sharpness in the bounds in favour of notational convenience.*

5 The continuation problem in Fourier space

With the formulation and the spaces well in hand we are now able to set up the problem for numerical solution. We look for a curve of solutions $x \in X$ such that $\widehat{f}(x) = 0$, where

$$\widehat{f} \stackrel{\text{def}}{=} (f_2^c, f_3^c, f_5^c, f^a, f^b),$$

with f_n^c, $n = 2, 3, 4$ and $f^a = (f_k^a)_{k \in \mathbb{N}_0}$ and $f^b = (f_m^b)_{m \in \mathbb{N}_0^2}$ defined below. To perform continuation we will append an equation $f_1^c = 0$ to $\widehat{f}$, i.e. $f \stackrel{\text{def}}{=} (f_1^c, \widehat{f}) = (f_n^c, f_k^a, f_m^b)$, so that the problem $f(x) = 0$ has a locally unique solution.

To be precise, for $k \in \mathbb{N}_0$

$$f_k^a \stackrel{\text{def}}{=} k^4 a_k - \kappa_1 k^2 [a_k - \mu \langle a^3 \rangle_k] + \kappa_1^2 \beta a_k,$$

and for $m \in \mathbb{N}_0^2$

$$f_m^b \stackrel{\text{def}}{=} \mathbf{m}^4 b_m - \kappa_2 \mathbf{m}^2 [b_m - \mu \langle b^3 \rangle_m] + \kappa_2^2 \beta b_m.$$

Furthermore

$$f_2^c \stackrel{\text{def}}{=} E_a - E_b = \sum_{k \in \mathbb{Z}_0} \left[\frac{1}{\kappa_1} k^2 - 1 + \kappa_1 \beta k^{-2} \right] a_k^2 + \frac{\mu}{2} \left[\langle a^4 \rangle_0 - 1 \right]$$
$$- \left\{ \sum_{m \in \mathbb{Z}_0^2} \left[\frac{1}{\kappa_2} \mathbf{m}^2 - 1 + \kappa_2 \beta \mathbf{m}^{-2} \right] b_m^2 + \frac{\mu}{2} \left[\langle b^4 \rangle_0 - 1 \right] \right\},$$

and

$$f_3^c \stackrel{\text{def}}{=} \sum_{k \in \mathbb{Z}_0} (k^2 - \kappa_1^2 \beta k^{-2}) a_k^2,$$
$$f_4^c \stackrel{\text{def}}{=} \sum_{m \in \mathbb{Z}_0^2} (\mathbf{m}^2 - \kappa_2^2 \beta \mathbf{m}^{-2}) b_m^2.$$

We will do our computations in the context of pseudo-arclength continuation. In particular, we assume we have two numerical zeros x_1 and x_2 of $\widehat{f}$ and set

$$\overline{x} \stackrel{\text{def}}{=} \frac{x_1 + x_2}{2} \qquad \text{and} \qquad \underline{x} \stackrel{\text{def}}{=} \frac{x_2 - x_1}{2},$$

so that

$$\widehat{x}(s) \stackrel{\text{def}}{=} \overline{x} + s\, \underline{x} = \tfrac{1-s}{2} x_1 + \tfrac{1+s}{2} x_2 \qquad \text{with } s \in [-1, 1],$$

interpolates linearly between $\overline{x} - \underline{x} = x_1$ and $\overline{x} + \underline{x} = x_2$. We also assume we have two numerical tangent vectors δ_1 and δ_2 (approximately tangent to the solution curve $\{x : \widehat{f}(x) = 0\}$ at x_1 and x_2, respectively). We define $\overline{\delta} \stackrel{\text{def}}{=} (\delta_1 + \delta_2)/2$ and $\underline{\delta} \stackrel{\text{def}}{=} (\delta_2 - \delta_1)/2$, as well as the interpolation

$$\delta(s) \stackrel{\text{def}}{=} \overline{\delta} + s\, \underline{\delta} = \tfrac{1-s}{2} \delta_1 + \tfrac{1+s}{2} \delta_2. \tag{5.1}$$

Then the continuation equation is given by

$$f_1^c \stackrel{\text{def}}{=} (x - \widehat{x}(s), \delta(s))_F = 0, \tag{5.2}$$

where $(\cdot, \cdot)_F$ denotes the standard inner product in the finite dimensional computational subspace X_F of X. In particular $(x, \tilde{x})_F = (x_F, \tilde{x}_F)_F$ in the notation introduced below. We collect all these equations in $f = (f^c, f^a, f^b)$ and we want to solve

$$f(x(s); s) = 0 \in X$$

for some $x(s) \in X$. Here s acts as a parameter (not a variable/unknown), and we will often suppress it in the notation. The derivative Df denotes derivation with respect to x only.

Remark 5.1. *When comparing spots to the uniform state, i.e., the mixed-spots transition described by the outer curve in the bifurcation diagram in Figure 1.1, we still have f^b, f_1^c and f_4^c, we drop f_3^c and f^a, and we simply take $f_2^c = E_b$ instead of $f_2^c = E_a - E_b$.*

Choosing two computational parameters K and M we define the finite dimensional projections: $a_F = (a_k)_{k=1}^K$, $b_F = (b_m)_{m\in\mathbb{N}_0^2, 1\le m_\infty \le M}$, where we choose

$$m_\infty \stackrel{\text{def}}{=} \max\{|m_1|, |m_2|\},$$

since it fits well with the matrix data structure. We set $x_F = (\beta, \mu, \kappa_1, \kappa_2, a_F, b_F) \in X_F = \mathbb{R}^4 \times \mathbb{R}^K \times \mathbb{R}^{M^2+2M}$, and similarly f_F^a, f_F^b and f_F. The dimension of X_F is $N_F \stackrel{\text{def}}{=} 4+K+M^2+2M$.

To transfer from computational space to the full space, we will need the extensions by 0, namely $a_F^0 \in X_1^1$ is defined by

$$(a_F^0)_k = (a_F)_k \text{ for } 1 \le k \le K, \qquad (a_F^0)_k = 0 \text{ for } k > K,$$

and similarly for b_F^0 and x_F^0. Note that $\overline{x}$, $\underline{x}$, $\overline{\delta}$ and $\underline{\delta}$ are all essentially finite dimensional: $\overline{x}_F^0 = \overline{x}$, etc.

For the approximate solution $\overline{x} = (\overline{\beta}, \overline{\mu}, \overline{\kappa}_1, \overline{\kappa}_2, \overline{a}, \overline{b})$ we will use in all formulas concerning convolutions the following notational convention: the symmetries $\overline{a}_{-k} = \overline{a}_k$ and $\overline{b}_{\pm m_1, \pm m_2} = \overline{b}_{m_1,m_2}$, as well as $\overline{a}_0 = 1$ and $\overline{b}_{0,0} = 1$. For $\underline{x}$ we use the same convention.

To conclude this notational agony, we introduce the complementary infinite dimensional projections $a_\infty = (a_k)_{k=K+1}^\infty$, and similarly b_∞ and x_∞. The extensions by 0 in the finite part are denoted by a_∞^0, b_∞^0 and x_∞^0. In particular, $a = a_F^0 + a_\infty^0$, etc.

6 The fixed point formulation

We now introduce the fixed points operator in X

$$T(x;s) \stackrel{\text{def}}{=} x - Af(x;s).$$

Here A is a linear operator of the form

$$\begin{aligned}(Ax)_F &= A_F x_F \\ (Ax)_\infty &= \Lambda^{-1} x_\infty.\end{aligned}$$

The $N_F \times N_F$ matrix A_F is determined via a computer calculation, namely a numerical (i.e. not exact) inverse of the Jacobian J_F of the finite dimensional map $x_F \to f_F(x_F^0)$). Furthermore, Λ is the diagonal operator on X_∞ given by

$$\begin{aligned}\pi_k^a(\Lambda x_\infty) &= \lambda_k^a \pi_k^a x_\infty, \\ \pi_m^b(\Lambda x_\infty) &= \lambda_m^b \pi_m^b x_\infty,\end{aligned}$$

for $k \ge K+1$ and $m_\infty \ge M+1$, with

$$\begin{aligned}\lambda_k^a &\stackrel{\text{def}}{=} k^4 - \overline{\kappa}_1 k^2 + \overline{\kappa}_1^2 \overline{\beta} \\ \lambda_m^b &\stackrel{\text{def}}{=} \mathbf{m}^4 - \overline{\kappa}_2 \mathbf{m}^2 + \overline{\kappa}_2^2 \overline{\beta}.\end{aligned}$$

Remark 6.1. *We note that λ_k^a and λ_m^b do not depend on the variables, hence A is a constant linear operator (independent of x).*

Note that we will always suppress the dependence of T on s and write $T(x)$ rather than $T(x;s)$. The derivative DT denotes derivation with respect to x only.

To set up the fixed point (contraction) argument on a small ball

$$B_r(\widehat{x}(s)) \stackrel{\text{def}}{=} \widehat{x}(s) + r\mathcal{B},$$

we will construct positive constants $Y = (Y_1^c, Y_2^c, Y_3^c, Y_4^c, Y^a, Y^b) \in X$ and polynomial functions $Z = (Z_1^c, Z_2^c, Z_3^c, Z_4^c, Z^a, Z^b)(r) \in X$ that provide the bounds

$$
\begin{aligned}
|\pi_n^c(T(\widehat{x}(s)) - \widehat{x}(s))| &\le Y_n^c \qquad n = 1,2,3,4 && (6.1a)\\
\|\pi^a(T(\widehat{x}(s)) - \widehat{x}(s))\|_1 &\le Y^a && (6.1b)\\
\|\pi^b(T(\widehat{x}(s)) - \widehat{x}(s))\|_2 &\le Y^b && (6.1c)\\
\sup_{v,w\in\mathcal{B}} \big|\pi_n^c(DT(\widehat{x}(s)+rw)rv)\big| &\le Z_n^c(r) \qquad n = 1,2,3,4 && (6.1d)\\
\sup_{v,w\in\mathcal{B}} \big\|\pi^a(DT(\widehat{x}(s)+rw)rv)\big\|_1 &\le Z^a(r) && (6.1e)\\
\sup_{v,w\in\mathcal{B}} \big\|\pi^b(DT(\widehat{x}(s)+rw)rv)\big\|_2 &\le Z^b(r), && (6.1f)
\end{aligned}
$$

for all $s \in [-1,1]$.

Remark 6.2. *The estimates* (6.1d)-(6.1f) *contain a "trivial" multiplicative factor r compared to the formulation in Section 1.2. We use the above formulation to be consistent with earlier work, see the references below.*

Remark 6.3. *In Sections 7 and 9 it may be convenient to think of Y and $Z(r)$ as polynomials in $|s|$. The coefficients of these polynomials are all positive, hence the uniform estimates for all $s \in [-1,1]$ are obtained via $Y(s) \le Y(1) \equiv Y$ and $Z(r,s) \le Z(r,1) \equiv Z(r)$. For compactness of notation we will not stipulate the dependence of the bounds on s.*

We need to find a radius r that satisfies the six inequalities

$$
\begin{aligned}
Y_n^c + Z_n^c(r) &< \omega_{c,n} r \qquad n = 1,2,3,4 && (6.2a)\\
Y^a + Z^a(r) &< \omega_a r && (6.2b)\\
Y^b + Z^b(r) &< \omega_b r. && (6.2c)
\end{aligned}
$$

The six inequalities can be verified rigorously via interval arithmetic. Since we will find bounds Z that depend quadratically on r, the information in (6.2) can be reformulated in terms of so-called radii polynomials, see Section 9. We stress that this approach is not new and has been adopted for a variety of problems in both dynamical systems [13, 33, 32, 18] and PDES [15, 16, 6].

The line piece interpolating the "numerical solutions" x_1 and x_2 represents a solution curve in the following precise sense:

Lemma 6.1. *Assume there exists an $r > 0$ such that the inequalities* (6.2) *hold for all $s \in [-1,1]$. Then there exists a smooth map $\chi : [-1,1] \to X$ such that $f(\chi(s); s) = 0$. In particular, χ parametrizes a continuous curve of zeros of $\widehat{f}$, i.e. $\widehat{f}(\chi(s)) = 0$ for all $s \in [-1,1]$. Furthermore, χ is unique in the sense that for each $s \in [-1,1]$ the only solution of $f(x; s) = 0$ in $B_r(\widehat{x}(s))$ is given by $x = \chi(s)$.*

Proof. It is not hard to infer that the inequalities (6.2) imply that for each $s \in [-1,1]$ the map T is a contraction on $B_r(\widehat{x}(s))$, with contraction rate uniform in s. The uniform contraction theorem then implies the existence a unique smooth map χ of fixed points of T given by $x = \chi(s)$, $s \in [-1,1]$. More details can be found in e.g. [34, 5]. The fixed points correspond to a solution curve of f, and hence of $\widehat{f}$, since A (and especially A_F) is injective. Indeed, the inequalities (6.2) imply that $\|DT(\overline{x})\| = \|I - ADf(\overline{x})\| < 1$, hence in particular $\|I_{N_F} - A_F J_F\| < 1$, from which we infer that A_F is invertible. Here we have used that J_F, which is defined as the Jacobian of $x_F \to f_F(x_F^0; 0)$ evaluated at $x_F = \overline{x}_F$, is also characterized by $Df(\overline{x})v_F^0 = J_F v_F$ for all $v \in \mathcal{B}$. $\square$

We need to verify an additional inequality to conclude that the solution curve is smooth and hence no bifurcation occurs. We define

$$
\begin{aligned}
\tau_1 &\stackrel{\text{def}}{=} \sum_{n=1}^{4} \omega_{c,n} \pi_n^c |\underline{\delta}| + \omega_a \|\pi^a \underline{\delta}\|_1^{0*} + \omega_b \|\pi^b \underline{\delta}\|_2^{0*},\\
\tau_2 &\stackrel{\text{def}}{=} \min\big\{ \big(\underline{x}, \overline{\delta} - \underline{\delta}\big)_F, \big(\underline{x}, \overline{\delta} + \underline{\delta}\big)_F \big\},
\end{aligned}
$$

which can be computed using interval arithmetic. We note that $\tau_1 = Q_1^c$, where the latter is defined in (A.6). The values of τ_1 and τ_2 are both expected to be on the order of the step size, since $\underline{x}$ and $\overline{\delta} \pm \underline{\delta}$ are almost parallel.

Lemma 6.2. *Assume there exists an $r > 0$ such that the inequalities (6.2) hold for all $s \in [-1, 1]$. If, in addition, $r\tau_1 - \tau_2 < 0$, then the solution curve χ obtained in Lemma 6.1 is a smooth curve: $\frac{d\chi}{ds} \not\equiv 0$ for $s \in [-1, 1]$. Furthermore, the curve is locally unique in the sense that for any $s \in (-1, 1)$ all solutions of $\widehat{f}(x) = 0$ in a sufficiently small neighborhood of $x = \chi(s)$ lie on the curve χ. The dimension of the null space of $D\widehat{f}(\chi(s))$ is 1 for all $s \in [-1, 1]$.*

Proof. We adapt the construction in [34, Lemma 10] to our setting. By differentiating the identity $f_1^c(\chi(s), s) = 0$ with respect to s we obtain

$$\left(\tfrac{d\chi}{ds}, \delta(s)\right)_F = \left(\underline{x}, \delta(s)\right)_F - (\chi(s) - \widehat{x}(s), \underline{\delta})_F. \tag{6.3}$$

The terms in the right hand side can be estimated by

$$\left(\underline{x}, \delta(s)\right)_F \geq \tau_2 \qquad \text{and} \qquad \left(\chi(s) - \widehat{x}(s), \underline{\delta}\right)_F \leq r\tau_1,$$

since $\chi(s) \in B_r(\widehat{x}(s))$. Here we have used the characterization of the dual space of $X^0_{1,2}$. Combining these estimates with (6.3) and using that $\tau_2 - r\tau_1 > 0$, we conclude that $\frac{d\chi}{ds} \not\equiv 0$. For additional details on the assertion about regularity of the curve we refer to [5, Corollary 2]. $\square$

We now glue two piece of curve together. Let x_1, x_2 and x_3 be three numerical approximations of solutions, with corresponding predictors δ_1, δ_2 and δ_3. Let $\widehat{x}_1(s)$ be the interpolation between x_1 and x_2, and let $\widehat{x}_2(s)$ be the interpolation between x_2 and x_3. Let χ_1 and χ_2 be the parameterization of the solution curves for the interpolations $\widehat{x}_1$ between $\widehat{x}_2$, respectively, using the corresponding interpolations of the predictors. We define the union

$$\chi_{1,2}(s) \stackrel{\text{def}}{=} \begin{cases} \chi_1(s-1) & \text{for } s \in [-2, 0], \\ \chi_2(s+1) & \text{for } s \in (0, 2]. \end{cases}$$

Lemma 6.3. *Let χ_1 and χ_2 be obtained through Lemma 6.1 as described above. Then $\chi_{1,2}$ is continuous. If, in addition, Lemma 6.2 is applicable for both χ_1 and χ_2, then $\chi_{1,2}$ defines a smooth curve.*

Proof. Let $T_1(x; s) = x - A_1 f_1(x; s)$ and $T_2(x; s) = x - A_2 f_2(x; s)$ be the fixed point maps for the two interpolations. Then the fixed points of $T^1(x; 1)$ and $T^2(x; -1)$ coincide, since $f_1(x; 1) = f_2(x; -1)$. It follows immediately from the uniqueness statement in Lemma 6.1 that $\chi_1(1) = \chi_2(-1)$, since the two balls around x_2 on which T_1 and T_2 are contractions are necessarily nested. Hence the union of the curves is continuous. Smoothness of the union then follows from Lemma 6.2 and the fact that the solution curves can be extended to open intervals slightly larger than $[-1, 1]$ due to the strictness of the inequalities (6.2). These slightly extended smooth curves χ_1 and χ_2 have an overlap with nonempty interior, hence the union is smooth. For a detailed proof we refer to [5, Theorem 6] $\square$

Remark 6.4. *Let us discuss what to do when the computational parameters are different for the two steps in which the pieces of parametrized solution curves χ_1 and χ_2 are determined.*

1. *If the weights ω are different for the two steps, then an additional check has to be performed to guarantee that $\chi_1(1) = \chi_2(-1)$. In particular, one needs to check that there are* nested *balls around x_2 on which T^1 and T^2 contract. Namely, let the inequalities (6.2) hold on intervals $r \in [r^1_{\min}, r^1_{\max}]$ and $r \in [r^2_{\min}, r^2_{\max}]$ for χ_1 and χ_2, respectively. Let $\omega^1 = (\omega^1_j)$ and $\omega^2 = (\omega^2_j)$, $j = 1, \ldots, 6$ be the weights used for χ_1 and χ_2. Then one needs to verify that either the six inequalities*

$$\omega^1_j r^1_{\min} < \omega^2_j r^2_{\max}, \quad j = 1, \ldots, 6 \qquad \text{or} \qquad \omega^1_j r^1_{\max} > \omega^2_j r^2_{\min}, \quad j = 1, \ldots, 6 \tag{6.4}$$

hold.

2. *Furthermore, if the above direct verification fails, one may perform an extra intermediate computation at x_2 with the two different sets of computational parameters. Namely, one may set up a contraction problem $\tilde{T}$ at $\overline{x} = x_2$ with $\underline{x} = 0$. One then works for a single $\tilde{T}$ with the two sets of parameter values used to find χ_1 and χ_2. This leads to (relatively large) intervals $r \in [\tilde{r}^1_{\min}, \tilde{r}^1_{\max}]$ and $r \in [\tilde{r}^2_{\min}, \tilde{r}^2_{\max}]$ where the inequalities (6.2) hold for $\tilde{T}^1 = \tilde{T}^2 = \tilde{T}$ with weights ω^1 and ω^2, respectively. One may then verify (6.4) with these $\tilde{r}^{1,2}_{\min,\max}$, to conclude that there are nested contracting balls for $\tilde{T}^1$ and $\tilde{T}^2$. Since the contracting balls for $T^1(x;1)$ and $\tilde{T}^1$ are necessarily nested, as are those for $T^2(x;-1)$ and $\tilde{T}^2$, one then concludes that $\chi_1(1) = \chi_2(-1)$. We note that in practice we never needed to perform this intermediate step in our final computation of the solution curve.*

3. *An analogous check should be performed when changing $\xi_{1,2}$ between steps, but we did not pursue that here.*

4. *The computational constants K and M may change from step to step as long as at the "midpoint" the smaller of the values are used for x_2 and δ_2.*

7 Structure of the estimates

In this section we discuss the structure of the estimates that are need to find the bounds in (6.1). Explicit expressions for the constants defined here are given in Appendix A.

7.1 bounds Y

For the componentwise estimates we use the notation

$$\begin{aligned} |\pi^c_n(T(\widehat{x}(s)) - \widehat{x}(s))| &\le \bar{Y}^c_n \qquad && n = 1,2,3,4 \\ |\pi^a_k(T(\widehat{x}(s)) - \widehat{x}(s))| &\le \bar{Y}^a_k \qquad && k \ge 1 \\ |\pi^b_m(T(\widehat{x}(s)) - \widehat{x}(s))| &\le \bar{Y}^b_m \qquad && m \in \mathbb{N}^2_0, \end{aligned}$$

all uniform for $s \in [-1,1]$. The finite part $1 \le n \le 4$, $1 \le k \le K$ and $1 \le m_\infty \le M$ of $\bar{Y}$ is denoted by $\bar{Y}_F$. In particular, $Y^c_n = \bar{Y}^c_n = (\bar{Y}_F)^c_n$.

We first note that for $f^a_k(\widehat{x}(s)) = 0$ for $k \ge 3K+1$ and $f^b_m(\widehat{x}(s)) = 0$ for $m_\infty \ge 3M+1$. Hence we may simply set

$$\bar{Y}^a_k = 0, \qquad \bar{Y}^b_m = 0.$$

The first component of f is the only one that depends on s explicitly, and it needs separate treatment in the estimates. We recall that $\widehat{x}(s) = \overline{x} + s\underline{x}$, and note that, by definition,

$$f^c_1(\widehat{x}(s); s) = 0 \qquad \text{for all } s. \tag{7.1}$$

The other components of f do not explicitly depend on s. The strategy is to expand these as

$$f(\widehat{x}(s)) = f(\overline{x}) + sDf(\overline{x})\underline{x} + \tfrac{1}{2}s^2 C(s), \tag{7.2}$$

with

$$C(s) = 2s^{-2}[f(\widehat{x}(s)) - f(\overline{x}) - sDf(\overline{x})\underline{x}].$$

Note that, in view of (7.1), the first component of $f(\overline{x})$, $Df(\overline{x})\underline{x}$ and $C(s)$ in (7.2) should be read as 0. Furthermore, by the choice of $\underline{x}$ the term $Df_F(\overline{x})\underline{x}$ will be small (and clearly $f_F(\overline{x})$ is also small).

We now want an estimate of the form

$$|A \cdot C(s)| \le S \qquad \text{for all } s \in [-1,1], \tag{7.3}$$

where S is obtained *componentwise* via the remainder formula for Taylor series:

$$S = \max_{\eta \in [\overline{x}-\underline{x}, \overline{x}+\underline{x}]} |A \cdot D^2 f(\eta)(\underline{x}, \underline{x})|. \tag{7.4}$$

Note that the above formula, and similar formulas throughout the paper, should be interpreted as finding some $S \in X$ such that the estimate

$$\max_{\eta \in [\overline{x}-\underline{x}, \overline{x}+\underline{x}]} |A \cdot D^2 f(\eta)(\underline{x}, \underline{x})| \leq S$$

holds componentwise.

Let us make this more explicit. The finite part

$$S_F = \max_{\eta \in [\overline{x}-\underline{x}, \overline{x}+\underline{x}]} |A_F \cdot D^2 f_F(\eta)(\underline{x}, \underline{x})| \tag{7.5}$$

can be determined by simply evaluating $D^2 f_F(\boldsymbol{\eta})$ with $\boldsymbol{\eta} \stackrel{\text{def}}{=} [\overline{x}-\underline{x}, \overline{x}+\underline{x}]$, since these intervals are reasonably small. We then write for the finite part

$$\bar{Y}_F = |\widehat{A}_F \cdot f_F(\overline{x})| + |\widehat{A}_F \cdot Df_F(\overline{x})\underline{x}| + \tfrac{1}{2} S_F,$$

where the matrix

$$(\widehat{A}_F)_{ij} = \begin{cases} 0 & \text{if } j = 1, \\ (A_F)_{ij} & \text{if } j \geq 2, \end{cases}$$

has vanishing first column in view of (7.1). Note that replacing A_F by $\widehat{A}_F$ in (7.5) is irrelevant, since $D^2 f_1^c$ vanishes anyway.

For the intermediate part $K+1 \leq k \leq 3K$ and $M+1 \leq m_\infty \leq 3M$, we obtain

$$S_k^a = \frac{1}{\lambda_k^a} \max_{\eta \in [\overline{x}-\underline{x}, \overline{x}+\underline{x}]} |D^2 f_k^a(\eta)(\underline{x}, \underline{x})| \tag{7.6a}$$

$$S_m^b = \frac{1}{\lambda_m^b} \max_{\eta \in [\overline{x}-\underline{x}, \overline{x}+\underline{x}]} |D^2 f_m^b(\eta)(\underline{x}, \underline{x})|, \tag{7.6b}$$

where each component involves convolution terms only (see Section A.2 for explicit formulas), each of which is a finite sum, and an estimate on the maximum can again be obtained using interval arithmetic with $\boldsymbol{\eta} = [\overline{x}-\underline{x}, \overline{x}+\underline{x}]$. Hence

$$\bar{Y}_k^a = \frac{1}{\lambda_k^a} |f_k^a(\overline{x})| + \frac{1}{\lambda_k^a} |Df_k^a(\overline{x})\underline{x}| + \tfrac{1}{2} S_k^a$$

$$\bar{Y}_m^b = \frac{1}{\lambda_m^b} |f_m^b(\overline{x})| + \frac{1}{\lambda_m^b} |Df_m^b(\overline{x})\underline{x}| + \tfrac{1}{2} S_m^b,$$

for $K+1 \leq k \leq 3K$ and $M+1 \leq m_\infty \leq 3M$, where evaluating $f_k^a(\overline{x})$ and $Df_k^a(\overline{x})\underline{x}$ again involves convolution terms only, each of which is a finite sum (and similarly for f_m^b).

Since $\bar{Y}^a$ and $\bar{Y}^b$ have only finitely many nonzero components, we just compute

$$Y^c = \bar{Y}^c \qquad \text{and} \qquad Y^a = \|\bar{Y}^a\|_1 \qquad \text{and} \qquad Y^b = \|\bar{Y}^b\|_2 .$$

Remark 7.1. *Using the explicit formulas for the first and second derivative of f in Section A the Y can thus be computed directly (without additional estimates) using interval arithmetic. Indeed, interval arithmetic is used not only to control rounding error (this involves very small intervals), but also to efficiently determine (upper bounds on) the maxima in* (7.5) *and* (7.6) *rigorously (involving intervals $\boldsymbol{\eta}$ of intermediate size).*

7.2 bounds Z

In this section we explain how to find bounds on $DT(\widehat{x}(s)+rw)rv$ uniform for $s \in [-1,1]$ and $v, w \in \mathcal{B}$ (defined in (4.3)). We write

$$Df(\widehat{x}(s)+rw)rv = Jrv + [Df(\widehat{x}(s)+rw) - J]rv,$$

where J is an approximate Jacobian defined by

$$\begin{aligned}(Jv)_F &= J_F v_F,\\ \pi^a_k (Jv)_\infty &= \lambda^a_k \pi^a_k v,\\ \pi^b_m (Jv)_\infty &= \lambda^b_m \pi^b_m v.\end{aligned}$$

Hence, J is block-diagonal and purely diagonal in the tail $k \geq K+1$ and $m_\infty \geq M+1$. We recall that J_F is the (exact) Jacobian of the finite dimensional map $x_F \to f_F(x^0_F;0)$, i.e. $J_F v_F = Df_F(\overline{x};0)v^0_F$. In this notation we have

$$DT(\widehat{x}(s)+rw)rv = [I-AJ]rv + A[Df(\widehat{x}(s)+rw)-J]rv, \tag{7.7}$$

where

$$\begin{aligned}([I-AJ]v)_F &= (I-A_F J_F)v_F\\ ([I-AJ]v)_\infty &= 0.\end{aligned}$$

Since A_F is an approximate, numerical inverse of J_F, the term $(I-A_F J_F)v_F$ will be small. In Section A.3 we derive explicit estimates

$$\begin{aligned}\sup_{v\in\mathcal{B}} \pi^c_n([I-A_F J_F]v_F) &\leq O^c_n\\ \sup_{v\in\mathcal{B}} \|\pi^a([I-A_F J_F]v_F)\|_1 &\leq O^a\\ \sup_{v\in\mathcal{B}} \|\pi^b([I-A_F J_F]v_F)\|_2 &\leq O^b.\end{aligned}$$

We move on to the second term in (7.7). Let us again first consider the first component. It is the only one depending explicitly on s:

$$Df^c_1(\widehat{x}(s)+rw;s)rv - \pi^c_1 Jv = r\big(v,\delta(s)\big)_F - r\big(v_F,\overline{\delta}\big)_F = rs\big(v,\underline{\delta}\big)_F, \tag{7.8}$$

since $Df^c_1(x;0)v = (v,\overline{\delta})_F = (v_F,\overline{\delta})_F$. For all other components we write

$$[Df(\widehat{x}(s)+rw)-J]rv = [Df(\widehat{x}(s))-J]rv + r^2R(r,s) = r[Df(\overline{x})-J]v + rs\,Q(s) + r^2R(r,s),$$

where

$$\begin{aligned}\bar{Q}(s,v) &\stackrel{\text{def}}{=} s^{-1}[Df(\overline{x}+s\underline{x})-Df(\overline{x})]v\\ \bar{R}(r,s,v,w) &\stackrel{\text{def}}{=} r^{-1}[Df(\overline{x}+s\underline{x}+rw)-Df(\overline{x}+s\underline{x})]v.\end{aligned}$$

We now want estimates of the form (*notice that we omit A compared to* (7.3))

$$\begin{aligned}[Df(\overline{x}))-J]v &\leq P,\\ |\bar{Q}(s,v)| &\leq Q,\\ |\bar{R}(r,s,v,w)| &\leq R,\end{aligned}$$

for all $s\in[-1,1]$, $0\leq r\leq r_*$, and $v,w\in\mathcal{B}$. Here r_* is an a priori bound on r. The bounds Q and R are once again obtained *componentwise* via the (integral) remainder formulas:

$$P \stackrel{\text{def}}{=} \max_{v\in\mathcal{B}} |[Df(\overline{x})-J]v|, \tag{7.9a}$$

$$Q \stackrel{\text{def}}{=} \max_{\eta\in[\overline{x}-\underline{x},\overline{x}+\underline{x}],v\in\mathcal{B}} |D^2f(\eta)(\underline{x},v)|, \tag{7.9b}$$

$$R \stackrel{\text{def}}{=} \max_{\eta\in[\overline{x}-\underline{x},\overline{x}+\underline{x}],v,w\in\mathcal{B}} \frac{1}{r_*}\left|\int_0^{r_*} D^2f(\eta+rw)(v,w)dr\right|. \tag{7.9c}$$

The choice for the integral remainder formula allows for additional flexibility in obtaining the estimate on R, which we exploit to get slightly better control on the dependence on r_*, see Section A.7. These estimates are noticeably harder than (7.4) because of the presence of $v, w \in \mathcal{B}$. In view of (7.8) one should read the first components as

$$P_1^c = 0 \qquad Q_1^c = \sup_{v\in\mathcal{B}} \left|\left(v, \underline{\delta}\right)_F\right| \qquad \text{and} \qquad R_1^c = 0,$$

where an explicit estimate for Q_1^c will be given in Section A.6.

The main part of the analysis is finding good bounds P, Q and R. Each of these splits along a finite and infinite dimensional part, i.e., $U = U_F^0 + U_\infty^0$ for $U = P, Q, R$. For the infinite dimensional parts we set for $|k| > K$ and $m_\infty > M$

$$\widehat{U}_k^a = \frac{1}{\lambda_k^a} \pi_k^a U_\infty \qquad \text{and} \qquad \widehat{U}_k^b = \frac{1}{\lambda_m^b} \pi_m^b U_\infty$$

for $U = P, Q, R$, and, rather than obtaining component-wise bounds, we bound the norms

$$\|\widehat{U}^a\|_1 \leq U_\infty^a \qquad \text{and} \qquad \|\widehat{U}^b\|_2 \leq U_\infty^b.$$

Once we have those, we can write

$$Z^c = r\,(O^c + \pi^c(|A_F| \cdot P_F)) + r\,\pi^c(|A_F| \cdot Q_F) + r^2\,\pi^c(|A_F| \cdot R_F), \tag{7.10a}$$

as well as

$$\begin{aligned} Z^a = r\,(O^a + \|\pi^a(|A_F| \cdot P_F)\|_1 + P_\infty^a) + r\,(\|\pi^a(|A_F| \cdot Q_F)\|_1 + Q_\infty^a) \\ + r^2\,(\|\pi^a(|A_F| \cdot R_F)\|_1 + R_\infty^a), \end{aligned} \tag{7.10b}$$

$$\begin{aligned} Z^b = r\,(O^b + \|\pi^b(|A_F| \cdot P_F)\|_2 + P_\infty^b) + r\,(\|\pi^b(|A_F| \cdot Q_F)\|_2 + Q_\infty^b) \\ + r^2\,(\|\pi^b(|A_F| \cdot R_F)\|_2 + R_\infty^b). \end{aligned} \tag{7.10c}$$

Remark 7.2. *In this approach we never need to compute more than two derivatives of f. However, to improve the estimates, we occasionally, namely for convolution terms, implicitly use a third derivative, see Section A.7.*

Remark 7.3. *We use the triangle inequality to split the estimate of, for example, $(A[Df(\overline{x}) - J]v)_F$ into an estimate P_F for $|([Df(\overline{x}) - J]v)_F|$ and a componentwise estimate $|A_F|$. One could postpone using the triangle inequality until after the multiplication by A_F, thus sharpening the estimate, but we did not pursue this in the present paper.*

8 Setup for the limit $\mu \to 0$

The problem is highly degenerate at $\mu = 0$. We need to rescale to obtain a sensible problem in the limit $\mu \to 0$, i.e., a problem with a nontrivial isolated solution at $\mu = 0$. In this section we describe how to set up the desingularized limit problem. We focus on the differences with the general case only, and do not go into details about the parts of the construction that are completely analogous.

8.1 The rescaled variables

We rescale

$$\begin{aligned} \beta(\mu, \tilde{\beta}) &\stackrel{\text{def}}{=} \frac{1}{4} + \mu\tilde{\beta} \\ \kappa_1(\mu, \tilde{\kappa}_1) &\stackrel{\text{def}}{=} 2 + \mu\tilde{\kappa}_1 \\ \kappa_2(\mu, \tilde{\kappa}_2) &\stackrel{\text{def}}{=} 8 + \mu\tilde{\kappa}_2. \end{aligned}$$

Note that we will keep using both κ_1 and $\tilde{\kappa}_1$, etcetera, in the notation, since this makes the notation more compact, hence one has to read carefully to distinguish between them. In this scaling there are a few special modes in the singular limit, which we identify by

$$\mathcal{I}^1 \stackrel{\text{def}}{=} \{-1,0,1\}$$
$$\mathcal{I}^2 \stackrel{\text{def}}{=} \{(0,0),(1,1),(-1,-1),(-1,1),(1,-1),(2,0),(-2,0)\},$$

and we define their complements

$$\mathbb{Z}_1 \stackrel{\text{def}}{=} \mathbb{Z} \setminus \mathcal{I}^1 \qquad \mathbb{N}_1 \stackrel{\text{def}}{=} \mathbb{Z} \cap \mathbb{N}$$
$$\mathbb{Z}_1^2 \stackrel{\text{def}}{=} \mathbb{Z}^2 \setminus \mathcal{I}^2 \qquad \mathbb{N}_1^2 \stackrel{\text{def}}{=} \mathbb{Z}_1^2 \cap \mathbb{N}^2.$$

Since we need to rescale the components $a_k \to \mu \tilde{a}_k$ for $k \in \mathbb{Z}_1$ and $b_m \to \mu \tilde{b}_m$ for $m \in \mathbb{Z}_1^2$, but not the components with index in $\mathcal{I}^1$ and $\mathcal{I}^2$, we introduce the orthogonal splitting

$$a = \hat{a} + \mu \tilde{a} \qquad \text{and} \qquad b = \hat{b} + \mu \tilde{b},$$

where

$$\begin{aligned}
\hat{a}_k &= 0 \quad \text{for } k \notin \mathcal{I}^1 \qquad \text{and } \hat{a}_0 = 1\\
\tilde{a}_k &= 0 \quad \text{for } k \in \mathcal{I}^1\\
\hat{b}_m &= 0 \quad \text{for } m \notin \mathcal{I}^2 \qquad \text{and } \hat{b}_0 = 1\\
\tilde{b}_m &= 0 \quad \text{for } m \in \mathcal{I}^2.
\end{aligned}$$

We assume symmetry throughout, and we write

$$\hat{b}_1 \equiv \hat{b}_{(1,1)} \qquad \text{and} \qquad \hat{b}_2 \equiv \hat{b}_{(2,0)}.$$

Instead of pseudo-arclength continuation, we simply perform a single parameter continuation step in the parameter μ, starting from $\mu = 0$. Since μ is thus a parameter, the variables are $x = (\tilde{\beta}, \tilde{\kappa}_1, \tilde{\kappa}_2, \hat{a}_1, \hat{b}_1, \hat{b}_2, \tilde{a}, \tilde{b})$, which form a Banach space with norm

$$\|x\| = \max\big\{\|(\tilde{\beta}, \tilde{\kappa}_1, \tilde{\kappa}_2, \hat{a}_1, \hat{b}_1, \hat{b}_2)\|_\infty, \omega_{\tilde{a}}^{-1}\|\tilde{a}\|_1, \omega_{\tilde{b}}^{-1}\|\tilde{b}\|_2\big\}$$
$$\|(\tilde{\beta}, \tilde{\kappa}_1, \tilde{\kappa}_2, \hat{a}_1, \hat{b}_1, \hat{b}_2)\|_\infty \stackrel{\text{def}}{=} \max\big\{\omega_{\tilde{\beta}}^{-1}|\tilde{\beta}|, \omega_{\tilde{\kappa}_1}^{-1}|\tilde{\kappa}_1|, \omega_{\tilde{\kappa}_2}^{-1}|\tilde{\kappa}_2|, \omega_{\hat{a}}^{-1}|\hat{a}_1|, \omega_{\hat{b}}^{-1}|\hat{b}_1|, \omega_{\hat{b}}^{-1}|\hat{b}_2|\big\}.$$

In this limit problem we have decided to use the norm $|m| \equiv |m_1| + |m_2|$ in the decay rates for the $\|\cdot\|_2$. The corresponding projections are denoted by $\pi^{\tilde{c}} x = (\tilde{\beta}, \tilde{\kappa}_1, \tilde{\kappa}_2, \hat{a}_1, \hat{b}_1, \hat{b}_2) \in \mathbb{R}^6$, $\pi^{\tilde{a}} x = \tilde{a} \in \tilde{X}_1^0$ and $\pi^{\tilde{b}} x = \tilde{b} \in \tilde{X}_2^0$. The ball of radius 1 in the tangent space is given explicitly by

$$v = (v^{\tilde{c}}, v^{\tilde{a}}, v^{\tilde{b}}) \in \widetilde{\mathcal{B}} \Leftrightarrow \begin{cases} |v_n^{\tilde{c}}| \leq \omega_{\tilde{c},n},\ n = 2,3,4,5,6,7 \\ v_0^{\tilde{a}} = 0,\ v_1^{\tilde{a}} = 0,\ v_{-k}^{\tilde{a}} = v_k^{\tilde{a}},\ \|v^{\tilde{a}}\|_1 \leq \omega_{\tilde{a}} \\ v_0^{\tilde{b}} = 0,\ v_{(1,1)}^{\tilde{b}} = 0,\ v_{(2,0)}^{\tilde{b}},\ v_{(m_1,m_2)}^{\tilde{b}} = v_{(|m_1|,|m_2|)}^{\tilde{b}},\ \|v^{\tilde{b}}\|_2 \leq \omega_{\tilde{b}}, \end{cases} \tag{8.1}$$

where $(\omega_{\tilde{c},n})_{n=2}^7 = (\omega_{\tilde{\beta}}, \omega_{\tilde{\kappa}_1}, \omega_{\tilde{\kappa}_2}, \omega_{\hat{a}}, \omega_{\hat{b}}, \omega_{\hat{b}})$. We will write $v^a = v^{\hat{a}} + \mu v^{\tilde{a}}$ throughout, where $v_1^{\hat{a}} = \pi_5^{\tilde{c}} v$ and $v^{\tilde{a}} = \pi^{\tilde{a}} v$, and similarly $v^b = v^{\hat{b}} + \mu v^{\tilde{b}}$. For $v \in \widetilde{\mathcal{B}}$ we have

$$\|v^a\|_1 = \|v^{\hat{a}}\|_1 + \mu\|v^{\tilde{a}}\|_1 = 2|v_1^{\hat{a}}|\xi_1 + \mu\|v^{\tilde{a}}\|_1 \tag{8.2a}$$
$$\|v^b\|_2 = \|v^{\hat{b}}\|_2 + \mu\|v^{\tilde{b}}\|_2 = (4|v_1^{\hat{b}}| + 2|v_2^{\hat{b}}|)\xi_2^2 + \mu\|v^{\tilde{b}}\|_2, \tag{8.2b}$$

where choosing the norm $|m| \equiv |m_1| + |m_2|$ in the decay rates for the $\|\cdot\|_2$ leads to the factor ξ_2^2 (it would be slightly different for the choice $|m| \equiv \max\{|m_1|, |m_2|\}$).

We introduce norms on the duals of $\tilde{X}_1^0$ and $\tilde{X}_2^0$:

$$\|\tilde{a}\|_1^{*1} \stackrel{\text{def}}{=} \sup_{k \in \mathbb{N}_1} |\tilde{a}_k| \xi_1^{-k} \qquad \text{and} \qquad \|\tilde{b}\|_2^{*1} \stackrel{\text{def}}{=} \sup_{m \in \mathbb{N}_1^2} |\tilde{b}_m| \xi_2^{-|m|}.$$

Hence, for $v \in \widetilde{\mathcal{B}}$,

$$|\langle av^a\rangle_k| \le |\langle av^{\hat a}\rangle_k| + \mu|\langle av^{\tilde a}\rangle_k| \le \omega_{\hat a}\langle |a|\delta^{\hat a}\rangle_k + \mu\omega_{\tilde a}\|\sigma_k a\|_1^{*1},$$
$$|\langle bv^b\rangle_m| \le |\langle bv^{\hat b}\rangle_m| + \mu|\langle bv^{\tilde b}\rangle_m| \le \omega_{\hat b}\langle |b|\delta^{\hat b}\rangle_m + \mu\omega_{\tilde b}\|\sigma_m b\|_2^{*1},$$

where

$$\delta_k^{\hat a} \stackrel{\text{def}}{=} \begin{cases} 1 & k = \pm 1 \\ 0 & k = 0, k \in \mathbb{Z}_1 \end{cases} \qquad \text{and} \qquad \delta_m^{\hat b} \stackrel{\text{def}}{=} \begin{cases} 1 & m \in \mathcal{I}^2 \setminus 0 \\ 0 & m = 0, m \in \mathbb{Z}_1^2. \end{cases} \tag{8.3}$$

Finally, by using $\|\delta^{\hat a}\|_1 = 2\xi_1$ and $\|\delta^{\hat b}\|_2 = 6\xi_2^2$, one obtains estimates in terms of norms (for $v \in \widetilde{\mathcal{B}}$):

$$\|\langle av^a\rangle\|_1 \le 2\omega_{\hat a}\xi_1\|a\|_1 + \mu\omega_{\tilde a}\|a\|_1, \qquad \text{and} \qquad \|\langle bv^b\rangle\|_2 \le 6\omega_{\hat b}\xi_2^2\|b\|_2 + \mu\omega_{\tilde b}\|b\|_2. \tag{8.4}$$

8.2 The rescaled equations

We rescale the equations, starting with

$$f^a = \mu\tilde f^a \qquad \text{and} \qquad f^b = \mu\tilde f^b,$$

where for $k = 1$

$$\begin{aligned}\tilde f_1^a &= \mu^{-1}\left\{[1 - \kappa_1 + \kappa_1^2\beta]\hat a_1 + \kappa_1\mu\langle a^3\rangle_1\right\} \\ &\stackrel{\text{def}}{=} \left[\kappa_1^2\tilde\beta + \tfrac14\mu\tilde\kappa_1^2\right]\hat a_1 + \kappa_1\langle a^3\rangle_1,\end{aligned}$$

while for $k \in \mathbb{N}_1$

$$\tilde f_k^a \stackrel{\text{def}}{=} \left[k^4 - \kappa_1 k^2 + \kappa_1^2\beta\right]\tilde a_k + \kappa_1 k^2\langle a^3\rangle_k.$$

Similarly, for the special modes $m = (1,1)$ and $m = (2,0)$ we set

$$\begin{aligned}\tilde f_m^b &= \mu^{-1}\left\{[16 - 4\kappa_2 + \kappa_2^2\beta]\hat b_m + 4\kappa_2\mu\langle b^3\rangle_1\right\} \\ &\stackrel{\text{def}}{=} \left[\kappa_2^2\tilde\beta + \tfrac14\mu\tilde\kappa_2^2\right]\hat b_m + 4\kappa_2\langle b^3\rangle_m,\end{aligned}$$

whereas for $m \in \mathbb{N}_1^2$ we have

$$\tilde f_m^b \stackrel{\text{def}}{=} \left[\mathbf{m}^4 - \kappa_2\mathbf{m}^2 + \kappa_2^2\beta\right]\tilde b_m + \kappa_2\mathbf{m}^2\langle b^3\rangle_m.$$

Next, the energy needs to be rescaled: $f_2^c = \mu\tilde f_2^c$ with

$$\begin{aligned}\tilde f_2^c \stackrel{\text{def}}{=} {}& 2\left[\kappa_1\tilde\beta + \tfrac14\mu\kappa_1^{-1}\tilde\kappa_1^2\right]\hat a_1^2 + \mu\sum_{k\in\mathbb{Z}_1}\left[\kappa_1^{-1}k^2 - 1 + \kappa_1\beta k^{-2}\right]\tilde a_k^2 + \frac12\left[\langle a^4\rangle_0 - 1\right] \\ &- \left\{\frac12\left[\kappa_2\tilde\beta + \tfrac14\mu\kappa_2^{-1}\tilde\kappa_2^2\right]\left[2\hat b_1^2 + \hat b_2^2\right] + \mu\sum_{k\in\mathbb{Z}_1^2}\left[\kappa_2^{-1}\mathbf{m}^2 - 1 + \kappa_2\beta\mathbf{m}^{-2}\right]\tilde b_m^2 + \frac12\left[\langle b^4\rangle_0 - 1\right]\right\}\end{aligned}$$

Finally, the energy optimisation (with respect to domain size) equations (3.4) and (3.8) also need to be rescaled by a factor μ:

$$\begin{aligned}\tilde f_3^c &\stackrel{\text{def}}{=} -2\left[\tilde\kappa_1 + \kappa_1^2\tilde\beta + \tfrac14\mu\tilde\kappa_1^2\right]\hat a_1^2 + \mu\sum_{k\in\mathbb{Z}_1}\left(k^2 - \kappa_1^2\beta k^{-2}\right)\tilde a_k^2, \\ \tilde f_4^c &\stackrel{\text{def}}{=} -\frac12\left[4\tilde\kappa_2 + \kappa_2^2\tilde\beta + \tfrac14\mu\tilde\kappa_2^2\right]\left[2\hat b_1^2 + \hat b_2^2\right] + \mu\sum_{m\in\mathbb{Z}_1^2}\left(\mathbf{m}^2 - \kappa_2^2\beta\mathbf{m}^{-2}\right)\tilde b_m^2.\end{aligned}$$

We will do parameter continuation in μ, hence there is *no* f_1^c. We set

$$\tilde{\lambda}_k^{\tilde{a}} \stackrel{\text{def}}{=} k^4 - 2k^2 + 1$$
$$\tilde{\lambda}_m^{\tilde{b}} \stackrel{\text{def}}{=} \mathbf{m}^4 - 8\mathbf{m}^2 + 16,$$

and we define the fixed point map analogously to the general case, i.e.,

$$\tilde{T}(x;\mu) \stackrel{\text{def}}{=} x - \tilde{A}\tilde{f}(x;\mu),$$

where $\tilde{A}$ is a linear operator of the form

$$(\tilde{A}x)_F = \tilde{A}_F x_F$$
$$(\tilde{A}x)_\infty = \tilde{\Lambda}^{-1} x_\infty.$$

8.3 The bounds Y and Z

We focus on the differences with the general case only. We will verify a single step starting at $\mu = 0$. We decompose

$$\tilde{f}(x;\mu) = g(x) + \mu h(x;\mu),$$

and compute Dg, $D^2 g$ and $Dh(x;\mu)$, but not the second derivative of h. To find the bounds Y we write, componentwise,

$$g(\overline{x} + \mu\underline{x};\mu) = g(\overline{x}) + \mu Dg(\overline{x})\underline{x} + \frac{1}{2}\mu^2 D^2 g(\eta)(\underline{x},\underline{x})$$
$$h(\overline{x} + \mu\underline{x};\mu) = \mu h(\overline{x};0) + \mu^2 D_\mu h(\overline{x};\mu') + \mu^2 D_x h(\eta';\mu)\underline{x},$$

for some $\eta, \eta' \in [\overline{x}, \overline{x} + \mu\underline{x}]$ and $\mu' \in [0,\mu]$. Here $\overline{x}$ is an (approximate) zero of g_F, whereas the predictor $\underline{x}$ is approximately a solution of $Dg_F(\overline{x})\underline{x} = -h_F(\overline{x};0)$. As in Section 7.1, it is better to include multiplication by $\tilde{A}_F$ before using the Taylor estimate. In particular, for fixed a priori bound μ_* on μ, we define *componentwise*

$$S_F = \max\bigl\{D^2 g_F(\eta)(\underline{x},\underline{x}) \,:\, \eta \in [\overline{x}, \overline{x} + \mu_*\underline{x}]\bigr\}$$
$$\widetilde{S}_F = \max\bigl\{D_\mu h_F(\overline{x};\mu) \,:\, \mu \in [0,\mu_*]\bigr\}$$
$$\widetilde{\widetilde{S}}_F = \max\bigl\{D_x h_F(\eta;\mu)\underline{x} \,:\, \eta \in [\overline{x}, \overline{x} + \mu_*\underline{x}], \mu \in [0,\mu_*]\bigr\},$$

computed using interval evaluation with intervals $\boldsymbol{\eta} = [\overline{x}, \overline{x} + \mu_*\underline{x}]$ and $\boldsymbol{\mu} = [0,\mu_*]$. Then

$$\bar{Y}_F = \Bigl|\tilde{A}_F \cdot g_F(\overline{x})\Bigr| + \mu\Bigl|\tilde{A}_F \cdot \bigl[Dg_F(\overline{x})\underline{x} + h_F(\overline{x};0)\bigr]\Bigr| + \mu^2\Bigl|\tilde{A}_F \cdot \bigl[\tfrac{1}{2}S_F + \widetilde{S}_F + \widetilde{\widetilde{S}}_F\bigr]\Bigr|.$$

Here μ can still be viewed as a free parameter, although a priori bounded by μ_*. The term linear in μ is small due to the choice of the predictor $\underline{x}$. For $K+1 \le k \le 3K$ and $M+1 \le m_\infty \le 3M$ we set

$$\bar{Y}_k^{\tilde{a}} = \frac{1}{\tilde{\lambda}_k^{\tilde{a}}}\max\bigl\{|g_k^a(\eta) + \mu h_k^a(\eta;\mu)| \,:\, \eta \in [\overline{x}, \overline{x} + \mu_*\underline{x}], \mu \in [0,\mu_*]\bigr\}$$
$$\bar{Y}_m^{\tilde{b}} = \frac{1}{\tilde{\lambda}_m^{\tilde{b}}}\max\bigl\{|g_m^b(\eta) + \mu h_m^b(\eta;\mu)| \,:\, \eta \in [\overline{x}, \overline{x} + \mu_*\underline{x}], \mu \in [0,\mu_*]\bigr\},$$

where the evaluation, which involves the convolution term only, is done using interval arithmetic. As before, $\bar{Y}_k^a = 0$ for $k > 3M$, and $\bar{Y}_m^b = 0$ for $m_\infty > 3M$. Finally, we compute

$$Y^{\tilde{c}} = \bar{Y}^{\tilde{c}} \qquad \text{and} \qquad Y^{\tilde{a}} = \|\bar{Y}^{\tilde{a}}\|_1 \qquad \text{and} \qquad Y^{\tilde{b}} = \|\bar{Y}^{\tilde{b}}\|_2\,.$$

For the Z bounds, we write (again componentwise)

$$[D_x f(\overline{x} + \mu\underline{x} + rw;\mu) - \tilde{J}]rv = [Dg(\overline{x}) - \tilde{J}]rv + \mu r D^2 g(\eta)(v,\underline{x}) + r^2 D^2 g(\zeta)(v,w) + \mu r D_x h(\zeta;\mu)v,$$

with $\zeta = \eta + r\tilde{v}$, where $\eta \in [\overline{x}, \overline{x} + \mu_* \underline{x}]$ and $\tilde{v} \in \widetilde{\mathcal{B}}$. In particular, we set

$$
\begin{aligned}
P &\stackrel{\text{def}}{=} \max\{|[Dg(\overline{x}) - \tilde{J}]v| \,:\, v \in \widetilde{\mathcal{B}}\} \\
Q &\stackrel{\text{def}}{=} \max\{|D^2 g(\eta)(\underline{x}, v)| \,:\, \eta \in [\overline{x}, \overline{x} + \mu_* \underline{x}], v \in \widetilde{\mathcal{B}}\} \\
\widetilde{Q} &\stackrel{\text{def}}{=} \max\{|D_x h(\eta + r_* \tilde{v}; \mu) v| \,:\, \eta \in [\overline{x}, \overline{x} + \mu_* \underline{x}], \mu \in [0, \mu_*], v, \tilde{v} \in \widetilde{\mathcal{B}}\} \\
R &\stackrel{\text{def}}{=} \max\{\left|D^2 g(\eta + r_* \tilde{v})(v, w)\right| \,:\, \eta \in [\overline{x}, \overline{x} + \mu_* \underline{x}], w, v, \tilde{v} \in \widetilde{\mathcal{B}}\}.
\end{aligned}
$$

The computation of O, bounding $(I - \tilde{A}\tilde{J})v$, is easily adapted from Section A.3 to the present setting.

As we will see explicitly in Section B.1, when we choose $K \geq 3$ and $M \geq 6$, then g_F depends on x_F only (and not on x_∞). This implies that $Dg_F(\overline{x})v - \tilde{J}v_F = Dg_F(\overline{x})v^0_\infty = 0$. Furthermore, see Section B.2, $Dg^a_k(x) = \tilde{\lambda}^{\tilde{a}}_k \tilde{a}_k$ for $k > 3$ and $Dg^b_m(x) = \tilde{\lambda}^{\tilde{b}}_m \tilde{b}_m$ for $m_\infty > 6$, hence $Dg_\infty = \tilde{\Lambda}$. We conclude that P *vanishes*.

Moreover, $D^2 g^a_k \equiv 0$ for $k > 3$ and $D^2 g^b_m \equiv 0$ for $m_\infty > 6$. We choose $K \geq 3$ and $M \geq 6$, hence $D^2 g_\infty \equiv 0$. In particular, this implies that $Q^{a,b}_\infty$ and $R^{a,b}_\infty$ vanish.

The remainder of the setup is the same as in the general case and we obtain

$$
Z^c = r\, O^c + r\mu_*\, \pi^{\tilde{c}}(|\tilde{A}_F| \cdot [Q_F + \widetilde{Q}_F]) + r^2\, \pi^{\tilde{c}}(|\tilde{A}_F| \cdot R_F),
$$

as well as

$$
\begin{aligned}
Z^a &= r\, O^a + r\mu_* \,(\|\pi^{\tilde{a}}(|\tilde{A}_F| \cdot [Q_F + \widetilde{Q}_F])\|_1 + \widetilde{Q}^a_\infty) + r^2\, \|\pi^{\tilde{a}}(|\tilde{A}_F| \cdot R_F)\|_1, \\
Z^b &= r\, O^b + r\mu_* \,(\|\pi^{\tilde{b}}(|\tilde{A}_F| \cdot [Q_F + \widetilde{Q}_F])\|_2 + \widetilde{Q}^b_\infty) + r^2\, \|\pi^{\tilde{b}}(|\tilde{A}_F| \cdot R_F)\|_2.
\end{aligned}
$$

Remark 8.1. *If one chooses to use analytic expressions for $\overline{x}$ (see Section B.7) and one takes $\tilde{A}_F$ as the exact inverse (rather than a numerical approximation) of the Jacobian of $x_F \to g_F(x^0_F)$ at $\overline{x}$, then $g_F(\overline{x}) \equiv 0$ and $O \equiv 0$. This would come at the cost of $\tilde{A}_F$ being a matrix of intervals rather than a matrix of floats, and we do not pursue that approach here.*

9 Computational and algorithmic aspects

In this section we first present key implementation details, grouped into three lists: general computational matters, issues related to the bifurcation at $\mu = 0$, and considerations associated with continuation of the solution curve. Continuation in the context of rigorous numerics has been implemented previously, and we refer to [34, 5] for a general description. Here we comment on special features of our particular problem only. We finish the section with two remarks about choosing the weights, as well as a short discussion of the computation of the mixed-spots branch.

We start with the main general comments.

1. The algorithm was implemented in Matlab. All interval arithmetic computations were performed using Intlab [26]. The code is available at [35].

2. All computations were performed on a standard MacBook Pro laptop. We halted the computation after 25000 continuation steps. It took about 3 days to complete and used approximately 1.5Gb of memory. This is of course not an insurmountable limitation in the approach. For example, while the scope for parallelizing the computation and verification of the solution branch is large, that is beyond the goals of the present paper.

3. As can be seen from the appendices, coding the bounds is a laborious task. In part this is due to the complexity of the problem. In particular, in deriving the estimates, the three energy equations f^2_c, f^3_c and f^4_c require the majority of the effort in comparison with the infinite sets of equations f^a_k and f^b_m, corresponding to the differential equation, which have a more easily accessible structure. Besides, analyzing the bifurcation essentially doubles the coding effort. Clearly, we need to develop more general approaches to reduce the coding overhead in the future.

4. Several computational parameters have to be chosen. After some experimentation we choose the exponential weights $\xi_1 = \xi_2 = 1.02$. The choice of weights ω changed from step to step, see Remark 9.1. The sizes K and M of the finite dimensional projections varied along the solution branch as described below.

5. For convenience we did include a_0 and b_0 in the data structures in the computations, but these are never considered as variables on the formal level (and the terms have no contribution to the values of the bounds).

6. The convolution products are computed using the discrete Fourier transform and zero-padding. In combination with interval arithmetic this gives exact results and it is computationally cheap. A disadvantage is that the wrapping effect causes the size of the intervals to grow, which is especially harmful in the computation at the bifurcation point since there we are computing with a rather large interval of μ-values. We combat this by "manually" setting some of the coefficients of the convolution products to zero, e.g., if $a_k = 0$ for $|k| \geq k_1$ and $\tilde{a}_k = 0$ for $|k| \geq k_2$ then clearly $\langle a\tilde{a}\rangle_k = 0$ for $|k| \geq k_1 + k_2 - 1$.

Next, we note the principal issues in proving the branch coming out of the bifurcation point.

1. The continuation starts at the bifurcation point, where we solve the rescaled problem from Section 8 with $\mu_* = 1.2 \cdot 10^{-5}$.

2. To obtain a proof with a single step in the rescaled problem, we choose weights

$$(\omega_{\tilde{a}}, \omega_{\tilde{b}}, \omega_{\tilde{\beta}}, \omega_{\tilde{\kappa}_1}, \omega_{\tilde{\kappa}_2}, \omega_{\hat{a}}, \omega_{\hat{b}}) = (10, 50, 1, 1, 1, 0.1, 0.3).$$

after some (manual) optimization.

3. Recall that the rescaled (bifurcation) problem is written as $\tilde{f}(x;\mu) = g(x) + \mu h(x;\mu) = 0$. At $\mu = 0$ we have the exact solution $\overline{x} = x_0$ of $\tilde{f}(x;0) = g(x) = 0$ given in Appendix B.7. A conspicuous choice for $\underline{x}$ would be the solution of $Dg(\overline{x})\underline{x} = -h(\overline{x};0)$. However, to facilitate the connection to the "main" continuation branch, i.e. the problem described in Section 5 in the "original" variables, we solve $\tilde{f}(x;\mu_*) = 0$ numerically to obtain a point x_1 that lies approximately on the solution curve. We then set $\underline{x} = (x_1 - x_0)/\mu_*$.

4. Since we need to connect the bifurcation branch, which is essentially continuation in the parameter μ, to the pseudo-arclength continuation on the main branch, we slowly change the vector δ used in (5.1). In particular, for the first point (the end point of the bifurcation branch) we choose δ to be exactly in the μ-direction. In the first 200 steps of the continuation we then gradually change δ to the direction tangent to the solution curve (numerically, for the finite dimensional projection). From then on we take δ to be the approximate tangent at every point along the branch.

5. To make sure the main continuation branch connects to the bifurcating branch, we need to perform some checks analogous to Remark 6.4. Let $r^{\mathrm{bif}}_{\max}$ be the maximal radius for which we can verify the step out of the bifurcation, and let $r^{\mathrm{con}}_{\min}$ be the minimal radius for which we can verify the first piece of the main continuation branch. Then we check that the following six inequalities hold (cf. (8.2)):

$$\begin{aligned}
r^{\mathrm{con}}_{\min}\omega_a &< r^{\mathrm{bif}}_{\max} \min\{2\xi_1\omega_{\hat{a}}, \mu_*\omega_{\tilde{a}}\} \\
r^{\mathrm{con}}_{\min}\omega_b &< r^{\mathrm{bif}}_{\max} \min\{2\xi_2^2\omega_{\hat{b}}, \mu_*\omega_{\tilde{b}}\} \\
r^{\mathrm{con}}_{\min}\omega_{\kappa_1} &< r^{\mathrm{bif}}_{\max}\mu_*\omega_{\tilde{\kappa}_1} \\
r^{\mathrm{con}}_{\min}\omega_{\kappa_2} &< r^{\mathrm{bif}}_{\max}\mu_*\omega_{\tilde{\kappa}_2} \\
r^{\mathrm{con}}_{\min}\omega_{\beta} &< r^{\mathrm{bif}}_{\max}\mu_*\omega_{\tilde{\beta}}.
\end{aligned}$$

These inequalities verify that the "verification neighborhoods" are nested, hence it guarantees that the solution at the end of the bifurcation branch is the same as the one at the start of the continuation branch.

The continuation of the solution curve leads to another set of computational considerations.

1. Since the three terms in (7.2) that contribute to the Y-bound are essentially treated separately in Section 7.1, and since the Z-bound is split into several pieces in Section 7.2, the inequalities (6.2) can be condensed into a problem of finding an $r > 0$ for which the quadratic polynomials, often called the *radii polynomials*,

$$p_i(r;|s|) = \mathrm{Y}_i^1 + |s|\mathrm{Y}_i^2 + s^2\mathrm{Y}_i^3 + r\mathrm{Z}_i^1 + r|s|\mathrm{Z}_i^2 + r^2\mathrm{Z}_i^3 - \omega_i r, \qquad i = 1,\dots,6 \tag{9.1}$$

are negative simultaneously. Here $\mathrm{Y}_i^j, \mathrm{Z}_i^j$ are positive, computable numbers. To rigorously prove a piece of solution curve parametrized by $s \in [-1,1]$, we set $\mathrm{a}_i = \mathrm{Z}_i^3$, $\mathrm{b}_i = -\omega_i + \mathrm{Z}_i^1 + \mathrm{Z}_i^2$ and $\mathrm{c}_i = \mathrm{Y}_i^1 + \mathrm{Y}_i^2 + \mathrm{Y}_i^3$, and compute

$$r_{\min}^i = \frac{-\mathrm{b}_i - \sqrt{\mathrm{b}_i^2 - 4\mathrm{a}_i\mathrm{c}_i}}{2\mathrm{a}_i} \qquad \text{and} \qquad r_{\max}^i = \frac{-\mathrm{b}_i + \sqrt{\mathrm{b}_i^2 - 4\mathrm{a}_i\mathrm{c}_i}}{2\mathrm{a}_i}. \tag{9.2}$$

Finally, we compute $r_{\min} = \max_{i=1,\dots,6} r_{\min}^i$ and $r_{\max} = \max_{i=1,\dots,6} r_{\max}^i$, and we check that $r_{\min} < r_{\max}$.

2. If a step is successful, then we have strict inequalities $p_i(r;1) < 0$ for all $i = 1,\dots,6$ for all $r \in (r_{\min}, r_{\max})$. Hence we could have taken $|s|$, and thus the step size, slightly larger. In particular, we choose $r_0 = (r_{\min} + r_{\max})/2$ and interpret $p(r_0;|s|)$ as a quadratic polynomial in s to obtain an estimate on how big a step size could have been taken. Hence, we set $\mathrm{d}_i = \mathrm{Y}_i^3$, $\mathrm{e}_i = \mathrm{Y}_i^2 + r_0\mathrm{Z}_i^2$, $\mathrm{f}_i = -\omega_i r_0 + \mathrm{Y}_i^1 + r_0\mathrm{Z}_i^1 + r_0^2\mathrm{Z}_i^3$, and compute

$$s_{\max} \stackrel{\text{def}}{=} \frac{-\mathrm{e}_i + \sqrt{\mathrm{e}_i^2 - 4\mathrm{d}_i\mathrm{f}_i}}{2\mathrm{d}_i} > 1. \tag{9.3}$$

The idea is that the step size can roughly be increased by a factor $s_{\max}$. However, we note this does not take into account that the coefficients in (9.1) have been obtained assuming $|s| \le 1$.

3. After a successful step, we may change the step size. Based on the discussion above, if $s_{\max} > 1.1$ we increase the step size by a factor $(1 + 2s_{\max})/3$, whereas if $s_{\max} < 1.05$ we decrease the step size by factor a $(1 + s_{\max})/2$. Besides, we also halve the stepsize after a change in the number of modes, see below. Finally, we decrease the step size by a factor 0.9 if a step is unsuccessful (but this rarely happens as we already decrease the step size if our estimate $s_{\max}$ is less than 1.05). One cannot interpret the step size in absolute terms, since there is no proper global normalization (even the weights in the norm in the Banach space X change from step to step, see below). In Figure 9.1 we depict the step size in terms of μ, β, κ_1 and κ_2 versus the iteration number. They all have a similar behaviour (with β decreasing rather than increasing). We see that the step size is small at first (the problem being ill-conditioned), reaches a maximum and then starts to decrease (since the values of the bounds grow as the number of modes needed to describe the solution increases).

4. After each successful step we adapt the weights to try to increase the step size that can be verified, see Remark 9.1. We also allow the weights to change immediately after changing the number of modes in the finite dimensional projection (see below). We can monitor how good the weights are by using the Perron-Frobenius eigenvalue, see Remark 9.2. The latter information is not used in the continuation algorithm or the proof, but gives an indication that we have chosen the weights reasonably well.

5. After each successful step, we check the inequalities (6.4) to guarantee that each two succesive pieces of curve connect continuously. Furthermore, we check the inequality in the assertion of Lemma 6.3 to verify smoothness of the parametrized solution curve.

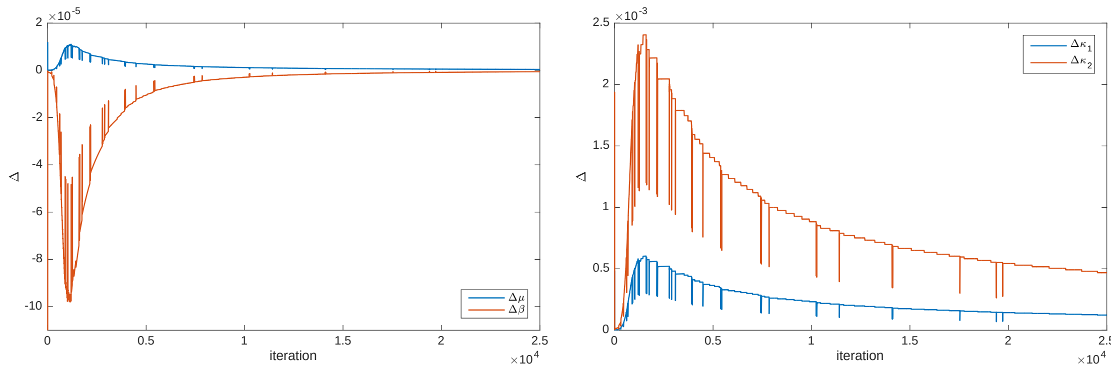

Figure 9.1: The step sizes for μ (left, upper graph), β (left, lower graph), κ_1 (right, lower graph) and κ_2 (right, upper graph) versus the iteration number.

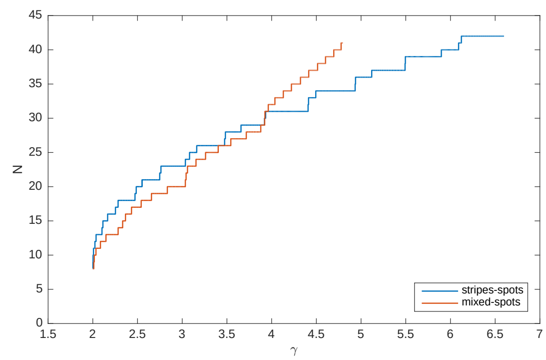

Figure 9.2: The number of modes N (i.e. $K = M = N - 1$, the total number of variables is $N^2 + N + 2$) versus the parameter $\gamma = \beta^{-1/2}$ for the stripes-spots branch (blue) and the mixed-spots branch (red).

6. We choose K and M to be equal throughout the computation, say $K = M = N - 1$. In the calculation for the bifurcation and in the initial phase of the continuation we set $N = 8$. To monitor the size of the (tail of the) residue $AF(\overline{x})$ we compute

$$\Xi_a \stackrel{\text{def}}{=} \max_{k \geq N} \frac{|f_k^a(\overline{x})|}{\lambda_k^a} \qquad \text{and} \qquad \Xi_b \stackrel{\text{def}}{=} \max_{|m| \geq N} \frac{|f_m^b(\overline{x})|}{\lambda_m^b}.$$

We increase N by 1 whenever $\max\{\Xi_a \xi_1^N, \Xi_b \xi_2^N\}$ exceeds 10^{-8}. We then simply pad the finite parts of $\overline{a}$, $\overline{b}$ and δ appropriately by zero(s). In other words, we do *not* change the center of the ball in the space X, nor do we change the continuation equation (5.2) at that point, but we simply increase the dimension of the finite dimensional projection. Notice that we only ever *increase* N along the solution curve, since the solution requires a growing number of Fourier modes to be described accurately as we move up (in terms of $\gamma = \beta^{-1/2}$) along the branch. In Figure 9.2 we depict N as a function of γ.

Remark 9.1 (Choice of weights)**.** *Initial weights have been chosen after some experimentation. After each successful iteration we adapt the weights. Our goal is to increase the step size, and we take $s_{\max}$ defined in (9.3) as its proxy. However, we do not want to make the interval $(r_{\min}, r_{\max})$, see (9.2), too small. Therefore we add $\log(r_{\max}/r_{\min})$ as a second target quantity. We use the* `gradient` *functionality of* INTLAB *to compute the derivative of both $s_{\max}$ and $\log(r_{\max}/r_{\min})$ with respect the six weights ω. We set*

$$\vec{\omega}_1 = \nabla_\omega \, s_{\max} \qquad \text{and} \qquad \vec{\omega}_2 = \nabla_\omega \log(r_{\max}/r_{\min}).$$

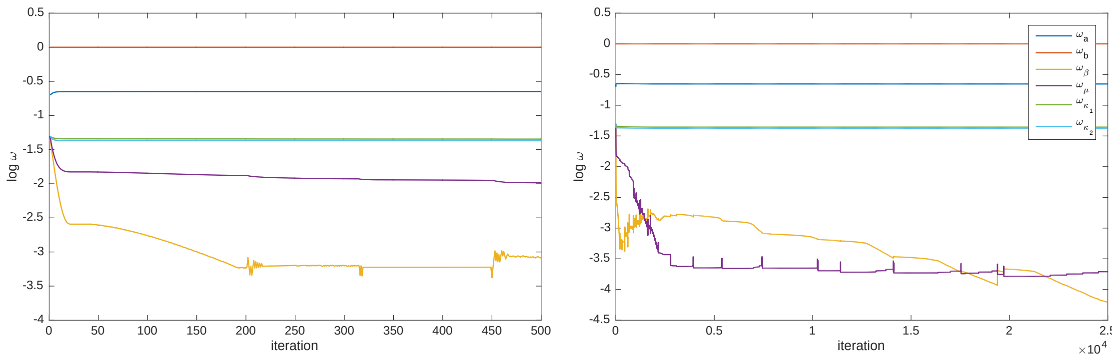

Figure 9.3: The log of the six weights ω as a function of the iteration number (the first few iterations are blown up on the left). From top to bottom (on the right) are ω_b (normalized at 1), ω_a, ω_{κ_1}, ω_{κ_2}, ω_μ and ω_β.

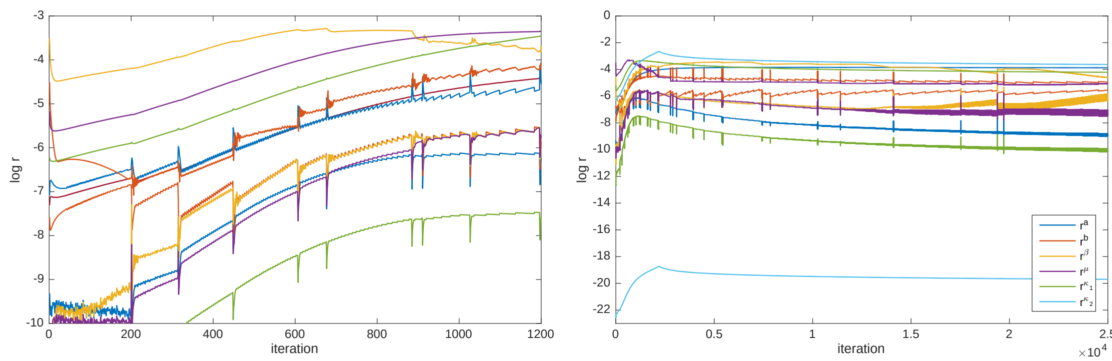

Figure 9.4: The log of the radii $r^i_{\min}$ (bottom six graphs) and $r^i_{\max}$ (top six graphs) as a function of the iteration number. The color coding is: a blue; b red; β orange; μ purple; κ_1 green; κ_2 cyan. On the right is the full picture, with on the left a blowup of (most of) the graphs for small iteration numbers, showcasing the frequent "switching" behaviour.

We want to increase both target quantities, hence we select $\vec{\omega}_0 = \vec{\omega}_1/|\vec{\omega}_1| + \vec{\omega}_2/|\vec{\omega}_2|$ *as the direction for changes in* ω*, since this would indeed increase both quantities if the dependencies were linear. We then take a small step in direction* $\vec{\omega}_0$*, allowing the individual weights to change by no more than 2% per iteration, except we are more lenient in the first few iterations after the bifurcation point mode and after each change in the number of modes, since then we are potentially far away from optimal step sizes and optimal weights. In Figure 9.3 we depict the six weights versus the iteration number. We see that after an initial transient phase, they are fairly stable.*

We note that $\log(r_{\max}/r_{\min})$ *does not depend smoothly on* ω*, since* $r_{\min}$ *and* $r_{\max}$ *may be attained by different radii polynomials for different values of the weights. This is illustrated on the right in Figure 9.4. The switching between radii polynomials that determine* $r_{\min}$ *and* $r_{\max}$ *can be clearly seen in the blowup on the left. By only allowing the weights to vary relatively cautiously from step to step, the (potential) problem related to this nonsmoothness does not cause (m)any unsuccessful steps.*

Finally, when increasing the number of modes (see above) leads to a failed continuation step because the intervals where the radii polynomials p_i *are negative have empty intersection (i.e.* $r_{max} < r_{\min}$*), then we change the weights in the direction* $\vec{\omega}_2$ *to try to obtain overlapping intervals.*

Remark 9.2 (Optimal weights)**.** *The bounds* Q *in* (7.9b)*, see also Section A.6, are linear in weights* ω*. These bounds correspond to to the term* Z_i^2 *in* (9.1) *through* (7.10)*. Therefore, the term*

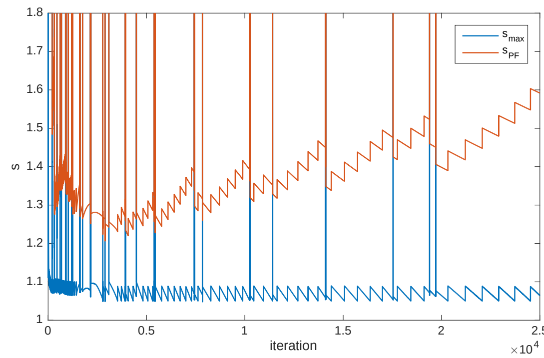

Figure 9.5: The upper bounds $s_{\rm PF}$ for any possible choice of weights (red, upper graph) and $s_{\max}$ for the particular weights used (blue, lower graph) versus the iteration number. The peaks are located at the iterations where the number of modes changes; the algorithm decreases the step size by 50% at these steps, hence the step sizes are temporarily far from optimal there. The algorithm keeps $s_{\max}$ between 1.05 and 1.1. The weight-independent "Perron-Frobenius" bound $s_{\rm PF}$ on the maximum step size gain varies between 1.2 and 1.6.

Z^2 can be interpreted as a 6×6 matrix $\mathcal{Q}$ with non-negative coefficients working on the weights vector $\omega = (\omega_i)_{i=1}^6$. A necessary condition for the inequalities $\mathrm{p}_i(r;1) < 0$ (and equivalently (6.2)) to hold for some range of r is thus that

$$s(\mathcal{Q}\omega)_i < \omega_i \qquad \text{for } i = 1, \ldots, 6.$$

This implies that if we ignore the other terms contributing to the bounds Y and Z, we may optimize the (predicted) maximal step size by solving the minimax problem

$$\min_{\omega>0} \max_{i=1,\ldots,6} \frac{(\mathcal{Q}\omega)_i}{\omega_i}.$$

This minimax problem is solved by the Perron-Frobenius *eigenvalue-eigenvector pair, since this is essentially the Collatz-Wielandt formula. In particular, the minimum value is the dominant eigenvalue λ_{PF} of $\mathcal{Q}$ (it is attained at weights corresponding to the positive eigenvector of $\mathcal{Q}$). An upper bound for the factor by which the step size can be increased is thus given by*

$$s_{\rm PF} \stackrel{\rm def}{=} \frac{1}{\lambda_{PF}(\mathcal{Q})}.$$

Since these considerations take just one term of the bounds Y and Z into account, the actual maximal step size gain will be less than this maximal factor $s_{\rm PF}$. The point is that $s_{\rm PF}$ is an upper bound no matter what weights one would choose. In Figure 9.5 we depict this (over)estimate $s_{\rm PF}$ of the maximal step size, together with the estimate $s_{\max}$, see (9.3), that takes all terms in the radii polynomial into account. We see that the (algorithmically) chosen weights lead to step sizes that are roughly within a factor 1.5 of the rigorous upper bound on the step size. The calculation of $s_{\rm PF}$ does not influence the bounds or the algorithm, but it gives us confidence that the algorithmic optimization of the weights works reasonably well.

Remark 9.3 (The mixed-spots branch)**.** *For the mixed-spots branch we pragmatically minimized the amount of changes to the code (compared to the stripes-spots branch). In particular, we just solve for $(a_k)_{k\in\mathbb{N}_0}$ even though we know they are trivial. The only somewhat subtle issue is that κ_1 is arbitrary for the mixed (homogeneous) state. Hence the derivative of f with respect to κ_1 vanishes, and when we invert the Jacobian we thus have to exclude the column corresponding to κ_1 and the row corresponding to f_3^c. With this modification, which appears in several places in the* *algorithm, we can run the code with a fixed (arbitrary) value of κ_1. To prevent overestimation we simply set $\omega_{\kappa_1} = 0$, and in A_F we set the column corresponding to κ_1 and the row corresponding to f_c^3 to 0. The starting point at $\mu = 0$ for the mixed-spots solution curve is given by the same formulas as in Section B.7, but with $\beta_0 = 37/30$ and $\bar{\hat{a}}_1 = 0$.*

A Analytic details of the estimates

We will write $v = (v_\beta, v_\mu, v_{\kappa_1}, v_{\kappa_2}, v^a, v^b)$ and $w = (w_\beta, w_\mu, w_{\kappa_1}, w_{\kappa_2}, w^a, w^b)$ throughout. In the notation for the first and second derivatives we use, in the convolution terms, the symmetry conventions for the variation v and w: $v^a_{-k} = v^a_k$ and $v^b_{\pm m_1, \pm m_2} = v^b_{m_1, m_2}$. Moreover, since no variations occur in the average, $v^a_0 = 0$ and $v^b_0 = 0$.

A.1 The first derivative

The derivative of f_1^c is the only one depending on s explicitly:

$$D f_1^c v = \big(v, \delta(s)\big)_F = \big(v, \bar{\delta} + s\underline{\delta}\big)_F.$$

Next, we compute

$$\begin{aligned}
D f_2^c v &= v_\beta \kappa_1 \sum_{k \in \mathbb{Z}_0} k^{-2} a_k^2 + \tfrac{1}{2} v_\mu \big[\langle a^4 \rangle_0 - 1\big] + v_{\kappa_1} \sum_{k \in \mathbb{Z}_0} (-\kappa_1^{-2} k^2 + \beta k^{-2}) a_k^2 \\
&\quad + 2 \sum_{k \in \mathbb{Z}_0} (\kappa_1^{-1} k^2 - 1 + \kappa_1 \beta k^{-2}) a_k v_k^a + 2\mu \langle a^3 v^a \rangle_0 \\
&\quad - \Bigg\{ v_\beta \kappa_2 \sum_{m \in \mathbb{Z}_0^2} \mathbf{m}^{-2} b_m^2 + \tfrac{1}{2} v_\mu \big[\langle b^4 \rangle_0 - 1\big] + v_{\kappa_2} \sum_{m \in \mathbb{Z}_0^2} (-\kappa_2^{-2} \mathbf{m}^2 + \beta \mathbf{m}^{-2}) b_m^2 \\
&\qquad + 2 \sum_{m \in \mathbb{Z}_0^2} (\kappa_2^{-1} \mathbf{m}^2 - 1 + \kappa_2 \beta \mathbf{m}^{-2}) b_m v_m^b + 2\mu \langle b^3 v^b \rangle_0 \Bigg\},
\end{aligned}$$

and

$$\begin{aligned}
D f_3^c v &= -[v_\beta \kappa_1^2 + 2 v_{\kappa_1} \kappa_1 \beta] \sum_{k \in \mathbb{Z}_0} k^{-2} a_k^2 + 2 \sum_{k \in \mathbb{Z}_0} (k^2 - \kappa_1^2 \beta k^{-2}) a_k v_k^a, \\
D f_4^c v &= -[v_\beta \kappa_2^2 + 2 v_{\kappa_2} \kappa_2 \beta] \sum_{m \in \mathbb{Z}_0^2} \mathbf{m}^{-2} b_m^2 + 2 \sum_{m \in \mathbb{Z}_0^2} (\mathbf{m}^2 - \kappa_2^2 \beta \mathbf{m}^{-2}) b_m v_m^b.
\end{aligned}$$

Finally

$$\begin{aligned}
D f_k^a v &= (v_\beta \kappa_1^2 + 2 v_{\kappa_1} \kappa_1 \beta - v_{\kappa_1} k^2) a_k + (k^4 - \kappa_1 k^2 + \kappa_1^2 \beta) v_k^a \\
&\quad + (v_\mu \kappa_1 + v_{\kappa_1} \mu) k^2 \langle a^3 \rangle_k + 3 \kappa_1 \mu k^2 \langle a^2 v^a \rangle_k, \\
D f_m^b v &= (v_\beta \kappa_2^2 + 2 v_{\kappa_2} \kappa_2 \beta - v_{\kappa_2} \mathbf{m}^2) b_m + (\mathbf{m}^4 - \kappa_2 \mathbf{m}^2 + \kappa_2^2 \beta) v_m^b \\
&\quad + (v_\mu \kappa_2 + v_{\kappa_2} \mu) \mathbf{m}^2 \langle b^3 \rangle_m + 3 \kappa_2 \mu \mathbf{m}^2 \langle b^2 v^b \rangle_m.
\end{aligned}$$

A.2 The second derivative

We shall need the formulas for the second derivative, which we denote by (the symmetric bilinear form)

$$D^2 f = D^2 f(x)(v, w) = D(Df(x)v)w. \tag{A.1}$$

Then, since f_1^c is linear,

$$D^2 f_1^c = 0.$$

This also means that $D^2 f$ does not depend on s explicitly, hence $D^2 f(x;s) = D^2 f(x)$. Next up is

$$\begin{aligned}
D^2 f_2^c = {}& 2(v_\beta \kappa_1 + v_{\kappa_1}\beta) \sum_{k\in\mathbb{Z}_0} k^{-2} a_k w_k^a + 2(w_\beta \kappa_1 + w_{\kappa_1}\beta) \sum_{k\in\mathbb{Z}_0} k^{-2} a_k v_k^a \\
& - 2v_{\kappa_1}\kappa_1^{-2} \sum_{k\in\mathbb{Z}_0} k^2 a_k w_k^a - 2w_{\kappa_1}\kappa_1^{-2} \sum_{k\in\mathbb{Z}_0} k^2 a_k v_k^a \\
& + 2v_{\kappa_1} w_{\kappa_1} \kappa_1^{-3} \sum_{k\in\mathbb{Z}_0} k^2 a_k^2 + (v_\beta w_{\kappa_1} + v_{\kappa_1} w_\beta) \sum_{k\in\mathbb{Z}_0} k^{-2} a_k^2 \\
& + 2 \sum_{k\in\mathbb{Z}_0} (\kappa_1^{-1} k^2 - 1 + \kappa_1 \beta k^{-2}) v_k^a w_k^a \\
& + 2v_\mu \langle a^3 w^a\rangle_0 + 2w_\mu \langle a^3 v^a\rangle_0 + 6\mu \langle a^2 w^a v^a\rangle_0 \\
& - \Bigg\{ 2(v_\beta \kappa_2 + v_{\kappa_2}\beta) \sum_{m\in\mathbb{Z}_0^2} \mathbf{m}^{-2} b_m w_m^b + 2(w_\beta \kappa_2 + w_{\kappa_2}\beta) \sum_{m\in\mathbb{Z}_0^2} \mathbf{m}^{-2} b_m v_m^b \\
& \quad - 2v_{\kappa_2}\kappa_2^{-2} \sum_{m\in\mathbb{Z}_0^2} \mathbf{m}^2 b_m w_m^b - 2w_{\kappa_2}\kappa_2^{-2} \sum_{m\in\mathbb{Z}_0^2} \mathbf{m}^2 b_m v_m^b \\
& \quad + 2v_{\kappa_2} w_{\kappa_2} \kappa_2^{-3} \sum_{m\in\mathbb{Z}_0^2} \mathbf{m}^2 b_m^2 + (v_\beta w_{\kappa_2} + v_{\kappa_2} w_\beta) \sum_{m\in\mathbb{Z}_0^2} \mathbf{m}^{-2} b_m^2 \\
& \quad + 2 \sum_{m\in\mathbb{Z}_0^2} (\kappa_2^{-1} \mathbf{m}^2 - 1 + \kappa_2 \beta \mathbf{m}^{-2}) v_m^b w_m^b \\
& \quad + 2v_\mu \langle b^3 w^b\rangle_0 + 2w_\mu \langle b^3 v^b\rangle_0 + 6\mu \langle b^2 w^b v^b\rangle_0 \Bigg\}.
\end{aligned}$$

Furthermore

$$\begin{aligned}
D^2 f_3^c = {}& -[2v_\beta \kappa_1^2 + 4v_{\kappa_1}\kappa_1\beta] \sum_{k\in\mathbb{Z}_0} k^{-2} a_k w_k^a - [2w_\beta \kappa_1^2 + 4w_{\kappa_1}\kappa_1\beta] \sum_{k\in\mathbb{Z}_0} k^{-2} a_k v_k^a \\
& - 2[(v_\beta w_{\kappa_1} + v_{\kappa_1} w_\beta)\kappa_1 + v_{\kappa_1} w_{\kappa_1}\beta] \sum_{k\in\mathbb{Z}_0} k^{-2} a_k^2 + 2 \sum_{k\in\mathbb{Z}_0} (k^2 - \kappa_1^2 \beta k^{-2}) v_k^a w_k^a, \\
D^2 f_4^c = {}& -[2v_\beta \kappa_2^2 + 4v_{\kappa_2}\kappa_2\beta] \sum_{m\in\mathbb{Z}_0^2} \mathbf{m}^{-2} b_m w_m^b - [2w_\beta \kappa_2^2 + 4w_{\kappa_2}\kappa_2\beta] \sum_{m\in\mathbb{Z}_0^2} \mathbf{m}^{-2} b_m v_m^b \\
& - 2[(v_\beta w_{\kappa_2} + v_{\kappa_2} w_\beta)\kappa_2 + v_{\kappa_2} w_{\kappa_2}\beta] \sum_{m\in\mathbb{Z}_0^2} \mathbf{m}^{-2} b_m^2 + 2 \sum_{m\in\mathbb{Z}_0^2} (\mathbf{m}^2 - \kappa_2^2 \beta \mathbf{m}^{-2}) v_m^b w_m^b,
\end{aligned}$$

and

$$\begin{aligned}
D^2 f_k^a = {}& (v_\beta \kappa_1^2 + 2v_{\kappa_1}\kappa_1\beta - v_{\kappa_1} k^2) w_k^a + (w_\beta \kappa_1^2 + 2w_{\kappa_1}\kappa_1\beta - w_{\kappa_1} k^2) v_k^a \\
& + 2[(v_\beta w_{\kappa_1} + v_{\kappa_1} w_\beta)\kappa_1 + v_{\kappa_1} w_{\kappa_1}\beta] a_k \\
& + 3(v_{\kappa_1}\mu + v_\mu \kappa_1) k^2 \langle a^2 w^a\rangle_k + 3(w_{\kappa_1}\mu + w_\mu \kappa_1) k^2 \langle a^2 v^a\rangle_k \\
& + [v_\mu w_{\kappa_1} + v_{\kappa_1} w_\mu] k^2 \langle a^3\rangle_k + 6\kappa_1 \mu k^2 \langle a w^a v^a\rangle_k, \\
D^2 f_m^b = {}& (v_\beta \kappa_2^2 + 2v_{\kappa_2}\kappa_2\beta - v_{\kappa_2} k^2) w_m^b + (w_\beta \kappa_2^2 + 2w_{\kappa_2}\kappa_2\beta - w_{\kappa_2} k^2) v_m^b \\
& + 2[(v_\beta w_{\kappa_2} + v_{\kappa_2} w_\beta)\kappa_2 + v_{\kappa_2} w_{\kappa_2}\beta] b_m \\
& + 3(v_{\kappa_2}\mu + v_\mu \kappa_2) \mathbf{m}^2 \langle b^2 w^b\rangle_m + 3(w_{\kappa_2}\mu + w_\mu \kappa_2) \mathbf{m}^2 \langle b^2 v^b\rangle_m \\
& + [v_\mu w_{\kappa_2} + v_{\kappa_2} w_\mu] \mathbf{m}^2 \langle b^3\rangle_m + 6\kappa_2 \mu \mathbf{m}^2 \langle b w^b v^b\rangle_m.
\end{aligned}$$

A.3 Estimates for O

To estimate the term $[I - AJ]v$ in (7.7), we introduce the following notation: for any (k', m') in the index set

$$\mathcal{I}_F \stackrel{\text{def}}{=} \{(k,m) \in \mathbb{N}_0 \times \mathbb{N}_0^2 : 1 \le k \le K, 1 \le m_\infty \le M\}, \tag{A.2}$$

we define $\psi_{k',m'} \in X_F \cong \mathbb{R}^{N_F}$ to have all its components equal to 0 except for the six positive components

$$\begin{aligned} \pi^c_n \psi_{k',m'} &= \omega_{c,n} && \text{for } n = 1,2,3,4 \\ \pi^a_k \psi_{k',m'} &= \omega_a \xi_1^{-k} && \text{for } k = k' \\ \pi^b_m \psi_{k',m'} &= \omega_b \xi_2^{-|m|} && \text{for } m = m'. \end{aligned}$$

By the characterization of the dual space, we obtain "componentwise" estimates

$$\sup_{v\in\mathcal{B}} |\pi^c_n([I - A_F J_F]v_F)| \leq \max_{(k,m)\in\mathcal{I}_F} \pi^c_n(|[I - A_F J_F]| \cdot \psi_{k,m}) \stackrel{\text{def}}{=} O^c_n, \tag{A.3a}$$

$$\sup_{v\in\mathcal{B}} \|\pi^a([I - A_F J_F]v_F)\|_1 \leq \max_{(k,m)\in\mathcal{I}_F} \|\pi^a(|[I - A_F J_F]| \cdot \psi_{k,m})\|_1 \stackrel{\text{def}}{=} O^a, \tag{A.3b}$$

$$\sup_{v\in\mathcal{B}} \|\pi^b([I - A_F J_F]v_F)\|_2 \leq \max_{(k,m)\in\mathcal{I}_F} \|\pi^b(|[I - A_F J_F]| \cdot \psi_{k,m})\|_2 \stackrel{\text{def}}{=} O^b. \tag{A.3c}$$

By exploiting linearity, these maxima are computed efficiently as follows. Let M_0 be the matrix of absolute values $|I_{N_F} - A_F J_F|$. Let M_1 be the diagonal $N_F \times N_F$ matrix such that

$$\begin{aligned} \pi^c_n(M_1 v_F) &= \pi^c_n v_F \\ \pi^a_k(M_1 v_F) &= \xi_1^{-k} \pi^a_k v_F \\ \pi^b_m(M_1 v_F) &= \xi_2^{-|m|} \pi^b_m v_F. \end{aligned}$$

Let M_2 be the $6 \times N_F$ matrix given by

$$\begin{aligned} (M_2 v_F)_n &= \pi^c_n v_F && \text{for } n = 1,2,3,4 \\ (M_2 v_F)_5 &= \sum_{1\leq k\leq K} \xi_1^k \pi^a_k v_F \\ (M_2 v_F)_6 &= \sum_{1\leq m_\infty \leq M} \xi_2^{|m|} \pi^b_m v_F. \end{aligned}$$

Let $M_3 = M_2 M_0 M_1$ and decompose it as $M_3 v_F = M_3^a \pi^a v_F + M_3^b \pi^b v_F + M_3^c \pi^c v_F$. Let M_4 be the 6×6 matrix given by, for each $j = 1, \ldots, 6$,

$$\begin{aligned} (M_4)_{jn} &= (M_3^c)_{jn} && \text{for } n = 1, \ldots, 4 \\ (M_4)_{j5} &= \max_{1\leq k\leq K} (M_3^a)_{jk} \\ (M_4)_{j6} &= \max_{1\leq m_\infty\leq M} (M_3^b)_{jm}. \end{aligned}$$

Then we find for the maxima in (A.3)

$$\begin{bmatrix} O^c_1 \\ O^c_2 \\ O^c_3 \\ O^c_4 \\ O^a \\ O^b \end{bmatrix} = M_4 \begin{bmatrix} \omega_{c,1} \\ \omega_{c,2} \\ \omega_{c,3} \\ \omega_{c,4} \\ \omega_a \\ \omega_b \end{bmatrix}.$$

A.4 Estimates for P

The first tail-term estimate for the bounds Z is to find a bound on the linear term (in r):

$$\bar{P} \stackrel{\text{def}}{=} [Df(\overline{x};0) - J]v,$$

which for the finite part gives

$$\bar{P}_F = Df_F(\overline{x};0)v - Df_F(\overline{x};0)v^0_F = Df_F(\overline{x};0)v^0_\infty$$

term	constant	value of constant
$\langle \overline{a}^3 y_\infty^{a0} \rangle_0$	$\mathcal{C}_a^1$	$\Vert \langle \overline{a}^3 \rangle_\infty^0 \Vert_1^* = \max\{ \lvert \langle \overline{a}^3 \rangle_{k'} \rvert \xi_1^{-k'} \,:\, K+1 \leq k' \leq 3K \}$
$\langle \overline{b}^3 y_\infty^{b0} \rangle_0$	$\mathcal{C}_b^1$	$\Vert \langle \overline{b}^3 \rangle_\infty^0 \Vert_2^* = \max\{ \lvert \langle \overline{b}^3 \rangle_{m'} \rvert \xi_2^{-\lvert m' \rvert} \,:\, m' \in \mathbb{N}^2, M+1 \leq \lvert m' \rvert \leq 3M \}$
$\langle \overline{a}^2 y_\infty^{a0} \rangle_k$	$\mathcal{C}_{a,k}^2$	$\Vert (\sigma_k \langle \overline{a}^2 \rangle)_\infty^0 \Vert_1^{*\mathrm{s}}$
$\langle \overline{b}^2 y_\infty^{b0} \rangle_m$	$\mathcal{C}_{b,m}^2$	$\Vert (\sigma_m \langle \overline{b}^2 \rangle)_\infty^0 \Vert_2^{*\mathrm{s}}$
$\Vert \langle \overline{a}^2 y^a \rangle_\infty^0 \Vert_1$	$\mathcal{C}_a^3$	$\Vert \langle \overline{a}^2 \rangle \Vert_1$
$\Vert \langle \overline{b}^2 y^b \rangle_\infty^0 \Vert_2$	$\mathcal{C}_b^3$	$\Vert \langle \overline{b}^2 \rangle \Vert_2$
$\Vert (\frac{k^2}{\lambda_k^a} \langle \overline{a}^3 \rangle_k)_\infty^0 \Vert_1$	$\mathcal{C}_a^4$	$\sum_{K+1 \leq \lvert k' \rvert \leq 3K} \frac{k'^2}{\lambda_{k'}^a} \lvert \langle \overline{a}^3 \rangle_{k'} \rvert \xi_1^{\lvert k' \rvert} = 2 \sum_{K+1 \leq k' \leq 3K} \frac{k'^2}{\lambda_{k'}^a} \lvert \langle \overline{a}^3 \rangle_{k'} \rvert \xi_1^{k'}$
$\Vert (\frac{\mathbf{m}^2}{\lambda_m^b} \langle \overline{b}^3 \rangle_m)_\infty^0 \Vert_2$	$\mathcal{C}_b^4$	$\sum_{M+1 \leq \lvert m' \rvert \leq 3M} \frac{\mathbf{m}'^2}{\lambda_{m'}^b} \lvert \langle \overline{b}^3 \rangle_{m'} \rvert \xi_2^{\lvert m' \rvert}$

Table A.1: Constants $\mathcal{C}$ used in the expressions for the estimates P. On each row, the term in the left column is estimated by the expression in the right column, which is computable and defines the constant in the middle column. Here we have assumed that $y^a \in X_1^0$ with $\|y^a\|_1 \leq 1$ and $y^b \in X_2^0$ with $\|y^b\|_2 \leq 1$. The constants $\mathcal{C}_{a,k}^2$ and $\mathcal{C}_{b,m}^2$ are needed for (k,m) in the finite index set $\mathcal{I}_F$, see (A.2), only.

and for the infinite part gives

$$\bar{P}_\infty = Df_\infty(\overline{x};0)v - \Lambda v_\infty.$$

Both of these expressions now only involve the convolution terms ($\langle a^3 \rangle_k$ and $\langle a^4 \rangle_0$, etc.) since the linear terms cancel due to the choice of Λ, and the quadratic terms (in the finite part) vanish. Let us be explicit:

$$\begin{aligned}
\bar{P}_1^c &= 0 \\
\bar{P}_2^c &= 2\overline{\mu}(\langle \overline{a}^3 v_\infty^{a0} \rangle_0 - \langle \overline{b}^3 v_\infty^{b0} \rangle_0) \\
\bar{P}_3^c &= 0 \\
\bar{P}_4^c &= 0 \\
\bar{P}_k^a &= 3\overline{\kappa}_1 \overline{\mu} k^2 \langle \overline{a}^2 v_\infty^{a0} \rangle_k && 1 \leq k \leq K \\
\bar{P}_k^a &= (v_{\kappa_1}\overline{\mu} + v_\mu \overline{\kappa}_1) k^2 \langle \overline{a}^3 \rangle_k + 3\overline{\kappa}_1 \overline{\mu} k^2 \langle \overline{a}^2 v^a \rangle_k && K < k \leq 3K \\
\bar{P}_k^a &= 3\overline{\kappa}_1 \overline{\mu} k^2 \langle \overline{a}^2 v^a \rangle_k && k > 3K \\
\bar{P}_m^b &= 3\overline{\kappa}_2 \overline{\mu} \mathbf{m}^2 \langle \overline{b}^2 v_\infty^{b0} \rangle_m && 1 \leq m_\infty \leq M \\
\bar{P}_m^b &= (v_{\kappa_2}\overline{\mu} + v_\mu \overline{\kappa}_2) \mathbf{m}^2 \langle \overline{b}^3 \rangle_m + 3\overline{\kappa}_2 \overline{\mu} \mathbf{m}^2 \langle \overline{b}^2 v^b \rangle_m && M < m_\infty \leq 3M \\
\bar{P}_m^b &= 3\overline{\kappa}_2 \overline{\mu} \mathbf{m}^2 \langle \overline{b}^2 v^b \rangle_m && m_\infty > 3M.
\end{aligned}$$

Note that in the finite part v_∞^0 appears, whereas in the infinite part the full v appears. The convolutions are all finite sums; for the finite part they involve intermediate values ($K < k \leq 3K$ and $M < m_\infty \leq 3M$) of v_∞ only.

The estimates for the convolution terms are based on Remark 4.1, and they are summarized in Table A.1. Obviously, all estimates are linear in $\|y^a\|_1$ and $\|y^b\|_2$, hence it is straightforward to incorporate the fact that $\|v^a\|_1 \leq \omega_a$ and $\|v^b\|_2 \leq \omega_b$ for $v \in \mathcal{B}$.

Before we can write down the tail estimate for $\bar{P}$, we introduce

$$\begin{aligned}
\mathcal{L}_K^a &\stackrel{\text{def}}{=} \frac{1}{(K+1)^4 - \overline{\kappa}_1 (K+1)^2 + \overline{\kappa}_1^2 \overline{\beta}}, \\
\mathcal{L}_M^b &\stackrel{\text{def}}{=} \frac{1}{(M+1)^4 - \overline{\kappa}_2 (M+1)^2 + \overline{\kappa}_2^2 \overline{\beta}},
\end{aligned}$$

which is used in the following elementary lemma.

Lemma A.1. *Let*

$$G(\overline{\beta}) \stackrel{\text{def}}{=} \begin{cases} \frac{1}{2} + \left(\frac{1}{4} - \overline{\beta}\right)^{1/2} & \text{for } 0 < \overline{\beta} < \frac{1}{4} \\ \overline{\beta}^{1/2} & \text{for } \overline{\beta} \geq \frac{1}{4}. \end{cases} \tag{A.4}$$

Assume that

$$(K+1)^2 \geq \overline{\kappa}_1 G(\overline{\beta}) \qquad \text{and} \qquad (M+1)^2 \geq \overline{\kappa}_2 G(\overline{\beta}). \tag{A.5}$$

Then for any $c_1, c_2 \geq 0$

$$\begin{aligned} \frac{c_1 + c_2 k^2}{\lambda^a_k} &\leq [c_1 + c_2(K+1)^2]\mathcal{L}^a_K \quad \text{for all } k \geq K+1 \\ \frac{c_1 + c_2 \boldsymbol{m}^2}{\lambda^b_m} &\leq [c_1 + c_2(M+1)^2]\mathcal{L}^b_M \quad \text{for all } m_\infty \geq M+1. \end{aligned}$$

Provided (A.5) holds, this leads to the estimates

$$\begin{aligned} P^c_n &= 0 && n = 1,3,4 \\ P^c_2 &= 2\overline{\mu}\big[\omega_a \mathcal{C}^1_a + \omega_b \mathcal{C}^1_b\big] \\ P^a_k &= 3\overline{\kappa}_1 \overline{\mu} k^2 \omega_a \mathcal{C}^2_{a,k} && 1 \leq k \leq K \\ P^a_\infty &= [\overline{\mu}\omega_{\kappa_1} + \overline{\kappa}_1 \omega_\mu]\mathcal{C}^4_a + 3\overline{\kappa}_1\overline{\mu}(K+1)^2 \mathcal{L}^K_a \omega_a \mathcal{C}^3_a \\ P^b_m &= 3\overline{\kappa}_2 \overline{\mu} \mathbf{m}^2 \omega_b \mathcal{C}^2_{b,m} && 1 \leq m_\infty \leq M \\ P^b_\infty &= [\overline{\mu}\omega_{\kappa_2} + \overline{\kappa}_2 \omega_\mu]\mathcal{C}^4_b + 3\overline{\kappa}_2\overline{\mu}(M+1)^2 \mathcal{L}^M_b \omega_b \mathcal{C}^3_b. \end{aligned}$$

A.5 Additional convolution estimates

Before we proceed with the estimates for $\bar{Q}$ and $\bar{R}$, we derive additional convolution estimates based on Remark 4.1 and (4.2). To compute the bounds $\mathcal{D}^i$, $\mathcal{E}^i$, $\mathcal{F}^i$, $\mathcal{G}^i$ and $\mathcal{H}^i$ in Tables A.2, A.3 and A.4, we perform interval computations using

$$\begin{aligned} \eta_\beta &= [\overline{\beta} - \underline{\beta}, \overline{\beta} + \underline{\beta}] \\ \eta_\mu &= [\overline{\mu} - \underline{\mu}, \overline{\mu} + \underline{\mu}] \\ \eta_{\kappa_1} &= [\overline{\kappa}_1 - \underline{\kappa}_1, \overline{\kappa}_1 + \underline{\kappa}_1] \\ \eta_{\kappa_2} &= [\overline{\kappa}_2 - \underline{\kappa}_2, \overline{\kappa}_2 + \underline{\kappa}_2] \\ \eta^a_k &= [\overline{a}_k - \underline{a}_k, \overline{a}_k + \underline{a}_k] \quad \text{for } 1 \leq k \leq K \\ \eta^b_m &= [\overline{b}_m - \underline{b}_m, \overline{b}_m + \underline{b}_m] \quad \text{for } 1 \leq m_\infty \leq M. \end{aligned}$$

When calculating with η^a and η^b, one needs to use

$$\begin{aligned} \eta^a_0 &= 1 \qquad \text{and} \qquad \eta^a_k = 0 \quad \text{for } k \geq K+1, \\ \eta^b_0 &= 1 \qquad \text{and} \qquad \eta^b_m = 0 \quad \text{for } m_\infty \geq M+1. \end{aligned}$$

Remark A.1. *In the bounds $\mathcal{D}^2$, $\mathcal{E}^2$ and $\mathcal{F}^2$ we use the weaker estimate* (4.4) *from Remark 4.1(iii) to reduce the computation time, which amply compensates the slightly smaller stepsize resulting from the larger constants. We note that in the bound $\mathcal{C}^2$ we use the sharper, computationally more expensive, estimate from Remark 4.1(ii), since the need for small P^a_k and P^b_m easily outweighs the longer computation.*

Remark A.2. *There is an opportunity to battle the adverse influence of the wrapping effect in the interval arithmetic. Namely, since we are merely after estimates that are uniform in the continuation parameter (not the variable) s, one may replace the constants $\mathcal{E}^2$, $\mathcal{E}^3$ $\mathcal{F}^2$, $\mathcal{F}^3$, $\mathcal{H}^1$ and $\mathcal{H}^2$, which are all in essence norms of linear interpolations in the parameter s, by variants where the evaluation is in the endpoints of the interval only, e.g. for $\mathcal{E}^3_a$:*

$$\|\langle \eta^a \underline{a} \rangle\|_1 \to \max\big\{\|\langle(\overline{a} - \underline{a})\underline{a}\rangle\|_1, \|\langle(\overline{a} + \underline{a})\underline{a}\rangle\|_1\big\}.$$

However, for clarity of exposition and code, we did not pursue that line here.

term	constant	value
$\langle(\eta^a)^3 y^a\rangle_0$	$\mathcal{D}_a^1$	$\lVert\langle(\eta^a)^3\rangle\rVert_1^{*0}$
$\langle(\eta^b)^3 y^b\rangle_0$	$\mathcal{D}_b^1$	$\lVert\langle(\eta^b)^3\rangle\rVert_2^{*0}$
$\langle(\eta^a)^2 y^a\rangle_k$	$\mathcal{D}_{a,k}^2$	$\lVert\langle(\eta^a)^2\rangle\rVert_1 \xi_1^{-k}$
$\langle(\eta^b)^2 y^b\rangle_m$	$\mathcal{D}_{b,m}^2$	$\lVert\langle(\eta^b)^2\rangle\rVert_2 \xi_2^{-\lvert m\rvert}$
$\lVert\langle(\eta^a)^2 y^a\rangle_\infty^0\rVert_1$	$\mathcal{D}_a^3$	$\lVert\langle(\eta^a)^2\rangle\rVert_1$
$\lVert\langle(\eta^b)^2 y^b\rangle_\infty^0\rVert_2$	$\mathcal{D}_b^3$	$\lVert\langle(\eta^b)^2\rangle\rVert_2$
$\sum_{k\in\mathbb{Z}_0} k^{-2}\eta_k^a y_k^a$	$\mathcal{D}_a^4$	$\lVert(k^{-2}\eta_k^a)\rVert_1^{*0}$
$\sum_{m\in\mathbb{Z}_0^2} \mathbf{m}^{-2}\eta_m^b y_m^b$	$\mathcal{D}_b^4$	$\lVert(\mathbf{m}^{-2}\eta_m^b)\rVert_2^{*0}$
$\sum_{k\in\mathbb{Z}_0} k^{2}\eta_k^a y_k^a$	$\mathcal{D}_a^5$	$\lVert(k^{2}\eta_k^a)\rVert_1^{*0}$
$\sum_{m\in\mathbb{Z}_0^2} \mathbf{m}^{2}\eta_m^b y_m^b$	$\mathcal{D}_b^5$	$\lVert(\mathbf{m}^{2}\eta_m^b)\rVert_2^{*0}$

term	constant	value
$\langle(\eta^a)^2 \underline{a} y^a\rangle_0$	$\mathcal{E}_a^1$	$\lVert\langle(\eta^a)^2\underline{a}\rangle\rVert_1^{*0}$
$\langle(\eta^b)^2 \underline{b} y^b\rangle_0$	$\mathcal{E}_b^1$	$\lVert\langle(\eta^b)^2\underline{b}\rangle\rVert_2^{*0}$
$\langle\eta^a \underline{a} y^a\rangle_k$	$\mathcal{E}_{a,k}^2$	$\lVert\langle\eta^a\underline{a}\rangle\rVert_1 \xi_1^{-k}$
$\langle\eta^b \underline{b} y^b\rangle_m$	$\mathcal{E}_{b,m}^2$	$\lVert\langle\eta^b\underline{b}\rangle\rVert_2 \xi_2^{-\lvert m\rvert}$
$\lVert\langle\eta^a \underline{a} y^a\rangle_\infty^0\rVert_1$	$\mathcal{E}_a^3$	$\lVert\langle\eta^a\underline{a}\rangle\rVert_1$
$\lVert\langle\eta^b \underline{b} y^b\rangle_\infty^0\rVert_2$	$\mathcal{E}_b^3$	$\lVert\langle\eta^b\underline{b}\rangle\rVert_2$
$\sum_{k\in\mathbb{Z}_0} k^{-2}\underline{a}_k y_k^a$	$\mathcal{E}_a^4$	$\lVert(k^{-2}\underline{a}_k)\rVert_1^{*0}$
$\sum_{m\in\mathbb{Z}_0^2} \mathbf{m}^{-2}\underline{b}_m y_m^b$	$\mathcal{E}_b^4$	$\lVert(\mathbf{m}^{-2}\underline{b}_m)\rVert_2^{*0}$
$\sum_{k\in\mathbb{Z}_0} k^{2}\underline{a}_k y_k^a$	$\mathcal{E}_a^5$	$\lVert(k^{2}\underline{a}_k)\rVert_1^{*0}$
$\sum_{m\in\mathbb{Z}_0^2} \mathbf{m}^{2}\underline{b}_m y_m^b$	$\mathcal{E}_b^5$	$\lVert(\mathbf{m}^{2}\underline{b}_m)\rVert_2^{*0}$
$\sum_{k\in\mathbb{Z}_0} \underline{a}_k y_k^a$	$\mathcal{E}_a^6$	$\lVert\underline{a}\rVert_1^{*0}$
$\sum_{m\in\mathbb{Z}_0^2} \underline{b}_m y_m^b$	$\mathcal{E}_b^6$	$\lVert\underline{b}\rVert_2^{*0}$

Table A.2: Constants $\mathcal{D}$ and $\mathcal{E}$ used in the expressions for the estimates Q and R. On each row, the term in the left column is estimated by the expression in the right column, which is computable via a finite interval arithmetic computation and defines the constant in the middle column. The intervals involved are $\eta^a = [\overline{a} - \underline{a}, \overline{a} + \underline{a}]$ and $\eta^b = [\overline{b} - \underline{b}, \overline{b} + \underline{b}]$. In the estimates we have assumed that $y^a \in X_1^0$ with $\lVert y^a\rVert_1 \leq 1$ and $y^b \in X_2^0$ with $\lVert y^b\rVert_2 \leq 1$. All the estimates in this table are linear in the norm of y^a and y^b.

term	constant	value
$\langle(\eta^a)^2 y^a \tilde{y}^a\rangle_0$	$\mathcal{F}_a^1$	$\lVert\langle(\eta^a)^2\rangle\rVert_1^{*}$
$\langle(\eta^b)^2 y^b \tilde{y}^b\rangle_0$	$\mathcal{F}_b^1$	$\lVert\langle(\eta^b)^2\rangle\rVert_2^{*}$
$\langle\eta^a y^a \tilde{y}^a\rangle_k$	$\mathcal{F}_{a,k}^2$	$\lVert\eta^a\rVert_1 \xi_1^{-k}$
$\langle\eta^b y^b \tilde{y}^b\rangle_m$	$\mathcal{F}_{b,m}^2$	$\lVert\eta^b\rVert_2 \xi_2^{-\lvert m\rvert}$
$\lVert\langle\eta^a y^a \tilde{y}^a\rangle_\infty^0\rVert_1$	$\mathcal{F}_a^3$	$\lVert\eta^a\rVert_1$
$\lVert\langle\eta^b y^b \tilde{y}^b\rangle_\infty^0\rVert_2$	$\mathcal{F}_b^3$	$\lVert\eta^b\rVert_2$

Table A.3: Constants $\mathcal{F}$ used in the expressions for the estimates R. In the estimates we have assumed that $\lVert y^a\rVert_1, \lVert\tilde{y}^a\rVert_1 \leq 1$ and $\lVert y^b\rVert_2, \lVert\tilde{y}^b\rVert_2 \leq 1$. The estimates in this table are quadratic in the variations y and $\tilde{y}$, and once again exploit the characterization of the dual space in Section 4. See the caption of Table A.2 for additional information.

constant	value
$\mathcal{G}_a^1$	$\sum_{1\le\lvert k\rvert\le K} k^{-2}(\eta_k^a)^2$
$\mathcal{G}_b^1$	$\sum_{1\le m_\infty\le M} \mathbf{m}^{-2}(\eta_m^b)^2$
$\mathcal{G}_a^2$	$\sum_{1\le\lvert k\rvert\le K} k^{2}(\eta_k^a)^2$
$\mathcal{G}_b^2$	$\sum_{1\le m_\infty\le M} \mathbf{m}^{2}(\eta_m^b)^2$
$\mathcal{G}_{a,k}^3$	$\lvert\langle(\eta^a)^3\rangle_k\rvert$
$\mathcal{G}_{b,m}^3$	$\lvert\langle(\eta^b)^3\rangle_m\rvert$
$\mathcal{G}_a^4$	$\lVert\langle(\eta^a)^3\rangle_\infty^0\rVert_1$
$\mathcal{G}_b^4$	$\lVert\langle(\eta^b)^3\rangle_\infty^0\rVert_2$

constant	value
$\mathcal{H}_a^1$	$\lvert\sum_{1\le\lvert k\rvert\le K} k^{-2}\eta_k^a\underline{a}_k\rvert$
$\mathcal{H}_b^1$	$\lvert\sum_{1\le m_\infty\le M} \mathbf{m}^{-2}\eta_m^b\underline{b}_m\rvert$
$\mathcal{H}_a^2$	$\lvert\sum_{1\le\lvert k\rvert\le K} k^{2}\eta_k^a\underline{a}_k\rvert$
$\mathcal{H}_b^2$	$\lvert\sum_{1\le m_\infty\le M} \mathbf{m}^{2}\eta_m^b\underline{b}_m\rvert$
$\mathcal{H}_{a,k}^3$	$\lvert\langle(\eta^a)^2\underline{a}\rangle_k\rvert$
$\mathcal{H}_{b,m}^3$	$\lvert\langle(\eta^b)^2\underline{b}\rangle_m\rvert$
$\mathcal{H}_a^4$	$\lVert\langle(\eta^a)^2\underline{a}\rangle_\infty^0\rVert_1$
$\mathcal{H}_b^4$	$\lVert\langle(\eta^b)^2\underline{b}\rangle_\infty^0\rVert_2$
$\mathcal{H}_a^5$	$\lvert\langle(\eta^a)^3\underline{a}\rangle_0\rvert$
$\mathcal{H}_b^5$	$\lvert\langle(\eta^b)^3\underline{b}\rangle_0\rvert$

Table A.4: Constants $\mathcal{G}$ and $\mathcal{H}$ used in the expressions for the estimates Q and R. The constants should be interpreted as upper bounds, computed using interval arithmetic, for the corresponding expressions appearing in the second column. The intervals involved are given by $\eta^a = [\bar{a}-\underline{a}, \bar{a}+\underline{a}]$ and $\eta^b = [\bar{b}-\underline{b}, \bar{b}+\underline{b}]$.

A.6 Estimates for Q

These terms vanish for the non-continuation case $\underline{x} = 0$. since they are the coefficients of the rs term. For the first component we obtain, with the notation from Section A.3,

$$\begin{aligned} Q_1^c &= \max_{(k,m)\in\mathcal{I}_F} (\psi_{k,m}, |\underline{\delta}|) \\ &= \sum_{n=1}^{4} \omega_{c,n}\pi_n^c|\underline{\delta}| + \omega_a \max_{1\le k\le K} \xi_1^{-k}\pi_k^a|\underline{\delta}| + \omega_b \max_{1\le m_\infty\le M} \xi_2^{-|m|}\pi_m^b|\underline{\delta}|. \end{aligned} \tag{A.6}$$

For the other components we need to estimate the second derivative of f. We start with

$$\begin{aligned} Q_2^c = {} & 2(\omega_\beta\eta_{\kappa_1} + \omega_{\kappa_1}\eta_\beta)\mathcal{H}_a^1 + 2|\underline{\beta}\eta_{\kappa_1} + \underline{\kappa}_1\eta_\beta|\omega_a\mathcal{D}_a^4 \\ & + 2\omega_{\kappa_1}\eta_{\kappa_1}^{-2}\mathcal{H}_a^2 + 2|\underline{\kappa}_1|\eta_{\kappa_1}^{-2}\omega_a\mathcal{D}_a^5 \\ & + 2\omega_{\kappa_1}|\underline{\kappa}_1|\eta_{\kappa_1}^{-3}\mathcal{G}_a^2 + (\omega_\beta|\underline{\kappa}_1| + \omega_{\kappa_1}|\underline{\beta}|)\mathcal{G}_a^1 \\ & + 2\omega_a\left\{\eta_{\kappa_1}^{-1}\mathcal{E}_a^5 + \mathcal{E}_a^6 + \eta_{\kappa_1}\eta_\beta\mathcal{E}_a^4\right\} \\ & + 2|\underline{\mu}|\omega_a\mathcal{D}_a^1 + 2\omega_\mu\mathcal{H}_a^5 + 6\eta_\mu\omega_a\mathcal{E}_a^1 \\ & + 2(\omega_\beta\eta_{\kappa_2} + \omega_{\kappa_2}\eta_\beta)\mathcal{H}_b^1 + 2|\underline{\beta}\eta_{\kappa_2} + \underline{\kappa}_2\eta_\beta|\omega_b\mathcal{D}_b^4 \\ & + 2\omega_{\kappa_2}\eta_{\kappa_2}^{-2}\mathcal{H}_b^2 + 2|\underline{\kappa}_2|\eta_{\kappa_2}^{-2}\omega_b\mathcal{D}_b^5 \\ & + 2\omega_{\kappa_2}|\underline{\kappa}_2|\eta_{\kappa_2}^{-3}\mathcal{G}_b^2 + (\omega_\beta|\underline{\kappa}_2| + \omega_{\kappa_2}|\underline{\beta}|)\mathcal{G}_b^1 \\ & + 2\omega_b\left\{\eta_{\kappa_2}^{-1}\mathcal{E}_b^5 + \mathcal{E}_b^6 + \eta_{\kappa_2}\eta_\beta\mathcal{E}_b^4\right\} \\ & + 2|\underline{\mu}|\omega_b\mathcal{D}_b^1 + 2\omega_\mu\mathcal{H}_b^5 + 6\eta_\mu\omega_b\mathcal{E}_b^1. \end{aligned}$$

Also

$$\begin{aligned} Q_3^c = {} & [2\omega_\beta\eta_{\kappa_1}^2 + 4\omega_{\kappa_1}\eta_{\kappa_1}\eta_\beta]\mathcal{H}_a^1 + |2\underline{\beta}\eta_{\kappa_1}^2 + 4\underline{\kappa}_1\eta_{\kappa_1}\eta_\beta|\omega_a\mathcal{D}_a^4 \\ & + 2[(\omega_\beta|\underline{\kappa}_1| + \omega_{\kappa_1}|\underline{\beta}|)\eta_{\kappa_1} + \omega_{\kappa_1}|\underline{\kappa}_1|\eta_\beta]\mathcal{G}_a^1 + 2\omega_a\left\{\mathcal{E}_a^5 + \eta_{\kappa_1}^2\eta_\beta\mathcal{E}_a^4\right\}, \end{aligned}$$

and

$$\begin{aligned}Q_4^c &= [2\omega_\beta \eta_{\kappa_2}^2 + 4\omega_{\kappa_2}\eta_{\kappa_2}\eta_\beta]\mathcal{H}_b^1 + |2\underline{\beta}\eta_{\kappa_2}^2 + 4\underline{\kappa}_2\eta_{\kappa_2}\eta_\beta|\omega_b \mathcal{D}_b^4 \\ &\quad + 2[(\omega_\beta|\underline{\kappa}_2| + \omega_{\kappa_2}|\underline{\beta}|)\eta_{\kappa_2} + \omega_{\kappa_2}|\underline{\kappa}_2|\eta_\beta]\mathcal{G}_b^1 + 2\omega_b\left\{\mathcal{E}_b^5 + \eta_{\kappa_2}^2\eta_\beta\mathcal{E}_b^4\right\}.\end{aligned}$$

Furthermore for $1 \le k \le K$

$$\begin{aligned}Q_k^a = (\omega_\beta\eta_{\kappa_1}^2 &+ 2\omega_{\kappa_1}\eta_{\kappa_1}\eta_\beta + \omega_{\kappa_1}k^2)|\underline{a}_k| + |\underline{\beta}\eta_{\kappa_1}^2 + 2\underline{\kappa}_1\eta_{\kappa_1}\eta_\beta - \underline{\kappa}_1 k^2|\omega_a\xi_1^{-k} \\ &+ 2[(\omega_\beta|\underline{\kappa}_1| + \omega_{\kappa_1}|\underline{\beta}|)\eta_{\kappa_1} + \omega_{\kappa_1}|\underline{\kappa}_1|\eta_\beta]|\eta_k^a| \\ &+ 3|\underline{\kappa}_1\eta_\mu + \underline{\mu}\eta_{\kappa_1}|k^2\omega_a\mathcal{D}_{a,k}^2 + 3(\omega_{\kappa_1}\eta_\mu + \omega_\mu\eta_{\kappa_1})k^2\mathcal{H}_{a,k}^3 \\ &+ [\omega_\mu|\underline{\kappa}_1| + \omega_{\kappa_1}|\underline{\mu}|]k^2\mathcal{G}_{a,k}^3 + 6\eta_{\kappa_1}\eta_\mu k^2\omega_a\mathcal{E}_{a,k}^2.\end{aligned}$$

For $k \ge K+1$ we split into terms with and without k^2 and define

$$\begin{aligned}\Gamma_0^a &= \omega_a|\underline{\beta}\eta_{\kappa_1}^2 + 2\underline{\kappa}_1\eta_{\kappa_1}\eta_\beta| \\ \Gamma_1^a &= \omega_a|\underline{\kappa}_1| + 3|\underline{\kappa}_1\eta_\mu + \underline{\mu}\eta_{\kappa_1}|\omega_a\mathcal{D}_a^3 + 3[\omega_{\kappa_1}\eta_\mu + \omega_\mu\eta_{\kappa_1}]\mathcal{H}_a^4 \\ &\qquad + [\omega_\mu|\underline{\kappa}_1| + \omega_{\kappa_1}|\underline{\mu}|]\mathcal{G}_a^4 + 6\eta_{\kappa_1}\eta_\mu\omega_a\mathcal{E}_a^3,\end{aligned}$$

so that, incorporating the division by λ_k^a, we find from Lemma A.1 that

$$Q_\infty^a = [\Gamma_0^a + \Gamma_1^a(K+1)^2]\mathcal{L}_K^a,$$

where and we have assumed, as before, that $(K+1)^2 \ge \overline{\kappa}_1 G(\overline{\beta})$.

Finally, for $1 \le m_\infty \le M$

$$\begin{aligned}Q_m^b = (\omega_\beta\eta_{\kappa_2}^2 &+ 2\omega_{\kappa_2}\eta_{\kappa_2}\eta_\beta + \omega_{\kappa_2}\mathbf{m}^2)|\underline{b}_m| + |\underline{\beta}\eta_{\kappa_2}^2 + 2\underline{\kappa}_2\eta_{\kappa_2}\eta_\beta - \underline{\kappa}_2\mathbf{m}^2|\omega_b\xi_2^{-|m|} \\ &+ 2[(\omega_\beta|\underline{\kappa}_2| + \omega_{\kappa_2}|\underline{\beta}|)\eta_{\kappa_2} + \omega_{\kappa_2}|\underline{\kappa}_2|\eta_\beta]|\eta_m^b|, \\ &+ 3|\underline{\kappa}_2\eta_\mu + \underline{\mu}\eta_{\kappa_2}|\mathbf{m}^2\omega_b\mathcal{D}_{b,m}^2 + 3(\omega_{\kappa_2}\eta_\mu + \omega_\mu\eta_{\kappa_2})\mathbf{m}^2\mathcal{H}_{b,m}^3 \\ &+ [\omega_\mu|\underline{\kappa}_2| + \omega_{\kappa_2}|\underline{\mu}|]\mathbf{m}^2\mathcal{G}_{b,m}^3 + 6\eta_{\kappa_2}\eta_\mu\mathbf{m}^2\omega_b\mathcal{E}_{b,m}^2,\end{aligned}$$

and in the tail we set

$$\begin{aligned}\Gamma_0^b &= \omega_b|\underline{\beta}\eta_{\kappa_2}^2 + 2\underline{\kappa}_2\eta_{\kappa_2}\eta_\beta| \\ \Gamma_1^b &= \omega_b|\underline{\kappa}_2| + 3|\underline{\kappa}_2\eta_\mu + \underline{\mu}\eta_{\kappa_2}|\omega_b\mathcal{D}_b^3 + [\omega_{\kappa_2}\eta_\mu + \omega_\mu\eta_{\kappa_2}]\mathcal{H}_b^4 \\ &\qquad + [\omega_\mu|\underline{\kappa}_2| + \omega_{\kappa_2}|\underline{\mu}|]\mathcal{G}_b^4 + 6\eta_{\kappa_2}\eta_\mu\omega_b\mathcal{E}_b^3,\end{aligned}$$

so that

$$Q_\infty^b = [\Gamma_0^b + \Gamma_1^b(M+1)^2]\mathcal{L}_m^b,$$

where have assumed, once again, that $(M+1)^2 \ge \overline{\kappa}_2 G(\overline{\beta})$.

Remark A.3. *As already remarked upon in Remark 7.3, there is an opportunity to combat the overestimation that results from using the triangle inequality "too early", which, among others, leads to multiplication by $|A_F|$. Namely, one may exploit linearity to carry through the multiplication by A_F first, collecting terms that are linear in the components of v, and only use the triangle inequality afterwards. Moreover, it is possible to exploit the characterization of the dual to estimate the terms that are linear in v^a in v^b by extending the construction of Section A.3 to the much more complex context of these estimates Q. We did not explore either of these possibilities.*

A.7 Estimates for R

Our goal in this section is to find an explicit estimates

$$\max_{\eta\in[\overline{x}-\underline{x},\overline{x}+\underline{x}],v,w\in\mathcal{B}} \frac{1}{r_*}\left|\int_0^{r_*} D^2 f(\eta + rw)(v,w)dr\right| \le R.$$

For each term, say g, appearing in f we will find explicit constants U_0^g and U_1^g.

$$\max_{\eta\in[\overline{x}-\underline{x},\overline{x}+\underline{x}],v,w\in\mathcal{B}} |D^2 g(\eta+rw)(v,w)| \le U_0^g + rU_1^g, \qquad \text{for all } r\in[0,r_*], \tag{A.7}$$

which then contributes $U_0^g + \frac{1}{2}r_* U_1^g$ to the corresponding component of R. We note that for many of the terms we will just put $U_1^g = 0$ at the cost of cruder estimate U_0^g, but for the convolution terms we use the slightly more refined splitting in (A.7). To give an example:

$$\left|\langle(\eta^a + r\tilde{y}^a)^3 y^a\rangle_0\right| \le |\langle(\eta^a)^3 y^a\rangle_0| + 3r(\|\eta^a\|_1 + r)^2$$

for all $\|y^a\|_1, \|\tilde{y}^a\|_1 \le 1$.

As discussed before,

$$R_1^c = 0.$$

To estimate the nonzero components of the second derivative we will perform computer-assisted evaluation using interval arithmetic. In particular, we will compute with intervals (for fixed r_*)

$$\begin{aligned}
\zeta_\beta &= \left|[\overline{\beta}-\underline{\beta},\overline{\beta}+\underline{\beta}] + [-1,1]\omega_\beta r_*\right| \\
\zeta_\mu &= \left|[\overline{\mu}-\underline{\mu},\overline{\mu}+\underline{\mu}] + [-1,1]\omega_\mu r_*\right| \\
\zeta_{\kappa_1} &= \left|[\overline{\kappa}_1-\underline{\kappa_1},\overline{\kappa}_1+\underline{\kappa_1}] + [-1,1]\omega_{\kappa_1} r_*\right| \\
\zeta_{\kappa_2} &= \left|[\overline{\kappa}_2-\underline{\kappa_2},\overline{\kappa}_2+\underline{\kappa_2}] + [-1,1]\omega_{\kappa_2} r_*\right|.
\end{aligned}$$

Taking absolute values above is somewhat superfluous, since r_* is small and all values $\overline{\beta}$, $\overline{\mu}$, $\overline{\kappa}_1$ and $\overline{\kappa}_1$ are positive (but $\overline{\mu}$ may be quite small). We have chosen to incorporated the absolute values directly in these expressions for ζ, rather than putting absolute values in the formulas below. This does not make a difference in the present situation (in general one may suffer a loss of possible cancellations), since the estimates below are term by term anyway (in contrast, in the limit problem in Section B.5 we proceed a bit more prudently).

The intervals $\eta_k^a = [\overline{a}_k - \underline{a}_k, \overline{a}_k + \underline{a}_k]$ and $\eta_m^b = [\overline{b}_m - \underline{b}_m, \overline{b}_m + \underline{b}_m]$ are as before (see Section A.5). We write

$$r_*^a = r_*\omega_a \qquad \text{and} \qquad r_*^b = r_*\omega_b.$$

Additionally, we derive directly from the dual space formulation

$$\begin{aligned}
\textstyle\sum_{k\in\mathbb{Z}_0} y_k^a \tilde{y}_k^a &\le \xi_1^{-2} \\
\textstyle\sum_{m\in\mathbb{Z}_0^2} y_m^b \tilde{y}_m^b &\le \xi_2^{-2} \\
\textstyle\sum_{k\in\mathbb{Z}_0} k^{-2} y_k^a \tilde{y}_k^a &\le \xi_1^{-2} \\
\textstyle\sum_{m\in\mathbb{Z}_0^2} \mathbf{m}^{-2} y_m^b \tilde{y}_m^b &\le \xi_2^{-2} \\
\textstyle\sum_{k\in\mathbb{Z}_0} k^{2} y_k^a \tilde{y}_k^a &\le \ell_1(\xi_1) \\
\textstyle\sum_{m\in\mathbb{Z}_0^2} \mathbf{m}^{2} y_m^b \tilde{y}_m^b &\le \ell_2(\xi_2),
\end{aligned}$$

for all $y^a, \tilde{y}^a \in X_1^0$ with $\|y^a\|_1, \|\tilde{y}^a\|_1 \le 1$, and $y^b, \tilde{y}^b \in X_2^0$ with $\|y^b\|_2, \|\tilde{y}^b\|_2 \le 1$, where

$$\ell_1(\xi) \stackrel{\text{def}}{=} \begin{cases} (e\log\xi)^{-2} & \text{if } \xi < e \\ \xi^{-2} & \text{if } \xi \ge e \end{cases} \qquad \text{and} \qquad \ell_2(\xi) \stackrel{\text{def}}{=} \begin{cases} 4(e\log\xi)^{-2} & \text{if } \xi < e \\ 4\xi^{-2} & \text{if } \xi \ge e. \end{cases} \tag{A.8}$$

Remark A.4. *The multiplicative factor* 4 *in* ℓ_2 *in* (A.8) *is for the norm* $|m| \equiv \max\{|m_1|, |m_2|\}$ *in the decay rates for the* $\|\cdot\|_2$ *in* (4.1). *If one uses* $|m| \equiv |m_1| + |m_2|$ *instead, this factor is* 3.

Using estimates similar to the ones involved in P and Q, we find

$$
\begin{aligned}
R_2^c = \omega_a\Big\{ & 2(\omega_\beta\zeta_{\kappa_1}+\omega_{\kappa_1}\zeta_\beta)\left[2\mathcal{D}_a^4+r_*^a\xi_1^{-2}\right]+2\omega_{\kappa_1}\zeta_{\kappa_1}^{-2}\left[2\mathcal{D}_a^5+r_*^a\ell(\xi_1)\right]\Big\}\\
& +2\omega_{\kappa_1}^2\zeta_{\kappa_1}^{-3}\left[\mathcal{G}_a^2+r_*^a(\|\eta^a\|_1+r_*^a)\ell(\xi_1)\right]+2\omega_{\kappa_1}\omega_\beta\left[\mathcal{G}_a^1+r_*^a(\|\eta^a\|_1+r_*^a)\xi_1^{-2}\right]\\
& +2\omega_a^2\Big\{\zeta_{\kappa_1}^{-1}\ell(\xi_1)+\xi_1^{-2}+\zeta_{\kappa_1}\zeta_\beta\xi_1^{-2}\Big\}\\
& +2\omega_\mu\omega_a\left[2\mathcal{D}_a^1+3r_*^a(\|\eta^a\|_1+r_*^a)^2\right]+6\zeta_\mu\omega_a^2\left[\mathcal{F}_a^1+r_*^a(\|\eta^a\|_1+r_*^a)\right]\\
+\omega_b\Big\{ & 2(\omega_\beta\zeta_{\kappa_2}+\omega_{\kappa_2}\zeta_\beta)\left[2\mathcal{D}_b^4+r_*^b\xi_2^{-2}\right]+2\omega_{\kappa_2}\zeta_{\kappa_2}^{-2}\left[2\mathcal{D}_b^5+r_*^b\ell(\xi_2)\right]\Big\}\\
& +2\omega_{\kappa_2}^2\zeta_{\kappa_2}^{-3}\left[\mathcal{G}_b^2+r_*^b(\|\eta^b\|_2+r_*^b)\ell(\xi_2)\right]+2\omega_{\kappa_2}\omega_\beta\left[\mathcal{G}_b^1+r_*^b(\|\eta^b\|_2+r_*^b)\xi_2^{-2}\right]\\
& +2\omega_b^2\Big\{\zeta_{\kappa_2}^{-1}\ell(\xi_2)+\xi_2^{-2}+\zeta_{\kappa_2}\zeta_\beta\xi_2^{-2}\Big\}\\
& +2\omega_\mu\omega_b\left[2\mathcal{D}_b^1+3r_*^b(\|\eta^b\|_2+r_*^b)^2\right]+6\zeta_\mu\omega_b^2\left[\mathcal{F}_b^1+r_*^b(\|\eta^b\|_2+r_*^b)\right].
\end{aligned}
$$

We note that the expression in the (complicated) righthand side is an interval and we interpret the above expression to mean that R_2^c is an upper bound for this interval.

Also

$$
\begin{aligned}
R_3^c = {} & \omega_a\left[2\omega_\beta\zeta_{\kappa_1}^2+4\omega_{\kappa_1}\zeta_{\kappa_1}\zeta_\beta\right]\left[2\mathcal{D}_a^4+r_*^a\xi_1^{-2}\right]\\
& +\left[4\omega_\beta\omega_{\kappa_1}\zeta_{\kappa_1}+2\omega_{\kappa_1}^2\zeta_\beta\right]\left[\mathcal{G}_a^1+r_*^a(\|\eta^a\|_1+r_*^a)\xi_1^{-2}\right]+2\omega_a^2\Big\{\ell(\xi_1)+\zeta_{\kappa_1}^2\zeta_\beta\xi_1^{-2}\Big\},
\end{aligned}
$$

and

$$
\begin{aligned}
R_4^c = {} & \omega_b\left[2\omega_\beta\zeta_{\kappa_2}^2+4\omega_{\kappa_2}\zeta_{\kappa_2}\zeta_\beta\right]\left[2\mathcal{D}_b^4+r_*^b\xi_2^{-2}\right]\\
& +\left[4\omega_\beta\omega_{\kappa_2}\zeta_{\kappa_2}+2\omega_{\kappa_2}^2\zeta_\beta\right]\left[\mathcal{G}_b^1+r_*^b(\|\eta^b\|_2+r_*^b)\xi_2^{-2}\right]+2\omega_b^2\Big\{\ell(\xi_2)+2\zeta_{\kappa_2}^2\zeta_\beta\xi_2^{-2}\Big\}.
\end{aligned}
$$

Furthermore, for $1 \le k \le K$:

$$
\begin{aligned}
R_k^a = {} & 2\omega_a\xi_1^{-k}\left[\omega_\beta\zeta_{\kappa_1}^2+2\omega_{\kappa_1}\zeta_{\kappa_1}\zeta_\beta+\omega_{\kappa_1}k^2\right]\\
& +\left[2\omega_\beta\omega_{\kappa_1}\zeta_{\kappa_1}+\omega_{\kappa_1}^2\zeta_\beta\right]\left[2|\eta_k^a|+r_*^a\xi_1^{-k}\right]\\
& +6\omega_a k^2\left[\omega_{\kappa_1}\zeta_\mu+\omega_\mu\zeta_{\kappa_1}\right]\left[\mathcal{D}_{a,k}^2+r_*^a(\|\eta^a\|_1+r_*^a)\xi_1^{-k}\right]\\
& +k^2\omega_\mu\omega_{\kappa_1}\left[2\mathcal{G}_{a,k}^3+3r_*^a(\|\eta^a\|_1+r_*^a)^2\xi_1^{-k}\right]+3\zeta_{\kappa_1}\zeta_\mu\omega_a^2k^2\left[2\mathcal{F}_{a,k}^2+r_*^a\xi_1^{-k}\right].
\end{aligned}
$$

In the tails ($k \ge K+1$), we split in terms with and without k^2. We set

$$
\begin{aligned}
\Delta_0^a &= 2\omega_a\left[\omega_\beta\zeta_{\kappa_1}^2+2\omega_{\kappa_1}\zeta_{\kappa_1}\zeta_\beta\right]+r_*^a\left[2\omega_\beta\omega_{\kappa_1}\zeta_{\kappa_1}+\omega_{\kappa_1}^2\zeta_\beta\right]\\
\Delta_1^a &= 2\omega_a\omega_{\kappa_1}+6\omega_a\left[\omega_{\kappa_1}\zeta_\mu+\omega_\mu\zeta_{\kappa_1}\right]\left[\mathcal{D}_a^3+r_*^a(\|\eta^a\|_1+r_*^a)\right]\\
&\qquad +\omega_\mu\omega_{\kappa_1}\left[\mathcal{G}_a^4+3r_*^a(\|\eta^a\|_1+r_*^a)^2\right]+3\zeta_{\kappa_1}\zeta_\mu\omega_a^2\left[2\mathcal{F}_a^3+r_*^a\right],
\end{aligned}
$$

and we obtain (analogous to Section A.6)

$$
R_\infty^a \stackrel{\text{def}}{=} [\Delta_0^a+\Delta_1^a(K+1)^2]\mathcal{L}_K^a,
$$

where we have assumed, as before, that $(K+1)^2 \ge \overline{\kappa}_1 G(\overline{\beta})$.

Similarly, for $1 \le m_\infty \le M$

$$
\begin{aligned}
R_m^b = {} & 2\omega_b\xi_2^{-|m|}\left[\omega_\beta\zeta_{\kappa_2}^2+2\omega_{\kappa_2}\zeta_{\kappa_2}\zeta_\beta+\omega_{\kappa_2}\mathbf{m}^2\right]\\
& +\left[2\omega_\beta\omega_{\kappa_2}\zeta_{\kappa_2}+\omega_{\kappa_2}^2\zeta_\beta\right]\left[2|\eta_m^b|+r_*^b\xi_2^{-|m|}\right]\\
& +6\omega_b\mathbf{m}^2\left[\omega_{\kappa_2}\zeta_\mu+\omega_\mu\zeta_{\kappa_2}\right]\left[\mathcal{D}_{b,m}^2+r_*^b(\|\eta^b\|_2+r_*^b)\xi_2^{-|m|}\right]\\
& +\mathbf{m}^2\omega_\mu\omega_{\kappa_2}\left[2\mathcal{G}_{b,m}^3+3r_*^b(\|\eta^b\|_2+r_*^b)^2\xi_2^{-|m|}\right]+3\zeta_{\kappa_2}\zeta_\mu\omega_b^2\mathbf{m}^2\left[2\mathcal{F}_{b,m}^2+r_*^b\xi_2^{-|m|}\right].
\end{aligned}
$$

Finally,

$$\begin{aligned}
\Delta_0^b &= 2\omega_b \left[\omega_\beta \zeta_{\kappa_2}^2 + 2\omega_{\kappa_2}\zeta_{\kappa_2}\zeta_\beta\right] + r_*^b \left[2\omega_\beta\omega_{\kappa_2}\zeta_{\kappa_2} + \omega_{\kappa_2}^2\zeta_\beta\right] \\
\Delta_1^b &= 2\omega_b\omega_{\kappa_2} + 6\omega_b\left[\omega_{\kappa_2}\zeta_\mu + \omega_\mu\zeta_{\kappa_2}\right]\left[\mathcal{D}_b^3 + r_*^b(\|\eta^b\|_2 + r_*^b)\right] \\
&\quad + \omega_\mu\omega_{\kappa_2}\left[\mathcal{G}_b^4 + 3r_*^b(\|\eta^b\|_2 + r_*^b)^2\right] + 3\zeta_{\kappa_2}\zeta_\mu\omega_b^2\left[2\mathcal{F}_b^3 + r_*^b\right],
\end{aligned}$$

and

$$R_\infty^b \stackrel{\text{def}}{=} [\Delta_0^b + \Delta_1^b(M+1)^2]\mathcal{L}_M^b,$$

where we have assumed, as before, that $(M+1)^2 \geq \overline{\kappa}_2 G(\overline{\beta})$.

B Analytic details for the limit problem

B.1 Splitting of $\tilde{f}$

We write $\tilde{f}(x;\mu) = g(x) + \mu h(x;\mu)$. For convenience we introduce the notation $\widetilde{\pi}F(x;\mu) \stackrel{\text{def}}{=} \mu^{-1}[F(x;\mu) - F(x;0)]$, so that, in particular, $\widetilde{\pi}\tilde{f} = h$. More importantly,

$$\begin{aligned}
\widetilde{\pi}\langle a^3\rangle &= 3\langle \hat{a}^2\tilde{a}\rangle + 3\mu\langle \hat{a}\tilde{a}^2\rangle + \mu^2\langle\tilde{a}^3\rangle \\
\widetilde{\pi}\langle a^4\rangle &= 4\langle \hat{a}^3\tilde{a}\rangle + 6\mu\langle \hat{a}^2\tilde{a}^2\rangle + 4\mu^2\langle\hat{a}\tilde{a}^3\rangle + \mu^3\langle\tilde{a}^4\rangle,
\end{aligned}$$

which are used below, and analogous expressions hold for the convolutions of b.

The explicit expressions for the splitting are

$$\begin{aligned}
g_2^c &\stackrel{\text{def}}{=} 4\tilde{\beta}\hat{a}_1^2 + \tfrac{1}{2}\left[\langle\hat{a}^4\rangle_0 - 1\right] - \left\{4\tilde{\beta}\left[2\hat{b}_1^2 + \hat{b}_2^2\right] + \tfrac{1}{2}\left[\langle\hat{b}^4\rangle_0 - 1\right]\right\} \\
g_3^c &\stackrel{\text{def}}{=} -2\left[\tilde{\kappa}_1 + 4\tilde{\beta}\right]\hat{a}_1^2 \\
g_4^c &\stackrel{\text{def}}{=} -2\left[\tilde{\kappa}_2 + 16\tilde{\beta}\right]\left[2\hat{b}_1^2 + \hat{b}_2^2\right] \\
g_1^a &\stackrel{\text{def}}{=} 4\tilde{\beta}\hat{a}_1 + 2\langle\hat{a}^3\rangle_1 \\
g_k^a &\stackrel{\text{def}}{=} \left[k^4 - 2k^2 + 1\right]\tilde{a}_k + 2k^2\langle\hat{a}^3\rangle_k \\
g_{m'}^b &\stackrel{\text{def}}{=} 64\tilde{\beta}\hat{b}_{m'} + 32\langle\hat{b}^3\rangle_{m'} \\
g_m^b &\stackrel{\text{def}}{=} \left[\mathbf{m}^4 - 8\mathbf{m}^2 + 16\right]\tilde{b}_m + 8\mathbf{m}^2\langle\hat{b}^3\rangle_m
\end{aligned}$$

for $k \in \mathbb{N}_1$, $m \in \mathbb{N}_1^2$, $m' \in \{(1,1),(2,0)\}$, and

$$\begin{aligned}
h_2^c &\stackrel{\text{def}}{=} 2\left[\tilde{\kappa}_1\tilde{\beta} + \tfrac{1}{4}\kappa_1^{-1}\tilde{\kappa}_1^2\right]\hat{a}_1^2 + \sum_{k\in\mathbb{Z}_1}\left[\kappa_1^{-1}k^2 - 1 + \kappa_1\beta k^{-2}\right]\tilde{a}_k^2 + \tfrac{1}{2}\widetilde{\pi}\langle a^4\rangle_0 \\
&\quad - \left\{\tfrac{1}{2}\left[\tilde{\kappa}_2\tilde{\beta} + \tfrac{1}{4}\kappa_2^{-1}\tilde{\kappa}_2^2\right]\left[2\hat{b}_1^2 + \hat{b}_2^2\right] + \sum_{k\in\mathbb{Z}_1^2}\left[\kappa_2^{-1}\mathbf{m}^2 - 1 + \kappa_2\beta\mathbf{m}^{-2}\right]\tilde{b}_m^2 + \tfrac{1}{2}\widetilde{\pi}\langle b^4\rangle_0\right\} \\
h_3^c &\stackrel{\text{def}}{=} -2\left[(4\tilde{\kappa}_1 + \mu\tilde{\kappa}_1^2)\tilde{\beta} + \tfrac{1}{4}\tilde{\kappa}_1^2\right]\hat{a}_1^2 + \sum_{k\in\mathbb{Z}_1}\left(k^2 - \kappa_1^2\beta k^{-2}\right)\tilde{a}_k^2 \\
h_4^c &\stackrel{\text{def}}{=} -\tfrac{1}{2}\left[(16\tilde{\kappa}_2 + \mu\tilde{\kappa}_2^2)\tilde{\beta} + \tfrac{1}{4}\tilde{\kappa}_2^2\right]\left[2\hat{b}_1^2 + \hat{b}_2^2\right] + \sum_{m\in\mathbb{Z}_1^2}\left(\mathbf{m}^2 - \kappa_2^2\beta\mathbf{m}^{-2}\right)\tilde{b}_m^2 \\
h_1^a &\stackrel{\text{def}}{=} \left[(4\tilde{\kappa}_1 + \mu\tilde{\kappa}_1^2)\tilde{\beta} + \tfrac{1}{4}\tilde{\kappa}_1^2\right]\hat{a}_1 + \tilde{\kappa}_1\langle a^3\rangle_1 + 2\widetilde{\pi}\langle a^3\rangle_1 \\
h_k^a &\stackrel{\text{def}}{=} \left[-\tilde{\kappa}_1 k^2 + \tilde{\kappa}_1 + \kappa_1^2\tilde{\beta} + \tfrac{1}{4}\mu\tilde{\kappa}_1^2\right]\tilde{a}_k + \tilde{\kappa}_1 k^2\langle a^3\rangle_k + 2k^2\widetilde{\pi}\langle a^3\rangle_k \\
h_{m'}^b &\stackrel{\text{def}}{=} \left[(16\tilde{\kappa}_2 + \mu\tilde{\kappa}_2^2)\tilde{\beta} + \tfrac{1}{4}\tilde{\kappa}_2^2\right]\hat{b}_{m'} + 4\tilde{\kappa}_2\langle b^3\rangle_{m'} + 32\widetilde{\pi}\langle b^3\rangle_{m'} \\
h_m^b &\stackrel{\text{def}}{=} \left[-\tilde{\kappa}_2\mathbf{m}^2 + 4\tilde{\kappa}_2 + \kappa_2^2\tilde{\beta} + \tfrac{1}{4}\mu\tilde{\kappa}_2^2\right]\tilde{b}_m + \tilde{\kappa}_2\mathbf{m}^2\langle b^3\rangle_m + 8\mathbf{m}^2\widetilde{\pi}\langle b^3\rangle_m.
\end{aligned}$$

B.2 The first derivative

We use notation as before, in particular $v^a_0 = 0$ and $v^b_0 = 0$, and in addition we write

$$v^a = v^{\hat{a}} + \mu v^{\tilde{a}} \qquad \text{and} \qquad v^b = v^{\hat{b}} + \mu v^{\tilde{a}}.$$

We compute the derivative of g:

$$\begin{aligned}
Dg^c_2 v &= 4v_{\tilde{\beta}}\hat{a}_1^2 + 8\tilde{\beta}\hat{a}_1 v_1^{\hat{a}} + 2\langle \hat{a}^3 v^{\hat{a}}\rangle_0 - \left\{4v_{\tilde{\beta}}\left[2\hat{b}_1^2 + \hat{b}_2^2\right] + 8\tilde{\beta}\left[2\hat{b}_1 v_1^{\hat{b}} + \hat{b}_2 v_2^{\hat{b}}\right] + 2\langle \hat{b}^3 v^{\hat{b}}\rangle_0\right\}\\
Dg^c_3 v &= -2\left[v_{\tilde{\kappa}_1} + 4v_{\tilde{\beta}}\right]\hat{a}_1^2 - 4\left[\tilde{\kappa}_1 + 4\tilde{\beta}\right]\hat{a}_1 v_1^{\hat{a}}\\
Dg^c_4 v &= -2\left[v_{\tilde{\kappa}_2} + 16v_{\tilde{\beta}}\right]\left[2\hat{b}_1^2 + \hat{b}_2^2\right] - 4\left[\tilde{\kappa}_2 + 16\tilde{\beta}\right]\left[2\hat{b}_1 v_1^{\hat{b}} + \hat{b}_2 v_2^{\hat{b}}\right]\\
Dg^a_1 v &= 4v_{\tilde{\beta}}\hat{a}_1 + 4\tilde{\beta}v_1^{\hat{a}} + 6\langle \hat{a}^2 v^{\hat{a}}\rangle_1\\
Dg^a_k v &= \left[k^4 - 2k^2 + 1\right] v_k^{\tilde{a}} + 6k^2\langle \hat{a}^2 v^{\hat{a}}\rangle_k\\
Dg^b_{m'} v &= 64v_{\tilde{\beta}}\hat{b}_{m'} + 64\tilde{\beta}v_{m'}^{\hat{b}} + 96\langle \hat{b}^2 v^{\hat{b}}\rangle_{m'}\\
Dg^b_m v &= \left[\mathbf{m}^4 - 8\mathbf{m}^2 + 16\right] v_m^{\tilde{b}} + 24\mathbf{m}^2\langle \hat{b}^2 v^{\hat{b}}\rangle_m.
\end{aligned}$$

Next, the derivatives of h are, for $k \geq 2$, $m \in \mathbb{N}_1^2$ and $m' \in \{(1,1),(2,0)\}$,

$$\begin{aligned}
D_x h_2^c v = {}& 2\big[v_{\tilde\kappa_1}\tilde\beta + \tilde\kappa_1 v_{\tilde\beta} + \tfrac{1}{2}\kappa_1^{-1} v_{\tilde\kappa_1}\tilde\kappa_1 - \tfrac{1}{4} v_{\tilde\kappa_1}\kappa_1^{-2}\mu\tilde\kappa_1^2\big]\hat a_1^2 + [4\tilde\kappa_1\tilde\beta + \kappa_1^{-1}\tilde\kappa_1^2]\hat a_1 v_1^{\hat a} \\
& - v_{\tilde\kappa_1}\mu\kappa_1^{-2}\sum_{k\in\mathbb{Z}_1} k^2\tilde a_k^2 + \mu(v_{\tilde\kappa_1}\beta + v_{\tilde\beta}\kappa_1)\sum_{k\in\mathbb{Z}_1} k^{-2}\tilde a_k^2 \\
& + 2\sum_{k\in\mathbb{Z}_1}(\kappa_1^{-1}k^2 - 1 + \kappa_1\beta k^{-2})\tilde a_k v_k^{\tilde a} + 2\widetilde{\pi}\langle a^3 v^a\rangle_0 \\
& - \Big\{ \tfrac{1}{2}\big[v_{\tilde\kappa_2}\tilde\beta + \tilde\kappa_2 v_{\tilde\beta} + \tfrac{1}{2}\kappa_2^{-1} v_{\tilde\kappa_2}\tilde\kappa_2 - \tfrac{1}{4} v_{\tilde\kappa_2}\kappa_2^{-2}\mu\tilde\kappa_2^2\big][2\hat b_1^2 + \hat b_2^2] + [\tilde\kappa_2\tilde\beta + \tfrac{1}{4}\kappa_2^{-1}\tilde\kappa_2^2][2\hat b_1 v_1^{\hat b} + \hat b_2 v_2^{\hat b}] \\
& \quad - v_{\tilde\kappa_2}\mu\kappa_2^{-2}\sum_{m\in\mathbb{Z}_1^2}\mathbf{m}^2\tilde b_m^2 + \mu(v_{\tilde\kappa_2}\beta + v_{\tilde\beta}\kappa_2)\sum_{m\in\mathbb{Z}_1^2}\mathbf{m}^{-2}\tilde b_m^2 \\
& \quad + 2\sum_{m\in\mathbb{Z}_1^2}(\kappa_2^{-1}\mathbf{m}^2 - 1 + \kappa_2\beta\mathbf{m}^{-2})\tilde b_m v_m^{\tilde b} + 2\widetilde{\pi}\langle b^3 v^b\rangle_0 \Big\}, \\
D_x h_3^c v = {}& -2[v_{\tilde\kappa_1}(4 + 2\mu\tilde\kappa_1)\tilde\beta + (4\tilde\kappa_1 + \mu\tilde\kappa_1^2)v_{\tilde\beta} + \tfrac{1}{2}v_{\tilde\kappa_1}\tilde\kappa_1]\hat a_1^2 - 4[(4\tilde\kappa_1 + \mu\tilde\kappa_1^2)\tilde\beta + \tfrac{1}{4}\tilde\kappa_1^2]\hat a_1 v_1^{\hat a} \\
& - \mu[v_{\tilde\beta}\kappa_1^2 + 2v_{\tilde\kappa_1}\kappa_1\beta]\sum_{k\in\mathbb{Z}_1} k^{-2}\tilde a_k^2 + 2\sum_{k\in\mathbb{Z}_1}(k^2 - \kappa_1^2\beta k^{-2})\tilde a_k v_k^{\tilde a}, \\
D_x h_4^c v = {}& -\tfrac{1}{2}[v_{\tilde\kappa_2}(16 + 2\mu\tilde\kappa_2)\tilde\beta + (16\tilde\kappa_2 + \mu\tilde\kappa_2^2)v_{\tilde\beta} + \tfrac{1}{2}v_{\tilde\kappa_2}\tilde\kappa_2][2\hat b_1^2 + \hat b_2^2] \\
& - [(16\tilde\kappa_2 + \mu\tilde\kappa_2^2)\tilde\beta + \tfrac{1}{4}\tilde\kappa_2^2][2\hat b_1 v_1^{\hat b} + \hat b_2 v_2^{\hat b}] \\
& - \mu[v_{\tilde\beta}\kappa_2^2 + 2v_{\tilde\kappa_2}\kappa_2\beta]\sum_{m\in\mathbb{Z}_1^2}\mathbf{m}^{-2}\tilde b_m^2 + 2\sum_{m\in\mathbb{Z}_1^2}(\mathbf{m}^2 - \kappa_2^2\beta\mathbf{m}^{-2})\tilde b_m v_m^{\tilde b}. \\
D_x h_1^a v = {}& [v_{\tilde\kappa_1}(4 + 2\mu\tilde\kappa_1)\tilde\beta + (4\tilde\kappa_1 + \mu\tilde\kappa_1^2)v_{\tilde\beta} + \tfrac{1}{2}v_{\tilde\kappa_1}\tilde\kappa_1]\hat a_1 + [(4\tilde\kappa_1 + \mu\tilde\kappa_1^2)\tilde\beta + \tfrac{1}{4}\tilde\kappa_1^2]v^{\hat a} \\
& + v_{\tilde\kappa_1}\langle a^3\rangle_1 + 3\tilde\kappa_1\langle a^2 v^a\rangle_1 + 6\widetilde{\pi}\langle a^2 v^a\rangle_1, \\
D_x h_k^a v = {}& [-v_{\tilde\kappa_1}k^2 + 2v_{\tilde\kappa_1}\kappa_1\beta + \kappa_1^2 v_{\tilde\beta}]\tilde a_k + [-\tilde\kappa_1 k^2 + \tilde\kappa_1 + \kappa_1^2\tilde\beta + \tfrac{1}{4}\mu\tilde\kappa_1^2]v_k^{\tilde a} \\
& + v_{\tilde\kappa_1}k^2\langle a^3\rangle_k + 3\tilde\kappa_1 k^2\langle a^2 v^a\rangle_k + 6k^2\widetilde{\pi}\langle a^2 v^a\rangle_k, \\
D_x h_{m'}^b v = {}& [v_{\tilde\kappa_2}(16 + 2\mu\tilde\kappa_2)\tilde\beta + (16\tilde\kappa_2 + \mu\tilde\kappa_2^2)v_{\tilde\beta} + \tfrac{1}{2}v_{\tilde\kappa_2}\tilde\kappa_2]\hat b_{m'} + [(16\tilde\kappa_2 + \mu\tilde\kappa_2^2)\tilde\beta + \tfrac{1}{4}\tilde\kappa_2^2]v_{m'}^{\hat b} \\
& + 4v_{\tilde\kappa_2}\langle b^3\rangle_{m'} + 12\tilde\kappa_2\langle b^2 v^b\rangle_{m'} + 96\widetilde{\pi}\langle b^2 v^b\rangle_{m'}, \\
D_x h_m^b v = {}& [-v_{\tilde\kappa_2}\mathbf{m}^2 + 2v_{\tilde\kappa_2}\kappa_2\beta + \kappa_2^2 v_{\tilde\beta}]\tilde b_m + [-\tilde\kappa_2\mathbf{m}^2 + 4\tilde\kappa_2 + \kappa_2^2\tilde\beta + \tfrac{1}{4}\mu\tilde\kappa_2^2]v_m^{\tilde b} \\
& + v_{\tilde\kappa_2}\mathbf{m}^2\langle b^3\rangle_m + 3\tilde\kappa_2\mathbf{m}^2\langle b^2 v^b\rangle_m + 24\mathbf{m}^2\widetilde{\pi}\langle b^2 v^b\rangle_m,
\end{aligned}$$

where we have used the identity $2\kappa_1\beta = (1 + 2\mu\kappa_1\tilde\beta + \frac{1}{2}\mu\tilde\kappa_1)$, as well as the shorthand notation

$$\widetilde{\pi}\langle a^2 v^a\rangle = 2\langle\hat a\tilde a v^{\hat a}\rangle + \mu\langle\tilde a^2 v^{\hat a}\rangle + \langle a^2 v^{\tilde a}\rangle \tag{B.1a}$$

$$\widetilde{\pi}\langle a^3 v^a\rangle = 3\langle\hat a^2\tilde a v^{\hat a}\rangle + 3\mu\langle\hat a\tilde a^2 v^{\hat a}\rangle + \mu^2\langle\tilde a^3 v^{\hat a}\rangle + \langle a^3 v^{\tilde a}\rangle. \tag{B.1b}$$

Finally, the derivative of h with respect to μ are

$$
\begin{aligned}
D_\mu h_2^c &= -\tfrac{1}{2}\kappa_1^{-2}\tilde{\kappa}_1^3\hat{a}_1^2 + \sum_{k\in\mathbb{Z}_1}\left[-\kappa_1^{-2}\tilde{\kappa}_1 k^2 + (\tilde{\kappa}_1\beta+\kappa_1\tilde{\beta})k^{-2}\right]\tilde{a}_k^2 + \tfrac{1}{2}[6\langle\hat{a}^2\tilde{a}^2\rangle_0 + 8\mu\langle\hat{a}\tilde{a}^3\rangle_0 + 3\mu^2\langle\tilde{a}^4\rangle_0] \\
&\quad - \Bigg\{-\tfrac{1}{8}\kappa_2^{-2}\tilde{\kappa}_2^3\left[2\hat{b}_1^2+\hat{b}_2^2\right] + \sum_{k\in\mathbb{Z}_1^2}\left[-\kappa_2^{-2}\tilde{\kappa}_2\mathbf{m}^2 + (\tilde{\kappa}_2\beta+\kappa_2\tilde{\beta})\mathbf{m}^{-2}\right]\tilde{b}_m^2 \\
&\qquad\qquad + \tfrac{1}{2}[6\langle\hat{b}^2\tilde{b}^2\rangle_0 + 8\mu\langle\hat{b}\tilde{b}^3\rangle_0 + 3\mu^2\langle\tilde{b}^4\rangle_0]\Bigg\} \\
D_\mu h_3^c &= -2\tilde{\kappa}_1^2\tilde{\beta}\hat{a}_1^2 - (2\tilde{\kappa}_1\kappa_1\beta+\kappa_1^2\tilde{\beta})\sum_{k\in\mathbb{Z}_1}k^{-2}\tilde{a}_k^2 \\
D_\mu h_4^c &= -\tfrac{1}{2}\tilde{\kappa}_2^2\tilde{\beta}\left[2\hat{b}_1^2+\hat{b}_2^2\right] - (2\tilde{\kappa}_2\kappa_2\beta+\kappa_2^2\tilde{\beta})\sum_{m\in\mathbb{Z}_1^2}\mathbf{m}^{-2}\tilde{b}_m^2 \\
D_\mu h_1^a &= \tilde{\kappa}_1^2\tilde{\beta}\hat{a}_1 + 3\tilde{\kappa}_1[\langle\hat{a}^2\tilde{a}\rangle_1 + 2\mu\langle\hat{a}\tilde{a}^2\rangle_1 + \mu^2\langle\tilde{a}^3\rangle_1] + 2[3\langle\hat{a}\tilde{a}^2\rangle_1 + 2\mu\langle\tilde{a}^3\rangle_1] \\
D_\mu h_k^a &= (2\kappa_1\tilde{\kappa}_1\tilde{\beta}+\tfrac{1}{4}\tilde{\kappa}_1^2)\tilde{a}_k + 3\tilde{\kappa}_1 k^2[\langle\hat{a}^2\tilde{a}\rangle_k + 2\mu\langle\hat{a}\tilde{a}^2\rangle_k + \mu^2\langle\tilde{a}^3\rangle_k] + 2k^2[3\langle\hat{a}\tilde{a}^2\rangle_k + 2\mu\langle\tilde{a}^3\rangle_k] \\
D_\mu h_{m'}^b &= \tilde{\kappa}_2^2\tilde{\beta}\hat{b}_{m'} + 12\tilde{\kappa}_2[\langle\hat{b}^2\tilde{b}\rangle_{m'} + 2\mu\langle\hat{b}\tilde{b}^2\rangle_{m'} + \mu^2\langle\tilde{b}^3\rangle_{m'}] + 32[3\langle\hat{b}\tilde{b}^2\rangle_{m'} + 2\mu\langle\tilde{b}^3\rangle_{m'}] \\
D_\mu h_m^b &= (2\kappa_2\tilde{\kappa}_2\tilde{\beta}+\tfrac{1}{4}\tilde{\kappa}_2^2)\tilde{b}_m + 3\tilde{\kappa}_2\mathbf{m}^2[\langle\hat{b}^2\tilde{b}\rangle_m + 2\mu\langle\hat{b}\tilde{b}^2\rangle_m + \mu^2\langle\tilde{b}^3\rangle_m] + 8\mathbf{m}^2[3\langle\hat{b}\tilde{b}^2\rangle_m + 2\mu\langle\tilde{b}^3\rangle_m]
\end{aligned}
$$

B.3 The second derivative

Only the second derivative of g is used, which is quite compact (using the notation (A.1)):

$$
\begin{aligned}
D^2 g_2^c &= 8[v_{\tilde{\beta}}w_1^{\hat{a}} + w_{\tilde{\beta}}v_1^{\hat{a}}]\hat{a}_1 + 8\tilde{\beta}w_1^{\hat{a}}v_1^{\hat{a}} + 6\langle\hat{a}^2v^{\hat{a}}w^{\hat{a}}\rangle_0 \\
&\quad - \left\{8v_{\tilde{\beta}}\left[2\hat{b}_1w_1^{\hat{b}}+\hat{b}_2w_2^{\hat{b}}\right] + 8w_{\tilde{\beta}}\left[2\hat{b}_1v_1^{\hat{b}}+\hat{b}_2v_2^{\hat{b}}\right] + 8\tilde{\beta}\left[2w_1^{\hat{b}}v_1^{\hat{b}}+w_2^{\hat{b}}v_2^{\hat{b}}\right] + 6\langle\hat{b}^2v^{\hat{b}}w^{\hat{b}}\rangle_0\right\} \\
D^2 g_3^c &= -4\left[v_{\tilde{\kappa}_1}+4v_{\tilde{\beta}}\right]\hat{a}_1w_1^{\hat{a}} - 4\left[w_{\tilde{\kappa}_1}+4w_{\tilde{\beta}}\right]\hat{a}_1v_1^{\hat{a}} - 4\left[\tilde{\kappa}_1+4\tilde{\beta}\right]v_1^{\hat{a}}w_1^{\hat{a}} \\
D^2 g_4^c &= -4\left[v_{\tilde{\kappa}_2}+16v_{\tilde{\beta}}\right]\left[2\hat{b}_1w_1^{\hat{b}}+\hat{b}_2w_2^{\hat{b}}\right] - 4\left[w_{\tilde{\kappa}_2}+16w_{\tilde{\beta}}\right]\left[2\hat{b}_1v_1^{\hat{b}}+\hat{b}_2v_2^{\hat{b}}\right] \\
&\qquad - 4\left[\tilde{\kappa}_2+16\tilde{\beta}\right]\left[2v_1^{\hat{b}}w_1^{\hat{b}}+v_2^{\hat{b}}w_2^{\hat{b}}\right] \\
D^2 g_1^a &= 4v_{\tilde{\beta}}w_1^{\hat{a}} + 4w_{\tilde{\beta}}v_1^{\hat{a}} + 12\langle\hat{a}v^{\hat{a}}w^{\hat{a}}\rangle_1 \\
D^2 g_k^a &= 12k^2\langle\hat{a}v^{\hat{a}}w^{\hat{a}}\rangle_k \\
D^2 g_{m'}^b &= 64v_{\tilde{\beta}}w_{m'}^{\hat{b}} + 64w_{\tilde{\beta}}v_{m'}^{\hat{b}} + 192\langle\hat{b}v^{\hat{b}}w^{\hat{b}}\rangle_{m'} \\
D^2 g_m^b &= 48\mathbf{m}^2\langle\hat{b}v^{\hat{b}}w^{\hat{b}}\rangle_m
\end{aligned}
$$

We note that $D^2g_k^a = 0$ for $k > 3$ and $D^2g_m^b = 0$ for $m_\infty > 6$.

B.4 Estimates for Q

We define intervals $\eta \overset{\text{def}}{=} [\overline{x}, \overline{x} + \mu_* \underline{x}]$ with the appropriate symmetry in the components of $\eta^{\hat{a}}$, $\eta^{\hat{b}}$, $\eta^{\tilde{a}}$ and $\eta^{\tilde{b}}$. With $\delta^{\hat{a}}$ and $\delta^{\hat{b}}$ defined in (8.3), we find the estimates

$$\begin{aligned}
Q_2^c &= 8\omega_{\tilde{\beta}}|\underline{\hat{a}}_1||\eta_1^{\hat{a}}| + 8\omega_{\hat{a}}\left|\underline{\tilde{\beta}}\eta_1^{\hat{a}} + \eta_{\tilde{\beta}}\underline{\hat{a}}_1\right| + 6\omega_{\hat{a}}\langle|\langle(\eta^{\hat{a}})^2\underline{\hat{a}}\rangle|\delta^{\hat{a}}\rangle_0 \\
&\quad + \left\{8\omega_{\tilde{\beta}}\left|2\eta_1^{\hat{b}}\underline{\hat{b}}_1 + \eta_2^{\hat{b}}\underline{\hat{b}}_2\right| + 8\omega_{\hat{b}}\left(2\left|\underline{\tilde{\beta}}\eta_1^{\hat{b}} + \eta_{\tilde{\beta}}\underline{\hat{b}}_1\right| + \left|\underline{\tilde{\beta}}\eta_2^{\hat{b}} + \eta_{\tilde{\beta}}\underline{\hat{b}}_2\right|\right) + 6\omega_{\hat{b}}\langle|\langle(\eta^{\hat{b}})^2\underline{\hat{b}}\rangle|\delta^{\hat{b}}\rangle_0\right\} \\
Q_3^c &= 4\left[\omega_{\tilde{\kappa}_1} + 4\omega_{\tilde{\beta}}\right]|\eta_1^{\hat{a}}||\underline{\hat{a}}_1| + 4\omega_{\hat{a}}\left|\left[\underline{\tilde{\kappa}}_1 + 4\underline{\tilde{\beta}}\right]\eta_1^{\hat{a}} + \left[\eta_{\tilde{\kappa}_1} + 4\eta_{\tilde{\beta}}\right]\underline{\hat{a}}_1\right| \\
Q_4^c &= 4\left[\omega_{\tilde{\kappa}_2} + 16\omega_{\tilde{\beta}}\right]\left|2\eta_1^{\hat{b}}\underline{\hat{b}}_1 + \eta_2^{\hat{b}}\underline{\hat{b}}_2\right| \\
&\quad + 4\omega_{\hat{b}}\left(2\left|\left[\underline{\tilde{\kappa}}_2 + 16\underline{\tilde{\beta}}\right]\eta_1^{\hat{b}} + \left[\eta_{\tilde{\kappa}_2} + 16\eta_{\tilde{\beta}}\right]\underline{\hat{b}}_1\right| + \left|\left[\underline{\tilde{\kappa}}_2 + 16\underline{\tilde{\beta}}\right]\eta_2^{\hat{b}} + \left[\eta_{\tilde{\kappa}_2} + 16\eta_{\tilde{\beta}}\right]\underline{\hat{b}}_2\right|\right) \\
Q_1^a &= 4\omega_{\tilde{\beta}}|\underline{\hat{a}}_1| + 4\omega_{\hat{a}}|\underline{\tilde{\beta}}| + 12\omega_{\hat{a}}\langle|\langle\eta^{\hat{a}}\underline{\hat{a}}\rangle|\delta^{\hat{a}}\rangle_1 \\
Q_k^a &= 12k^2\omega_{\hat{a}}\langle|\langle\eta^{\hat{a}}\underline{\hat{a}}\rangle|\delta^{\hat{a}}\rangle_k \\
Q_{m'}^b &= 64\omega_{\tilde{\beta}}|\underline{\hat{b}}_{m'}| + 64\omega_{\hat{b}}|\underline{\tilde{\beta}}| + 192\omega_{\hat{b}}\langle|\langle\eta^{\hat{b}}\underline{\hat{b}}\rangle|\delta^{\hat{b}}\rangle_{m'} \\
Q_m^b &= 48\mathbf{m}^2\omega_{\hat{b}}\langle|\langle\eta^{\hat{b}}\underline{\hat{b}}\rangle|\delta^{\hat{b}}\rangle_m.
\end{aligned}$$

B.5 Estimates for R

Let us introduce, analogously to Section A.7, the intervals

$$\begin{aligned}
\zeta_{\tilde{\beta}} &\overset{\text{def}}{=} [\overline{\tilde{\beta}}, \overline{\tilde{\beta}} + \mu_*\underline{\tilde{\beta}}] + \omega_{\tilde{\beta}}r_*[-1,1] \\
\zeta_{\tilde{\kappa}_1} &\overset{\text{def}}{=} [\overline{\tilde{\kappa}}_1, \overline{\tilde{\kappa}}_1 + \mu_*\underline{\tilde{\kappa}}_1] + \omega_{\tilde{\kappa}_1}r_*[-1,1] \\
\zeta_{\tilde{\kappa}_2} &\overset{\text{def}}{=} [\overline{\tilde{\kappa}}_2, \overline{\tilde{\kappa}}_2 + \mu_*\underline{\tilde{\kappa}}_2] + \omega_{\tilde{\kappa}_2}r_*[-1,1] \\
\zeta_k^{\hat{a}} &\overset{\text{def}}{=} [\overline{\hat{a}}_k, \overline{\hat{a}}_k + \mu_*\underline{\hat{a}}_k] + \omega_{\hat{a}}r_*[-1,1] \qquad \text{for } k = \pm 1 \\
\zeta_m^{\hat{b}} &\overset{\text{def}}{=} [\overline{\hat{b}}_m, \overline{\hat{b}}_m + \mu_*\underline{\hat{b}}_m] + \omega_{\hat{b}}r_*[-1,1] \qquad \text{for } m \in \mathcal{I}^2 \setminus 0,
\end{aligned}$$

with appropriate symmetry in the components of $\zeta_k^{\hat{a}}$ and $\zeta_m^{\hat{b}}$, while

$$\begin{aligned}
\zeta_0^{\hat{a}} &\overset{\text{def}}{=} 1 \qquad \text{and} \qquad \zeta_k^{\hat{a}} \overset{\text{def}}{=} 0 \quad \text{for } k \notin \mathcal{I}^1 \\
\zeta_0^{\hat{b}} &\overset{\text{def}}{=} 1 \qquad \text{and} \qquad \zeta_m^{\hat{b}} \overset{\text{def}}{=} 0 \quad \text{for } m \notin \mathcal{I}^2.
\end{aligned}$$

With $\delta^{\hat{a}}$ and $\delta^{\hat{b}}$ defined in (8.3) we obtain

$$\begin{aligned}
R_2^c &= 16\omega_{\tilde{\beta}}\omega_{\hat{a}}|\zeta_1^{\hat{a}}| + 8\omega_{\hat{a}}^2|\zeta_{\tilde{\beta}}| + 6\omega_{\hat{a}}^2\langle|\langle(\zeta^{\hat{a}})^2\rangle|(\delta^{\hat{a}})^2\rangle_0 \\
&\quad + \left\{16\omega_{\tilde{\beta}}\omega_{\hat{b}}\left[2|\zeta_1^{\hat{b}}| + |\zeta_2^{\hat{b}}|\right] + 24\omega_{\hat{b}}^2|\zeta_{\tilde{\beta}}| + 6\omega_{\hat{b}}^2\langle|\langle(\zeta^{\hat{b}})^2\rangle|(\delta^{\hat{b}})^2\rangle_0\right\} \\
R_3^c &= 8\omega_{\hat{a}}\left[\omega_{\tilde{\kappa}_1} + 4\omega_{\tilde{\beta}}\right]|\zeta_1^{\hat{a}}| + 4\omega_{\hat{a}}^2\left|\zeta_{\tilde{\kappa}_1} + 4\zeta_{\tilde{\beta}}\right| \\
R_4^c &= 8\omega_{\hat{b}}\left[\omega_{\tilde{\kappa}_2} + 16\omega_{\tilde{\beta}}\right]\left[2|\zeta_1^{\hat{b}}| + |\zeta_2^{\hat{b}}|\right] + 12\omega_{\hat{b}}^2\left|\zeta_{\tilde{\kappa}_2} + 16\zeta_{\tilde{\beta}}\right| \\
R_1^a &= 8\omega_{\tilde{\beta}}\omega_{\hat{a}} + 12\omega_{\hat{a}}^2\langle|\zeta^{\hat{a}}|(\delta^{\hat{a}})^2\rangle_1 \\
R_k^a &= 12k^2\omega_{\hat{a}}^2\langle|\zeta^{\hat{a}}|(\delta^{\hat{a}})^2\rangle_k \\
R_{m'}^b &= 128\omega_{\tilde{\beta}}\omega_{\hat{b}} + +192\omega_{\hat{b}}^2\langle|\zeta^{\hat{b}}|(\delta^{\hat{b}})^2\rangle_{m'} \\
R_m^b &= 48\mathbf{m}^2\omega_{\hat{b}}^2\langle|\zeta^{\hat{b}}|(\delta^{\hat{b}})^2\rangle_m.
\end{aligned}$$

B.6 Estimates for $\widetilde{Q}$

We fix a priori bounds r_* and μ_* on r and μ respectively, and we use the notation

$$r_*^{\tilde{a}} = r_* \omega_{\tilde{a}} \qquad \text{and} \qquad r_*^{\tilde{b}} = r_* \omega_{\tilde{b}}.$$

For all $v \in \widetilde{\mathcal{B}}$ and all $\mu \in [0, \mu_*]$, we derive the following bounds from (8.2):

$$\|v^a\|_1 \leq q_a \stackrel{\text{def}}{=} 2\omega_{\hat{a}}\xi_1 + \mu_* \omega_{\tilde{a}} \tag{B.2a}$$

$$\|v^b\|_2 \leq q_b \stackrel{\text{def}}{=} 6\omega_{\hat{b}}\xi_2^2 + \mu_* \omega_{\tilde{b}}. \tag{B.2b}$$

Furthermore, analogously to (A.8), see also Remark A.4, we introduce

$$\tilde{\ell}_1(\xi) \stackrel{\text{def}}{=} \begin{cases} (e \log \xi)^{-2} & \text{if } \xi < e^{1/2} \\ 4\xi^{-4} & \text{if } \xi \geq e^{1/2} \end{cases} \qquad \text{and} \qquad \tilde{\ell}_2(\xi) \stackrel{\text{def}}{=} \begin{cases} 3(e \log \xi)^{-2} & \text{if } \xi < e \\ 3\xi^{-2} & \text{if } \xi \geq e, \end{cases} \tag{B.3}$$

which bound $\sum_{k \in \mathbb{Z}_1} k^2 y_k^{\tilde{a}} \tilde{y}_k^{\tilde{a}}$ and $\sum_{m \in \mathbb{Z}_1^2} \mathbf{m}^2 y_m^{\tilde{b}} \tilde{y}_m^{\tilde{b}}$, respectively. Having already introduced $\eta \stackrel{\text{def}}{=} [\overline{x}, \overline{x} + \mu_* \underline{x}]$, we write $\eta^a = \eta^{\hat{a}} + [0, \mu_*]\eta^{\tilde{a}}$ and $\eta^b = \eta^{\hat{b}} + [0, \mu_*]\eta^{\tilde{b}}$. We note that

$$\eta_k^a = 0 \quad \text{for } k > K \qquad \text{and} \qquad \eta_m^b = 0 \quad \text{for } m_\infty > M.$$

The (computable) constants $\mathcal{M}$ and $\mathcal{N}$ that appear in the estimates below are listed in Table B.1. The expressions for $\mathcal{N}^5$, $\mathcal{N}^6$ and $\mathcal{N}^7$ are derived from (B.1).

With ζ as in Section B.5 and additionally (to shorten the expressions)

$$\zeta_\beta \stackrel{\text{def}}{=} \tfrac{1}{4} + [0, \mu_*]\, \zeta_{\tilde{\beta}}$$

$$\zeta_{\kappa_1} \stackrel{\text{def}}{=} 2 + [0, \mu_*]\, \zeta_{\tilde{\kappa}_1}$$

$$\zeta_{\kappa_2} \stackrel{\text{def}}{=} 8 + [0, \mu_*]\, \zeta_{\tilde{\kappa}_2},$$

term	constant	value of constant
$\sum_{k\in\mathbb{Z}_1} k^{-2}(\eta_k^{\tilde a} + r_*^{\tilde a}\tilde y_k^{\tilde a})^2$	$\mathcal{M}_a^1$	$\sum_{k\in\mathbb{Z}_1} k^{-2}(\eta_k^{\tilde a})^2 + 2r_*^{\tilde a}\Vert(k^{-2}\eta_k^{\tilde a})\Vert_1^{*1} + (r_*^{\tilde a})^2\frac{1}{4}\xi_1^{-4}$
$\sum_{m\in\mathbb{Z}_1^2} \mathbf{m}^{-2}(\eta_m^{\tilde b} + r_*^{\tilde b}\tilde y_m^{\tilde b})^2$	$\mathcal{M}_b^1$	$\sum_{m\in\mathbb{Z}_1^2} \mathbf{m}^{-2}(\eta_m^{\tilde b})^2 + 2r_*^{\tilde b}\Vert(\mathbf{m}^{-2}\eta_m^{\tilde b})\Vert_2^{*1} + (r_*^{\tilde b})^2\xi_2^{-2}$
$\sum_{k\in\mathbb{Z}_1} k^{2}(\eta_k^{\tilde a} + r_*^{\tilde a}\tilde y_k^{\tilde a})^2$	$\mathcal{M}_a^2$	$\sum_{k\in\mathbb{Z}_1} k^{2}(\eta_k^{\tilde a})^2 + 2r_*^{\tilde a}\Vert(k^{2}\eta_k^{\tilde a})\Vert_1^{*1} + (r_*^{\tilde a})^2\tilde\ell_1(\xi_1)$
$\sum_{m\in\mathbb{Z}_1^2} \mathbf{m}^{2}(\eta_m^{\tilde b} + r_*^{\tilde b}\tilde y_m^{\tilde b})^2$	$\mathcal{M}_b^2$	$\sum_{m\in\mathbb{Z}_1^2} \mathbf{m}^{2}(\eta_m^{\tilde b})^2 + 2r_*^{\tilde b}\Vert(\mathbf{m}^{2}\eta_m^{\tilde b})\Vert_2^{*1} + (r_*^{\tilde b})^2\tilde\ell_2(\xi_2)$
$\sum_{k\in\mathbb{Z}_1} k^{-2}(\eta_k^{\tilde a} + r_*^{\tilde a}\tilde y_k^{\tilde a})y_k^{\tilde a}$	$\mathcal{M}_a^3$	$\Vert(k^{-2}\eta_k^{\tilde a})\Vert_1^{*1} + r_*^{\tilde a}\frac{1}{4}\xi_1^{-4}$
$\sum_{m\in\mathbb{Z}_1^2} \mathbf{m}^{-2}(\eta_m^{\tilde b} + r_*^{\tilde b}\tilde y_m^{\tilde b})y_m^{\tilde b}$	$\mathcal{M}_b^3$	$\Vert(\mathbf{m}^{-2}\eta_m^{\tilde b})\Vert_2^{*1} + r_*^{\tilde b}\xi_2^{-2}$
$\sum_{k\in\mathbb{Z}_1} k^{2}(\eta_k^{\tilde a} + r_*^{\tilde a}\tilde y_k^{\tilde a})y_k^{\tilde a}$	$\mathcal{M}_a^4$	$\Vert(k^{2}\eta_k^{\tilde a})\Vert_1^{*1} + r_*^{\tilde a}\tilde\ell_1(\xi)$
$\sum_{k\in\mathbb{Z}_1^2} \mathbf{m}^{2}(\eta_m^{\tilde b} + r_*^{\tilde b}\tilde y_m^{\tilde b})y_m^{\tilde b}$	$\mathcal{M}_b^4$	$\Vert(\mathbf{m}^{2}\eta_m^{\tilde b})\Vert_2^{*1} + r_*^{\tilde b}\tilde\ell_2(\xi_2)$
$\sum_{k\in\mathbb{Z}_1} (\eta_k^{\tilde a} + r_*^{\tilde a}\tilde y_k^{\tilde a})y_k^{\tilde a}$	$\mathcal{M}_a^5$	$\Vert\eta_k^{\tilde a}\Vert_1^{*1} + r_*^{\tilde a}\xi_1^{-4}$
$\sum_{m\in\mathbb{Z}_1^2} (\eta_m^{\tilde b} + r_*^{\tilde b}\tilde y_m^{\tilde b})y_m^{\tilde b}$	$\mathcal{M}_b^5$	$\Vert\eta_m^{\tilde b}\Vert_2^{*1} + r_*^{\tilde b}\xi_2^{-2}$
$\langle(\eta^a + r_*\tilde v^a)^3\rangle_k$	$\mathcal{N}_{a,k}^1$	$\lvert\langle(\eta^a)^3\rangle_k\rvert + 3r_*q_a(\Vert\eta^a\Vert_1 + r_*q_a)^2\xi_1^{-k}$
$\langle(\eta^b + r_*\tilde v^b)^3\rangle_m$	$\mathcal{N}_{b,m}^1$	$\lvert\langle(\eta^b)^3\rangle_m\rvert + 3r_*q_b(\Vert\eta^b\Vert_2 + r_*q_b)^2\xi_2^{-\lvert m\rvert}$
$\Vert\langle(\eta^a + r_*\tilde v^a)^3\rangle_\infty^0\Vert_1$	$\mathcal{N}_a^2$	$\Vert\langle(\eta^a)^3\rangle_\infty^0\Vert_1 + 3r_*q_a(\Vert\eta^a\Vert_1 + r_*q_a)^2$
$\Vert\langle(\eta^b + r_*\tilde v^b)^3\rangle_\infty^0\Vert_2$	$\mathcal{N}_b^2$	$\Vert\langle(\eta^b)^3\rangle_\infty^0\Vert_2 + 3r_*q_b(\Vert\eta^b\Vert_2 + r_*q_b)^2$
$\langle(\eta^a + r_*\tilde v^a)^2v^a\rangle_k$	$\mathcal{N}_{a,k}^3$	$\omega_{\hat a}\langle\lvert\langle(\eta^a)^2\rangle\rvert\delta^{\hat a}\rangle_k + \mu_*\omega_{\tilde a}\Vert\langle(\eta^a)^2\rangle\Vert_1\xi_1^{-k}$ $+2r_*q_a^2(\Vert\eta^a\Vert_1 + r_*q_a)\xi_1^{-k}$
$\langle(\eta^b + r_*\tilde v^b)^2v^b\rangle_m$	$\mathcal{N}_{b,m}^3$	$\omega_{\hat b}\langle\lvert\langle(\eta^b)^2\rangle\rvert\delta^{\hat b}\rangle_m + \mu_*\omega_{\tilde b}\Vert\langle(\eta^b)^2\rangle\Vert_2\xi_2^{-\lvert m\rvert}$ $+2r_*q_b^2(\Vert\eta^b\Vert_2 + r_*q_b)\xi_2^{-\lvert m\rvert}$
$\Vert\langle(\eta^a + r_*\tilde v^a)^2v^a\rangle_\infty^0\Vert_1$	$\mathcal{N}_a^4$	$\omega_{\hat a}\Vert\langle\lvert\langle(\eta^a)^2\rangle\rvert\delta^{\hat a}\rangle_\infty^0\Vert_1 + \mu_*\omega_{\tilde a}\Vert\langle(\eta^a)^2\rangle\Vert_1$ $+2r_*q_a^2(\Vert\eta^a\Vert_1 + r_*q_a)$
$\Vert\langle(\eta^b + r_*\tilde v^b)^2v^b\rangle_\infty^0\Vert_2$	$\mathcal{N}_b^4$	$\omega_{\hat b}\Vert\langle\lvert\langle(\eta^b)^2\rangle\rvert\delta^{\hat b}\rangle_\infty^0\Vert_2 + \mu_*\omega_{\tilde b}\Vert\langle(\eta^b)^2\rangle\Vert_2$ $+2r_*q_b^2(\Vert\eta^b\Vert_2 + r_*q_b)$
$\widetilde\pi\langle(\eta^a + r_*\tilde v^a)^2v^a\rangle_k$	$\mathcal{N}_{a,k}^5$	$2\omega_{\hat a}\langle\lvert\langle\zeta^{\hat a}\eta^{\tilde a}\rangle\rvert\delta^{\hat a}\rangle_k + 4r_*^{\tilde a}\omega_{\hat a}\Vert\zeta^{\hat a}\Vert_1\xi_1^{1-k}$ $+2\mu_*\omega_{\hat a}(\Vert\eta^{\tilde a}\Vert_1 + r_*^{\tilde a})^2\xi_1^{1-k}$ $+\omega_{\tilde a}\Vert\langle(\eta^a)^2\rangle\Vert_1\xi_1^{-k} + 2r_*q_a\omega_{\tilde a}(\Vert\eta^a\Vert_1 + r_*q_a)\xi_1^{-k}$
$\widetilde\pi\langle(\eta^b + r_*\tilde v^b)^2v^b\rangle_m$	$\mathcal{N}_{b,m}^5$	$2\omega_{\hat b}\langle\lvert\langle\zeta^{\hat b}\eta^{\tilde b}\rangle\rvert\delta^{\hat b}\rangle_m + 12r_*^{\tilde b}\omega_{\hat b}\Vert\zeta^{\hat b}\Vert_2\xi_2^{2-\lvert m\rvert}$ $+6\mu_*\omega_{\hat b}(\Vert\eta^{\tilde b}\Vert_2 + r_*^{\tilde b})^2\xi_2^{2-\lvert m\rvert}$ $+\omega_{\tilde b}\Vert\langle(\eta^b)^2\rangle\Vert_2\xi_2^{-\lvert m\rvert} + 2r_*q_b\omega_{\tilde b}(\Vert\eta^b\Vert_2 + r_*q_b)\xi_2^{-\lvert m\rvert}$
$\Vert\widetilde\pi\langle(\eta^a + r_*\tilde v^a)^2v^a\rangle_\infty^0\Vert_1$	$\mathcal{N}_a^6$	$2\omega_{\hat a}\Vert\langle\lvert\langle\zeta^{\hat a}\eta^{\tilde a}\rangle\rvert\delta^{\hat a}\rangle_\infty^0\Vert_1 + 4r_*^{\tilde a}\omega_{\hat a}\Vert\zeta^{\hat a}\Vert_1\xi_1$ $+2\mu_*\omega_{\hat a}(\Vert\eta^{\tilde a}\Vert_1 + r_*^{\tilde a})^2\xi_1$ $+\omega_{\tilde a}\Vert\langle(\eta^a)^2\rangle\Vert_1 + 2r_*q_a\omega_{\tilde a}(\Vert\eta^a\Vert_1 + r_*q_a)$
$\Vert\widetilde\pi\langle(\eta^b + r_*\tilde v^b)^2v^b\rangle_\infty^0\Vert_2$	$\mathcal{N}_b^6$	$2\omega_{\hat b}\Vert\langle\lvert\langle\zeta^{\hat b}\eta^{\tilde b}\rangle\rvert\delta^{\hat b}\rangle_\infty^0\Vert_2 + 12r_*^{\tilde b}\omega_{\hat b}\Vert\zeta^{\hat b}\Vert_2\xi_2^2$ $+6\mu_*\omega_{\hat b}(\Vert\eta^{\tilde b}\Vert_2 + r_*^{\tilde b})^2\xi_2^2$ $+\omega_{\tilde b}\Vert\langle(\eta^b)^2\rangle\Vert_2 + 2r_*q_b\omega_{\tilde b}(\Vert\eta^b\Vert_2 + r_*q_b)$
$\widetilde\pi\langle(\eta^a + r_*\tilde v^a)^3v^a\rangle_0$	$\mathcal{N}_a^7$	$3\omega_{\hat a}\langle\lvert\langle(\zeta^{\hat a})^2\eta^{\tilde a}\rangle\rvert\delta^{\hat a}\rangle_0 + 6r_*^{\tilde a}\omega_{\hat a}\Vert\langle(\zeta^{\hat a})^2\rangle\Vert_1\xi_1$ $+6\mu_*\omega_{\hat a}\Vert\zeta^{\hat a}\Vert_1(\Vert\eta^{\tilde a}\Vert_1 + r_*^{\tilde a})^2\xi_1$ $+2\mu_*^2\omega_{\hat a}(\Vert\eta^{\tilde a}\Vert_1 + r_*^{\tilde a})^3\xi_1$ $+\omega_{\tilde a}\Vert\langle(\eta^a)^3\rangle\Vert_1^{*1} + 3r_*q_a\omega_{\tilde a}(\Vert\eta^a\Vert_1 + r_*q_a)^2$
$\widetilde\pi\langle(\eta^b + r_*\tilde v^b)^3v^b\rangle_0$	$\mathcal{N}_b^7$	$3\omega_{\hat b}\langle\lvert\langle(\zeta^{\hat b})^2\eta^{\tilde b}\rangle\rvert\delta^{\hat b}\rangle_0 + 18r_*^{\tilde b}\omega_{\hat b}\Vert\langle(\zeta^{\hat b})^2\rangle\Vert_2\xi_2^2$ $+18\mu_*\omega_{\hat b}\Vert\zeta^{\hat b}\Vert_2(\Vert\eta^{\tilde b}\Vert_2 + r_*^{\tilde b})^2\xi_2^2$ $+6\mu_*^2\omega_{\hat b}(\Vert\eta^{\tilde b}\Vert_2 + r_*^{\tilde b})^3\xi_2^2$ $+\omega_{\tilde b}\Vert\langle(\eta^b)^3\rangle\Vert_2^{*1} + 3r_*q_b\omega_{\tilde b}(\Vert\eta^b\Vert_2 + r_*q_b)^2$

Table B.1: Constants $\mathcal{M}$ and $\mathcal{N}$ used in the expressions for the estimates $\widetilde{Q}$. On each row, the term in the left column is estimated by the expression in the right column, which is computable and defines the constant in the middle column. Here we have assumed that $y^{\tilde a}, \tilde y^{\tilde a} \in \tilde X_1^0$ with $\|y^{\tilde a}\|_1, \|\tilde y^{\tilde a}\|_1 \le 1$ and $y^{\tilde b}, \tilde y^{\tilde b} \in \tilde X_2^0$ with $\|y^{\tilde b}\|_2, \|\tilde y^{\tilde b}\|_2 \le 1$. Furthermore, $v, \tilde v \in \widetilde{\mathcal{B}}$. The constants q_a and q_b are given in (B.2), whereas $\tilde\ell_1$ and $\tilde\ell_2$ are defined in (B.3).

we obtain

$$
\begin{aligned}
\widetilde{Q}^c_2 &= 2\big[\omega_{\tilde\kappa_1}|\zeta_{\tilde\beta}| + \omega_{\tilde\beta}|\zeta_{\tilde\kappa_1}| + \tfrac12\omega_{\tilde\kappa_1}|\zeta_{\kappa_1}^{-1}||\zeta_{\tilde\kappa_1}| + \tfrac14\omega_{\tilde\kappa_1}\zeta_{\kappa_1}^{-2}\mu_*\zeta_{\tilde\kappa_1}^2\big](\zeta_1^{\hat a})^2 + \omega_{\hat a}|4\zeta_{\tilde\kappa_1}\zeta_{\tilde\beta} + \zeta_{\kappa_1}^{-1}\zeta_{\tilde\kappa_1}^2||\zeta_1^{\hat a}| \\
&\quad + \omega_{\tilde\kappa_1}\mu_*\zeta_{\kappa_1}^{-2}\mathcal{M}_a^2 + \mu_*(\omega_{\tilde\kappa_1}|\zeta_\beta| + \omega_{\tilde\beta}|\zeta_{\kappa_1}|)\mathcal{M}_a^1 + 2\omega_{\tilde a}(|\zeta_{\kappa_1}^{-1}|\mathcal{M}_a^4 + \mathcal{M}_a^5 + |\zeta_{\kappa_1}||\zeta_\beta|\mathcal{M}_a^3) + 2\mathcal{N}_a^7 \\
&\quad + \Bigg\{ \tfrac12\big[\omega_{\tilde\kappa_2}|\zeta_{\tilde\beta}| + \omega_{\tilde\beta}|\zeta_{\tilde\kappa_2}| + \tfrac12\omega_{\tilde\kappa_2}|\zeta_{\kappa_2}^{-1}||\zeta_{\tilde\kappa_2}| + \tfrac14\omega_{\tilde\kappa_2}\zeta_{\kappa_2}^{-2}\mu_*\zeta_{\tilde\kappa_2}^2\big][2(\zeta_1^{\hat b})^2 + (\zeta_2^{\hat b})^2] \\
&\qquad + \omega_{\hat b}\big|\zeta_{\tilde\kappa_2}\zeta_{\tilde\beta} + \tfrac14\zeta_{\kappa_2}^{-1}\zeta_{\tilde\kappa_2}^2\big|\big[2|\zeta_1^{\hat b}| + |\zeta_2^{\hat b}|\big] + \omega_{\tilde\kappa_2}\mu_*\zeta_{\kappa_2}^{-2}\mathcal{M}_b^2 + \mu_*(\omega_{\tilde\kappa_2}|\zeta_\beta| + \omega_{\tilde\beta}|\zeta_{\kappa_2}|)\mathcal{M}_b^1 \\
&\qquad + 2\omega_{\tilde b}(|\zeta_{\kappa_2}^{-1}|\mathcal{M}_b^4 + \mathcal{M}_b^5 + |\zeta_{\kappa_2}||\zeta_\beta|\mathcal{M}_b^3) + 2\mathcal{N}_b^7 \Bigg\}, \\
\widetilde{Q}^c_3 &= 2[\omega_{\tilde\kappa_1}(4 + 2\mu_*|\zeta_{\tilde\kappa_1}|)|\zeta_{\tilde\beta}| + \omega_{\tilde\beta}(4|\zeta_{\tilde\kappa_1}| + \mu_*\zeta_{\tilde\kappa_1}^2) + \tfrac12\omega_{\tilde\kappa_1}|\zeta_{\tilde\kappa_1}|](\zeta_1^{\hat a})^2 \\
&\quad + 4\omega_{\hat a}[(4|\zeta_{\tilde\kappa_1}| + \mu_*\zeta_{\tilde\kappa_1}^2)|\zeta_{\tilde\beta}| + \tfrac14\zeta_{\tilde\kappa_1}^2]|\zeta_1^{\hat a}| \\
&\qquad + \mu_*[\omega_{\tilde\beta}\zeta_{\kappa_1}^2 + 2\omega_{\tilde\kappa_1}|\zeta_{\kappa_1}||\zeta_\beta|]\mathcal{M}_a^1 + 2\omega_{\tilde a}\zeta_{\kappa_1}^2|\zeta_\beta|\mathcal{M}_a^3 + 2\omega_{\tilde a}\mathcal{M}_a^4, \\
\widetilde{Q}^c_4 &= \tfrac12[\omega_{\tilde\kappa_2}(16 + 2\mu_*|\zeta_{\tilde\kappa_2}|)|\zeta_{\tilde\beta}| + \omega_{\tilde\beta}(16|\zeta_{\tilde\kappa_2}| + \mu_*\zeta_{\tilde\kappa_2}^2) + \tfrac12\omega_{\tilde\kappa_2}|\zeta_{\tilde\kappa_2}|][2(\zeta_1^{\hat b})^2 + (\zeta_2^{\hat b})^2] \\
&\quad + \omega_{\hat b}[16|\zeta_{\tilde\kappa_2}| + \mu_*\zeta_{\tilde\kappa_2}^2]|\zeta_{\tilde\beta}| + \tfrac14\zeta_{\tilde\kappa_2}^2][2|\zeta_1^{\hat b}| + |\zeta_2^{\hat b}|] \\
&\qquad + \mu_*[\omega_{\tilde\beta}\zeta_{\kappa_2}^2 + 2\omega_{\tilde\kappa_2}|\zeta_{\kappa_2}||\zeta_\beta|]\mathcal{M}_b^1 + 2\omega_{\tilde b}\zeta_{\kappa_2}^2|\zeta_\beta|\mathcal{M}_b^3 + 2\omega_{\tilde b}\mathcal{M}_b^4, \\
\widetilde{Q}^a_1 &= [\omega_{\tilde\kappa_1}(4 + 2\mu_*|\zeta_{\tilde\kappa_1}|)|\zeta_{\tilde\beta}| + \omega_{\tilde\beta}(4|\zeta_{\tilde\kappa_1}| + \mu_*\zeta_{\tilde\kappa_1}^2) + \tfrac12\omega_{\tilde\kappa_1}|\zeta_{\tilde\kappa_1}|]|\zeta_1^{\hat a}| + \omega_{\hat a}[(4|\zeta_{\tilde\kappa_1}| + \mu_*\zeta_{\tilde\kappa_1}^2)|\zeta_{\tilde\beta}| + \tfrac14\zeta_{\tilde\kappa_1}^2] \\
&\quad + \omega_{\tilde\kappa_1}\mathcal{N}_{a,1}^1 + 3|\zeta_{\tilde\kappa_1}|\mathcal{N}_{a,1}^3 + 6\mathcal{N}_{a,1}^5, \\
\widetilde{Q}^a_k &= [\omega_{\tilde\kappa_1}k^2 + 2\omega_{\tilde\kappa_1}|\zeta_{\kappa_1}||\zeta_\beta| + \omega_{\tilde\beta}\zeta_{\kappa_1}^2](|\eta_k^{\tilde a}| + r_*^{\tilde a}\xi_1^{-k}) + \omega_{\tilde a}[|\zeta_{\tilde\kappa_1}|(k^2-1) + \zeta_{\kappa_1}^2|\zeta_{\tilde\beta}| + \tfrac14\mu_*\zeta_{\tilde\kappa_1}^2]\xi_1^{-k} \\
&\quad + \omega_{\tilde\kappa_1}k^2\mathcal{N}_{a,k}^1 + 3|\zeta_{\tilde\kappa_1}|k^2\mathcal{N}_{a,k}^3 + 6k^2\mathcal{N}_{a,k}^5, \\
\widetilde{Q}^b_{m'} &= [\omega_{\tilde\kappa_2}(16 + 2\mu_*|\zeta_{\tilde\kappa_2}|)|\zeta_{\tilde\beta}| + \omega_{\tilde\beta}(16|\zeta_{\tilde\kappa_2}| + \mu_*\zeta_{\tilde\kappa_2}^2) + \tfrac12\omega_{\tilde\kappa_2}|\zeta_{\tilde\kappa_2}|]|\zeta_{m'}^{\hat b}| + \omega_{\hat b}[(16|\zeta_{\tilde\kappa_2}| + \mu_*\zeta_{\tilde\kappa_2}^2)|\zeta_{\tilde\beta}| + \tfrac14\zeta_{\tilde\kappa_2}^2] \\
&\quad + 4\omega_{\tilde\kappa_2}\mathcal{N}_{b,m'}^1 + 12|\zeta_{\tilde\kappa_2}|\mathcal{N}_{b,m'}^3 + 96\mathcal{N}_{b,m'}^5, \\
\widetilde{Q}^b_m &= [\omega_{\tilde\kappa_2}\mathbf{m}^2 + 2\omega_{\tilde\kappa_2}|\zeta_{\kappa_2}||\zeta_\beta| + \omega_{\tilde\beta}\zeta_{\kappa_2}^2](|\eta_m^{\tilde b}| + r_*^{\tilde b}\xi_2^{-|m|}) + \omega_{\tilde b}[|\zeta_{\tilde\kappa_2}||\mathbf{m}^2 - 4| + \zeta_{\kappa_2}^2|\zeta_{\tilde\beta}| + \tfrac14\mu_*\zeta_{\tilde\kappa_2}^2]\xi_2^{-|m|} \\
&\quad + \omega_{\tilde\kappa_2}\mathbf{m}^2\mathcal{N}_{b,m}^1 + 3|\zeta_{\tilde\kappa_2}|\mathbf{m}^2\mathcal{N}_{b,m}^3 + 24\mathbf{m}^2\mathcal{N}_{b,m}^5.
\end{aligned}
$$

For $k > K$ and $m_\infty > M$ we split into terms with and without k^2 and $\mathbf{m}^2$, and we define

$$
\begin{aligned}
\Theta_0^a &= [2\omega_{\tilde\kappa_1}|\zeta_{\kappa_1}||\zeta_\beta| + \omega_{\tilde\beta}\zeta_{\kappa_1}^2]r_*^{\tilde a} + \omega_{\tilde a}[|\zeta_{\tilde\kappa_1}| + \zeta_{\kappa_1}^2|\zeta_{\tilde\beta}| + \tfrac14\mu_*\zeta_{\tilde\kappa_1}^2] \\
\Theta_0^b &= [2\omega_{\tilde\kappa_2}|\zeta_{\kappa_2}||\zeta_\beta| + \omega_{\tilde\beta}\zeta_{\kappa_2}^2]r_*^{\tilde b} + \omega_{\tilde b}[4|\zeta_{\tilde\kappa_2}| + \zeta_{\kappa_2}^2|\zeta_{\tilde\beta}| + \tfrac14\mu_*\zeta_{\tilde\kappa_2}^2] \\
\Theta_1^a &= \omega_{\tilde\kappa_1}r_*^{\tilde a} + \omega_{\tilde a}|\zeta_{\tilde\kappa_1}| + \omega_{\tilde\kappa_1}\mathcal{N}_a^2 + 3|\zeta_{\tilde\kappa_1}|\mathcal{N}_a^4 + 6\mathcal{N}_a^6 \\
\Theta_1^b &= \omega_{\tilde\kappa_2}r_*^{\tilde b} + \omega_{\tilde b}|\zeta_{\tilde\kappa_2}| + \omega_{\tilde\kappa_2}\mathcal{N}_b^2 + 3|\zeta_{\tilde\kappa_2}|\mathcal{N}_b^4 + 24\mathcal{N}_b^6
\end{aligned}
$$

so that, incorporating the division by $\tilde\lambda_k^{\tilde a}$ and $\tilde\lambda_m^{\tilde b}$, we find from Lemma A.1 (Section A.4) that

$$
\begin{aligned}
\widetilde{Q}^a_\infty &= \frac{\Theta_0^a + \Theta_1^a(K+1)^2}{((K+1)^2 - 1)^2}, \\
\widetilde{Q}^b_\infty &= \frac{\Theta_0^b + \Theta_1^b(M+1)^2}{((M+1)^2 - 4)^2}.
\end{aligned}
$$

B.7 Explicit solution for $\mu = 0$

Let

$$
\beta_0 \stackrel{\text{def}}{=} \frac{57 + 18\sqrt{6}}{10}.
$$

Then the solution for $\mu = 0$ is given by

$$
\begin{aligned}
\bar{\tilde{\beta}} &= -\beta_0 \\
\bar{\tilde{\kappa}}_1 &= 4\beta_0 \\
\bar{\tilde{\kappa}}_2 &= 16\beta_0 \\
\bar{\hat{a}}_1 &= \sqrt{\tfrac{2}{3}\beta_0 - 1} \\
\bar{\hat{b}}_1 &= -\tfrac{1}{15}\left(\sqrt{30\beta_0 - 36} + 3\right) \\
\bar{\hat{b}}_2 &= -\tfrac{1}{15}\left(\sqrt{30\beta_0 - 36} + 3\right),
\end{aligned}
$$

whereas the "slaved" modes are

$$
\begin{aligned}
\bar{\tilde{a}}_2 &= -\tfrac{8}{3}\left(\bar{\hat{a}}_1\right)^2 \\
\bar{\tilde{a}}_3 &= -\tfrac{9}{32}\left(\bar{\hat{a}}_1\right)^3 \\
\bar{\tilde{b}}_{(4,0)} &= -\tfrac{8}{3}[2(\bar{\hat{b}}_1)^3 + (\bar{\hat{b}}_1)^2] \\
\bar{\tilde{b}}_{(6,0)} &= -\tfrac{9}{32}(\bar{\hat{b}}_1)^3 \\
\bar{\tilde{b}}_{(3,1)} &= -9[(\bar{\hat{b}}_1)^3 + (\bar{\hat{b}}_1)^2] \\
\bar{\tilde{b}}_{(5,1)} &= -\tfrac{7}{6}(\bar{\hat{b}}_1)^3 \\
\bar{\tilde{b}}_{(0,2)} &= -9[(\bar{\hat{b}}_1)^3 + (\bar{\hat{b}}_1)^2] \\
\bar{\tilde{b}}_{(2,2)} &= -\tfrac{8}{3}[2(\bar{\hat{b}}_1)^3 + (\bar{\hat{b}}_1)^2] \\
\bar{\tilde{b}}_{(4,2)} &= -\tfrac{7}{6}(\bar{\hat{b}}_1)^3 \\
\bar{\tilde{b}}_{(1,3)} &= -\tfrac{7}{6}(\bar{\hat{b}}_1)^3 \\
\bar{\tilde{b}}_{(3,3)} &= -\tfrac{9}{32}(\bar{\hat{b}}_1)^3\,,
\end{aligned}
$$

and all other elements of $\bar{\tilde{a}}$ and $\bar{\tilde{b}}$ vanish.

References

[1] CAPD: Computer assisted proofs in dynamics, a package for rigorous numerics. `http://capd.ii.uj.edu.pl/`.

[2] G. Arioli and H. Koch. Computer-Assisted Methods for the Study of Stationary Solutions in Dissipative Systems, Applied to the Kuramoto-Sivashinski Equation. *Archive for Rational Mechanics and Analysis*, 197:1033–1051, 2010.

[3] G. Arioli and H. Koch. Integration of dissipative partial differential equations: a case study. *SIAM J. Applied Dynamical Systems*, 9:1119–1133, 2010.

[4] F.S. Bates and G.H. Fredrickson. Block copolymers - Designer soft materials. *Physics Today*, 52:32–38, 1999.

[5] M. Breden, J.P. Lessard, and M. Vanicat. Global bifurcation diagram of steady states of systems of PDEs via rigorous numerics: a 3-component reaction-diffusion system. *Acta Applicandae Mathematicae*, 128:113–152, 2013.

[6] R. Castelli, M. Gameiro, and J.-P. Lessard. Rigorous numerics for ill-posed PDEs: periodic orbits in the Boussinesq equation, 2015. Preprint.

[7] R. Choksi. Scaling laws in microphase separation of diblock copolymers. *J. Nonlinear Science*, 11:223–236, 2001.

[8] R. Choksi, M. Maras, and J.F. Williams. 2D phase diagram for minimizers of a Cahn-Hilliard functional with long-range interactions. *SIAM J. Applied Dynamical Systems*, 10:1344–1362, 2011.

[9] R. Choksi and M.A. Peletier. Small volume fraction limit of the diblock copolymer problem: I. Sharp-interface functional. *SIAM J. Mathematical Analysis*, 42:1334–1370, 2010.

[10] R. Choksi and M.A. Peletier. Small volume fraction limit of the diblock copolymer problem: II. diffuse-interface functional. *SIAM J. Mathematical Analysis*, 43:739–763, 2011.

[11] R. Choksi, M.A. Peletier, and J.F. Williams. On the phase diagram for microphase separation of diblock copolymers: an approach via a nonlocal Cahn-Hilliard functional. *SIAM J. On Applied Mathematics*, 69:1712–1738, 2009.

[12] R. Choksi and X.F. Ren. On the derivation of a density functional theory for microphase separation of diblock copolymers. *J. Statistical Physics*, 113:151–176, 2003.

[13] S. Day, J.P. Lessard, and K. Mischaikow. Validated continuation for equilibria of PDEs. *SIAM J. Nummerical Analysis*, 45:1398–1424, 2007.

[14] M. Gameiro and J.-P. Lessard. Analytic estimates and rigorous continuation for equilibria of higher-dimensional PDEs. *J. Differential Equations*, 249:2237–2268, 2010.

[15] M. Gameiro and J.-P. Lessard. Rigorous computation of smooth branches of equilibria for the three-dimensional Cahn-Hilliard equation. *Nummerische Mathematik*, 117:753–778, 2011.

[16] M. Gameiro and J.-P. Lessard. Efficient rigorous numerics for higher-dimensional PDEs via one-dimensional estimates. *SIAM J. Numerical Analysis*, 51:2063–2087, 2013.

[17] M. Gameiro, J.-P. Lessard, and A. Pugliese. Computation of smooth manifolds via rigorous multi-parameter continuation in infinite dimensions, 2016. To appear in Mathematics of Computation.

[18] A. Hungria, , J.-P. Lessard, and J.D. Mireles James. Rigorous numerics for analytic solutions of differential equations: the radii polynomial approach, 2016. To appear in Mathematics of Computation.

[19] D. Jeong, J. Shin, Y. Li, Y. Choi, J.-H. Jung, S. Lee, and J. Kim. Numerical analysis of energy-minimizing wavelengths of equilibrium states for diblock copolymers. *Current Applied Physics*, 14:1263–1272, 2014.

[20] A.K. Kassam and L.N. Trefethen. Fourth-order time-stepping for stiff PDEs. *SIAM J. Scientific Computing*, 26:1214–1233, 2005.

[21] L. Leibler. Theory of microphase separation in block co-polymers. *Macromolecules*, 13:1602–1617, 1980.

[22] J.-P. Lessard. Recent advances about the uniqueness of the slowly oscillating periodic solutions of Wrights equation. *J. Differential Equations*, 248:992–1016, 2010.

[23] M. T. Nakao. Numerical verification methods for solutions of ordinary and partial differential equations. *Numer. Funct. Anal. Optim.*, 22(3-4):321–356, 2001.

[24] Y. Nishiura and I. Ohnishi. Some mathematical aspects of the microphase separation in diblock copolymers. *Physica D*, 84:31–39, 1995.

[25] T. Ohta and K. Kawasaki. Equilibrium morphology of block copolymer melts. *Macromolecules*, 19:2621–2632, 1986.

[26] S.M. Rump. INTLAB - INTerval LABoratory. In Tibor Csendes, editor, *Developments in Reliable Computing*, pages 77–104. Kluwer Academic Publishers, Dordrecht, 1999.

[27] S.M. Rump. Verification methods: Rigorous results using floating-point arithmetic. *Acta Numerica*, 19:287–449, 2010.

[28] D. Shirokoff, R. Choksi, and J.C. Nave. Sufficient conditions for global minimality of metastable states in a class of non-convex functionals: a simple approach via quadratic lower bounds. *J. of Nonlinear Science*, 25(3):539–582, 2015.

[29] X.D. Sun and M.J. Ward. Dynamics and coarsening of interfaces for the viscous Cahn-Hilliard equation in one spatial dimension. *Studies in Applied Mathematics*, 105:203–234, 2000.

[30] T. Teramoto and Y. Nishiura. Double gyroid morphology in a gradient system with nonlocal effects. *J. of the Physical Society of Japan*, 71:1611–1614, 2002.

[31] T. Teramoto and Y. Nishiura. Morphological characterization of the diblock copolymer problem with topological computation. *Japan J. of Industrial and Applied Mathematics*, 27:175–190, 2010.

[32] J.B. van den Berg, C.M. Groothedde, and J.F. Williams. Rigorous computation of a radially symmetric localized solution in a ginzburg–landau problem. *SIAM J. Applied Dynamical Systems*, 14:423–447, 2015.

[33] J.B. van den Berg and J.-P. Lessard. Chaotic braided solutions via rigorous numerics: chaos in the Swift-Hohenberg equation. *SIAM J. Applied Dynamical Systems*, 7:988–1031, 2008.

[34] J.B. van den Berg, J.-P. Lessard, and K. Mischaikow. Global smooth solution curves using rigorous branch following. *Mathematics of Computation*, 79(271):1565–1584, 2010.

[35] J.B. van den Berg and J.F. Williams. MATLAB code for "Validation of the bifurcation diagram in the 2D Ohta-Kawasaki problem", 2016. `http://www.math.vu.nl/~janbouwe/code/ohtakawasaki/`.

[36] T. Wanner. Computer-assisted equilibrium validation for the diblock copolymer model, 2015. Preprint.

[37] N. Yamamoto. A numerical verification method for solutions of boundary value problems with local uniqueness by Banach's fixed-point theorem. *SIAM J. Numerical Analysis*, 35:2004–2013, 1998.

[38] P. Zgliczyński. Rigorous numerics for dissipative partial differential equations. II. Periodic orbit for the Kuramoto-Sivashinsky PDE—a computer-assisted proof. *Foundations of Computational Math.*, 4:157–185, 2004.